

Hurricanes: their formation, structure and likely role in the tropical circulation

By WILLIAM M. GRAY

Department of Atmospheric Science, Colorado State University, Fort Collins, Colorado 80523

SUMMARY

This paper discusses tropical cyclone frequency from a global point of view. Statistics are presented on global tropical cyclone frequency and its yearly, monthly and regional variability. Cyclone genesis frequency is shown in its relationship to specific climatological and individual day parameters. An extensive discussion of many of the likely physical processes responsible for tropical cyclone genesis is made. Information on the role of tropical cyclones in the global moisture and kinetic energy budgets is presented. These storms account for about 2% of the annual global rainfall and kinetic energy generation. They export kinetic energy in their upper tropospheric outflow levels. Much of this is accomplished by horizontal eddy processes. Recommendations on future tropical cyclone research are made.

1. INTRODUCTION

If we did not know that tropical cyclones occurred, it is doubtful that, with our current understanding of fluid mechanics and baroclinic instability processes, we would have believed their existence possible. They develop in regions of negligible tropospheric vertical wind shear. Although we have some physical understanding of the processes which probably lead to tropical cyclone intensification, meteorologists are at present not in agreement upon the processes which bring about tropical disturbance to cyclone transformation. Also, some of the dynamics of hurricane structure are in doubt. It is possible, nevertheless, to gather together a number of new observational facts which increase our understanding of a number of the likely relevant processes involved with these systems.

Tropical cyclones appear to be primarily a product of the long-term characteristics of the tropical general circulation. Their yearly frequency is quite steady. Because their local influence on man's activities can be so substantial, tropical cyclones appear worthy of careful study. As nature's most destructive weather event they also stimulate our curiosity as to the physical processes responsible for their generation and existence.

This paper will attempt to synthesize recent observational information as this may relate to an understanding of the physical mechanisms involved with tropical cyclone genesis and structure, and tropical cyclone-broad-scale interaction. Discussion will concentrate on the likely role which climatological and synoptic-scale flow features play in the generation and maintenance of tropical cyclones. As the opposite role, the importance of tropical cyclones to the general circulation, is believed not to be fundamental to the maintenance of the long-term tropical general circulation, this topic will be treated only briefly.

Much of the following discussion is based on observational studies which have been conducted on the author's research project in the last decade. The background to this discussion is contained in the Colorado State University tropical research reports of the author, his graduate students and associates. These include the reports of R. López, K. Williams, D. Shea, E. Ruprecht, W. Frank, R. Zehr, S. Erickson, C. Arnold, W. Fingerhut, J. McBride and forthcoming reports of J. Dewart and P. Grube. The references for these reports are in the following sections.

Much of the discussion of hurricane structure is taken from material contained in the Ph.D. thesis of W. Frank (1976).

2. ANALYSIS PHILOSOPHY AND COMPOSITING METHODOLOGY

Cloud clusters and tropical cyclones spend most of their lifetimes over the warm tropical oceans. Traditional data sources are very sparse in such regions, and daily tropical weather analyses are notoriously unreliable. The severe winds found in tropical cyclones further reduce the availability of such data. It is not possible to obtain enough rawinsonde data or surface observations around any individual storm or cluster at one time period to permit quantitative analysis of structure, dynamics or energetics.

Aircraft data have provided the best information concerning the activities in the intense central core regions of tropical cyclones. There are a number of case studies of individual storms based on northwest Atlantic hurricane flight data (Riehl and Malkus 1961; Miller 1962; LaSeur and Hawkins 1963; Sheets 1967a, 1967b, 1968; Hawkins and Rubsam 1968; Hawkins and Imbembo 1976) and also statistical treatment of the flight data (Gray 1962, 1965, 1966, 1967; Shea and Gray 1973; Gray and Shea 1973, 1976). However, logistical considerations have limited the ability of aircraft to provide information concerning the outer convective regions of the storm and its broader-scale environment. Aircraft data also have been limited to a few flight levels per storm time period, due to the usually low number of available aircraft, maximum aircraft ceilings of 200 mb or lower, and dangerous low-level flight conditions.

None of the above data sources can produce an accurate vertical profile of the radial wind pattern around a system. Without such a profile, it is impossible to compute meaningful budgets of energy, water vapour, momentum, vorticity, etc. In addition, vertical profiles of the other dynamic and thermodynamic variables cannot be determined fully over the mesoscale area. It is necessary to composite very large amounts of data from many similar weather systems at many time periods to obtain meaningful quantitative measurements.

Although the extreme variabilities and individual asymmetries of tropical cyclones and cloud clusters are well known, the nature of the basic dynamic and energetic processes which govern these systems must be largely invariant. Compositing allows quantitative

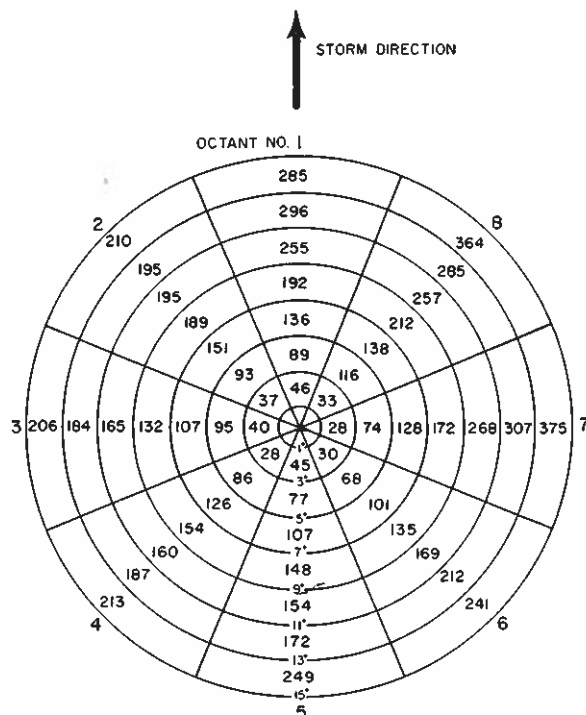


Figure 1. Compositing grid (15° latitude radius) with the number of rawinsonde reports in each octant and each 2° radial band for a typical stratification.

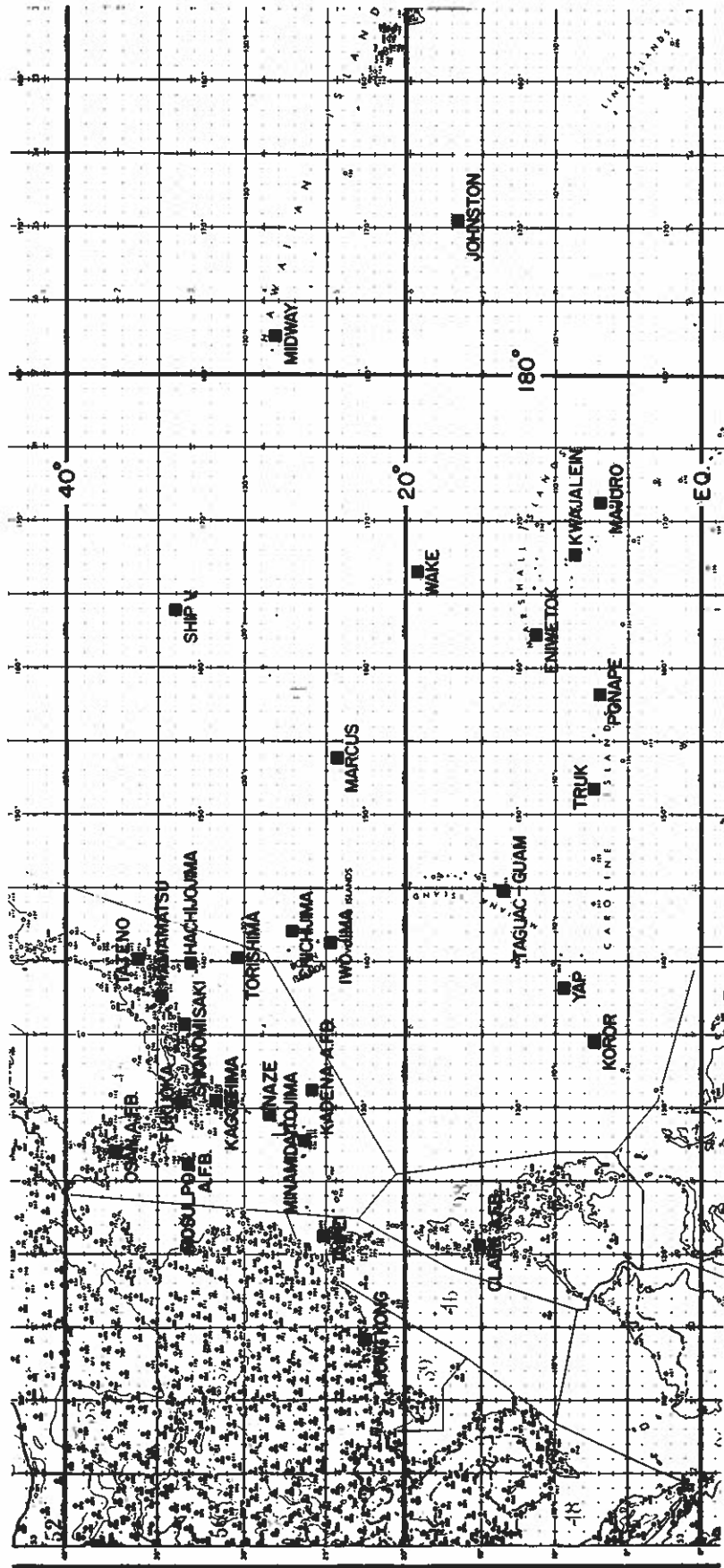


Figure 2. Western North Pacific rawinsonde data network.

al
er
er
or
nit

se
al
ler
8;
2,
al
he
so
er
w-

al
g-
es
he
ar

rd
es
ve

nt

analyses of these features. Any compositing system smoothes out many of the individual characteristics of single systems, but a great deal of information concerning asymmetrical or 'eddy' quantities can be deduced by the use of proper data-handling techniques.

Rawinsonde compositing has been performed on a 15° latitude radius cylindrical grid extending from sea level to 50 mb about many hundreds of tropical cloud clusters and cyclones. The system circulation centre was located at each time period using JTWC and NOAA Miami reports and/or satellite photographs, and the grid was positioned with the system based on the grid centre of the lowest level. Whenever available rawinsonde soundings fell on the grid at a given time period for a given storm, these soundings were positioned relative to the storm centre in cylindrical coordinates. Figure 1 shows the grid and the number of soundings per grid space for a typical class of cloud cluster or tropical cyclone stratification. All the parameters to be composited, whether directly measured or computed from the directly measured parameters, were determined at the observation station locations at 19 pressure levels.

The discussion to follow involves the use of ten years (1961-1970) of northwest Pacific rawinsonde data to provide high density data coverage around all cyclones occurring in that

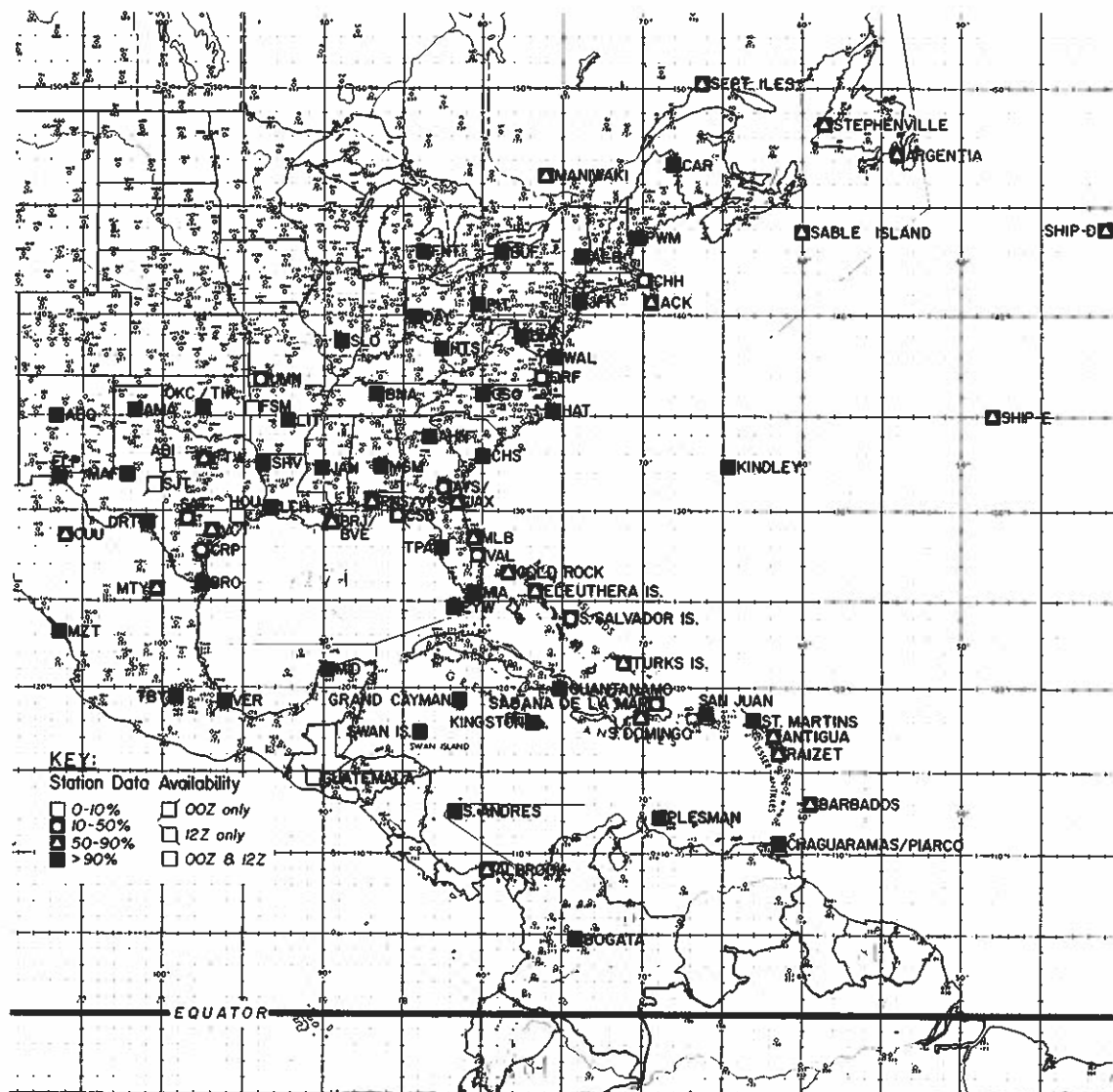


Figure 3. North Atlantic rawinsonde data network.

region. About 18 000 soundings from the 30 stations shown in Fig. 2 have been processed. A similarly sized data sample for west Atlantic stations (Fig. 3) for a 14-year period (1961–1974) has also been utilized.

All parameters were assigned to a point at the centre of the grid box in which the sounding fell. All soundings which fell in that grid space for the particular composite were averaged.

The data set was sufficiently large to allow compositing of various subsets. Data could be grouped according to any characteristic observed in individual systems such as location, season, intensity, motion, or intensity tendency, etc. By comparing the composites of different subsets, it is possible to analyse quantitatively persistent differences between the groups. It is also possible to remove obviously atypical systems or time periods from a data group to improve the quality of the data set.

Rawinsonde compositing procedures involve the use of four separate reference frames:

(1) With respect to the instantaneously fixed cyclone centre in a N–S or geographical coordinate system.

(2) With respect to the cyclone centre in a geographical coordinate system with the cyclone motion subtracted out of all the winds (portrayal of data relative to the moving cyclone centre in geographical coordinates).

(3) With respect to the instantaneously fixed cyclone centre and the direction to which the storm is moving.

(4) With respect to the cyclone centre and the direction to which the storm is moving with the cyclone motion subtracted out of all the winds.

The relative positions of the system and the balloon changed due to their respective motions during the balloon's ascent. These motions were estimated from the data, and the position of each was corrected at each pressure level.

In this study, horizontal eddy fluxes were estimated by compositing individual fluxes of quantities and comparing them to mean fluxes. The radial winds were initially composited and mass balanced from the surface to 100 mb by adding a small constant correction factor (ΔV_r) to each individual radial wind in a given radial band. Changes in mass of the volume within the radial band were neglected. For each sounding the product of the corrected V_r and the quantity being analysed was computed at each level. Such products for all the soundings in an octant were then composited as before, giving a mean transport value for each octant at each level, $\overline{V_r Q}$, where the bar denotes time and space averaging of the $V_r Q$ products. By subtracting the product of the mean $\overline{V_r}$ and the mean \overline{Q} one could achieve a good estimate of horizontal eddy transport; thus

$$\overline{V_r' Q'} \approx \overline{V_r Q} - \overline{V_r} \overline{Q} \quad (1)$$

3. STATISTICS ON TROPICAL CYCLONE OCCURRENCE

There are approximately 80 tropical cyclones with maximum sustained winds of 20–25 m s⁻¹ over the globe per year. Figure 4 shows the location of the initial genesis point of cyclones for a 20-year period. About half to two thirds of these cyclones reach hurricane strength (maximum sustained winds > 33 m s⁻¹). As shown by Table 1, the annual percentage variation in the global number of tropical cyclones over the last 20 years has ranged from –13% to +23%. The average annual variation is only 8% which, considering the individual 'ocean basin' variation, is quite small. This table also gives northern and southern hemisphere occurrences. The ratio of yearly northern to southern hemisphere cyclone frequency varied from 1.5 to 4.0. The numbers of tropical cyclone formations by month and

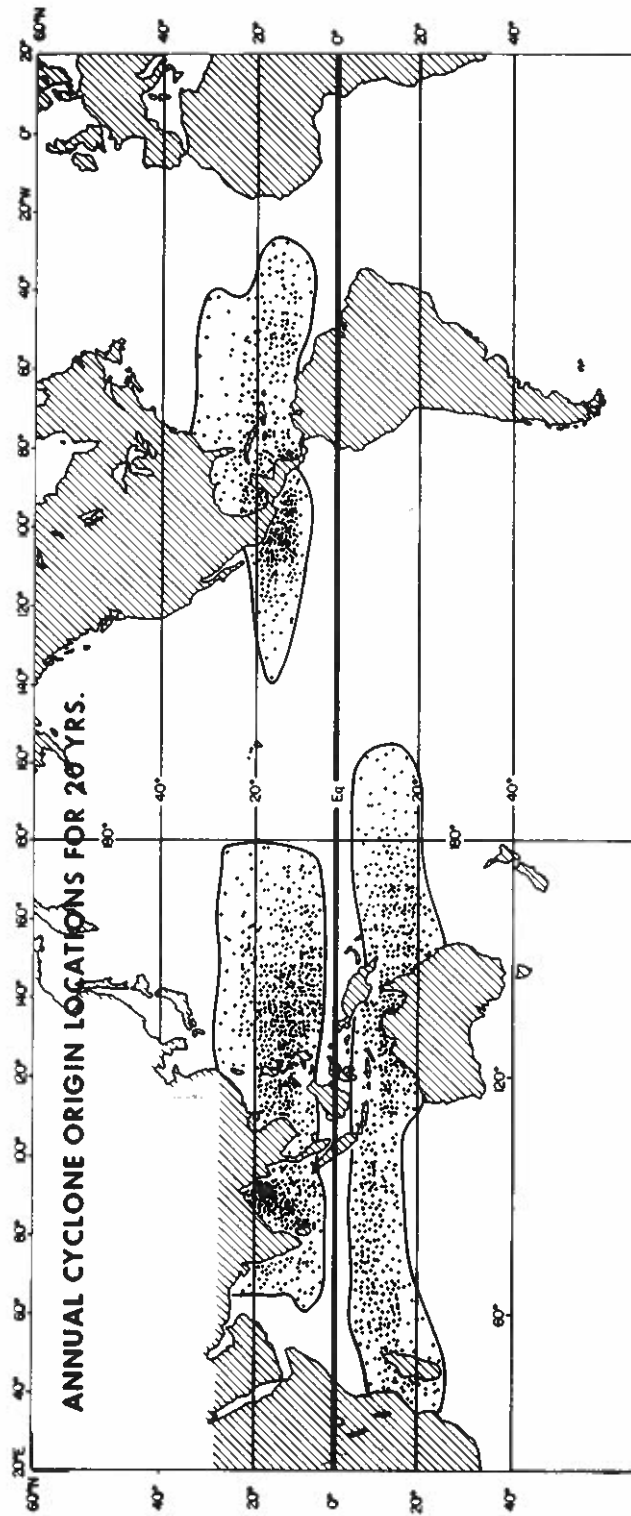


Figure 4.

TABLE 1. LAST 20 YEARS' STATISTICS ON TROPICAL CYCLONE ACTIVITY IN NORTHERN AND SOUTHERN HEMISPHERES

Year	Year		No. of cyclones		Total	% deviation from 20 yr average	Ratio NH. to SH.
	NH.	SH.	NH.	SH.			
1958		1958-59	52	25	77	-3	2.1
1959		1959-60	48	21	69	-13	2.3
1960		1960-61	48	22	70	-12	2.2
1961		1961-62	58	23	81	+2	2.5
1962		1962-63	50	30	80	+1	1.7
1963		1963-64	49	23	72	-9	2.1
1964		1964-65	65	19	84	+6	3.4
1965		1965-66	56	22	78	-1	2.5
1966		1966-67	64	16	78	-1	4.0
1967		1967-68	63	28	91	+15	2.2
1968		1968-69	61	23	84	+6	2.6
1969		1969-70	49	23	72	-9	2.1
1970		1970-71	56	26	82	+4	2.1
1971		1971-72	70	27	97	+23	2.6
1972		1972-73	54	35	91	+15	1.5
1973		1973-74	46	28	74	-6	1.6
1974		1974-75	55	19	75	-5	2.9
1975		1975-76	47	29	76	-4	1.6
1976		1976-77	55	30	85	+7	1.8
1977		1977-78	47	20	67	-15	2.3
Total			1093	489	1583		
Average			54.6	24.5	79.1	±8	2.3

year for the northern and southern hemispheres are given in Tables 2 and 3. Individual monthly variation is large. About $3\frac{1}{2}$ times as many cyclones occur in August and September as in April and May. Individual ocean basins can have wide annual differences in cyclone occurrences, as indicated in Table 4. Basins are defined in Fig. 5.

TABLE 2. FREQUENCY OF NORTHERN HEMISPHERE TROPICAL CYCLONE GENESIS BY YEAR AND MONTH

Year	Jan.	Feb.	Mar.	Apr.	May	June	July	Aug.	Sep.	Oct.	Nov.	Dec.	Total
1958	1	0	0	0	2	5	10	9	11	9	4	1	52
1959	0	0	0	1	2	6	7	11	9	8	2	2	48
1960	0	0	0	1	3	7	6	14	6	8	2	1	48
1961	1	1	1	1	4	5	10	5	14	9	6	1	58
1962	0	1	0	1	3	2	7	11	11	7	4	3	50
1963	0	0	0	1	3	5	6	5	14	11	0	4	49
1964	0	0	0	0	3	4	11	15	12	8	10	2	65
1965	2	2	1	1	4	8	8	8	12	3	4	3	56
1966	0	0	0	2	2	3	9	13	20	5	7	3	64
1967	2	1	1	1	2	4	10	12	12	13	3	2	63
1968	0	0	0	1	2	5	7	17	11	11	6	1	61
1969	1	0	1	1	1	0	7	13	10	9	4	2	49
1970	0	1	0	0	4	6	11	10	9	8	7	0	56
1971	1	0	1	3	7	3	15	11	15	9	4	1	70
1972	1	0	0	1	4	2	9	12	12	6	4	3	54
1973	0	0	0	0	0	5	12	8	8	7	5	1	46
1974	1	0	0	2	4	6	5	14	13	6	4	0	55
1975	2	0	0	0	2	3	6	11	9	8	6	0	47
1976	1	1	0	3	2	7	9	15	10	4	0	3	55
1977	0	0	1	0	3	4	8	4	13	9	4	1	47
Total	13	7	6	20	57	90	173	218	231	158	86	34	1093
Average	0.7	0.3	0.3	1.0	2.9	4.5	8.6	10.9	11.5	7.9	4.3	1.7	54.6

TABLE 3. FREQUENCY OF SOUTHERN HEMISPHERE TROPICAL CYCLONE GENESIS BY YEAR AND MONTH

Year	Oct.	Nov.	Dec.	Jan.	Feb.	Mar.	Apr.	May	Total
1958-59	1	1	3	5	7	6	2	0	25
1959-60	0	1	4	3	2	7	4	0	21
1960-61	0	1	1	9	7	4	0	0	22
1961-62	0	1	4	6	8	2	2	0	23
1962-63	1	0	4	6	9	5	2	3	30
1963-64	0	1	3	7	3	7	1	1	23
1964-65	0	2	5	4	5	3	0	0	19
1965-66	0	0	3	7	6	6	0	0	22
1966-67	0	1	3	5	1	3	2	1	16
1967-68	0	2	4	8	7	3	4	0	28
1968-69	1	1	3	7	8	2	1	0	23
1969-70	0	1	0	5	6	7	3	1	23
1970-71	1	3	6	4	7	4	1	0	26
1971-72	0	1	6	3	10	3	2	2	27
1972-73	1	3	4	10	6	7	3	1	35
1973-74	1	3	5	7	4	6	2	0	28
1974-75	0	0	2	6	2	5	4	0	19
1975-76	0	4	4	8	5	4	3	1	29
1976-77	1	0	4	8	9	5	3	0	30
1977-78	0	3	4	3	4	4	2	0	20
Total	7	29	72	121	117	93	41	10	489
Average	0.4	1.5	3.6	6.1	5.9	4.7	2.1	0.5	24.5

TABLE 4. YEARLY VARIATION OF TROPICAL CYCLONES BY OCEAN BASIN

Year	SH.	NW Atl.	NE Pac.	NW Pac.	N Indian	S Indian	Aust.	S Pac.	Total
1958	1958-59	12	13	22	5	11	11	7	81
1959	1959-60	11	13	18	6	6	13	2	69
1960	1960-61	6	10	28	4	6	8	8	70
1961	1961-62	11	12	29	6	12	7	4	81
1962	1962-63	6	9	30	5	8	17	3	78
1963	1963-64	9	9	25	6	9	7	7	72
1964	1964-65	13	6	39	7	6	9	4	84
1965	1965-66	5	11	34	6	12	7	4	79
1966	1966-67	11	13	31	9	5	5	6	80
1967	1967-68	8	14	35	6	11	9	8	91
1968	1968-69	7	20	27	7	8	7	8	84
1969	1969-70	14	10	19	6	10	7	6	72
1970	1970-71	8	18	23	7	11	12	3	82
1971	1971-72	14	16	34	6	7	14	6	97
1972	1972-73	4	14	28	6	13	12	10	88
1973	1973-74	7	12	21	6	4	16	8	74
1974	1974-75	8	17	23	7	6	10	3	74
1975	1975-76	8	16	17	6	8	16	5	76
1976	1976-77	8	18	24	5	9	12	9	85
1977	1977-78	6	17	19	5	6	7	7	67
Total		176	268	526	121	168	206	118	1583
Average		8.8	13.4	26.3	6.4	8.4	10.3	5.9	79.1

Figures 6 and 7 show the location of cyclone initial occurrence by latitude. Note that only about 13% of cyclones form poleward of 20° latitude and nearly all these occur in the northern hemisphere. Large land-sea monsoonal influences do not occur in the southern hemisphere and the poleward penetration of the equatorial trough is much more restricted than in the northern hemisphere. About two thirds of all cyclones occur in the northern hemisphere. Similarly, about two thirds of all tropical cyclones form in the eastern as opposed to the western hemisphere.

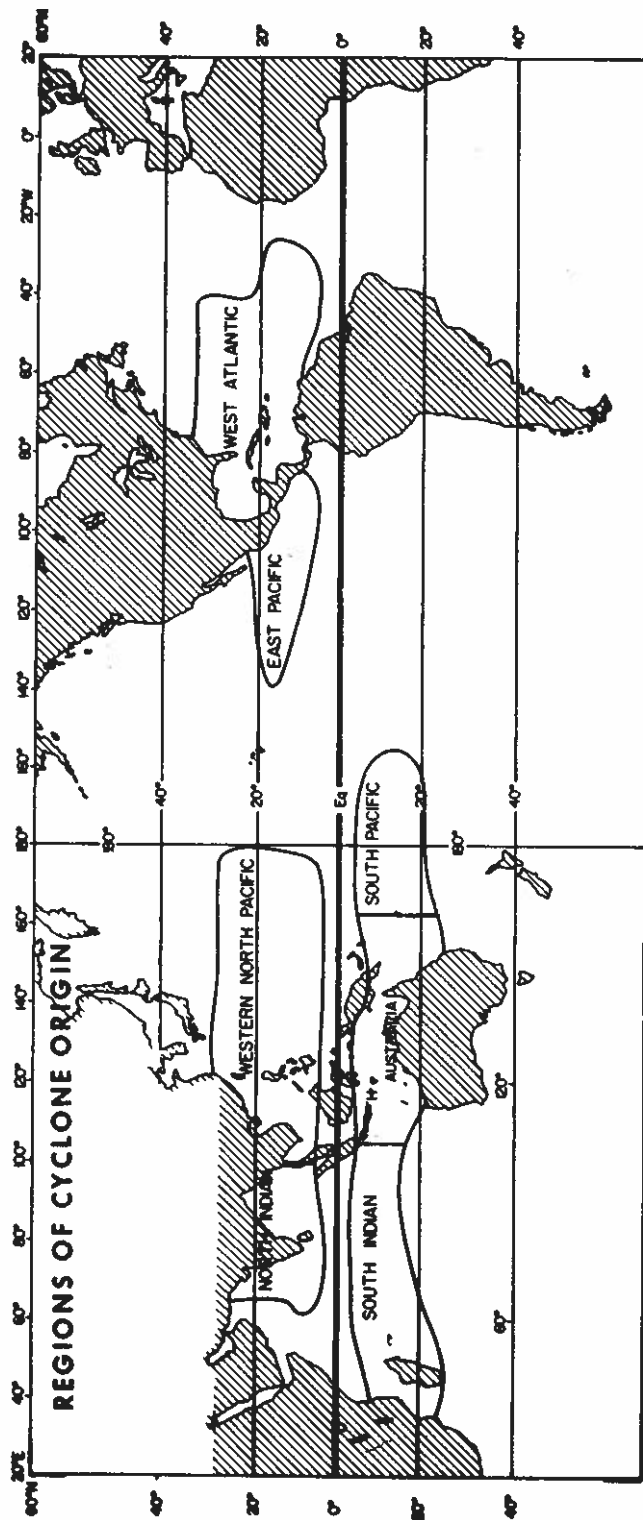


Figure 5.

total

- 31
- 59
- 70
- 31
- 78
- 72
- 34
- 79
- 30
- 31
- 34
- 72
- 32
- 37
- 38
- 74
- 74
- 76
- 35
- 57

33
79-1

hat
the
ern
ted
ern
sed

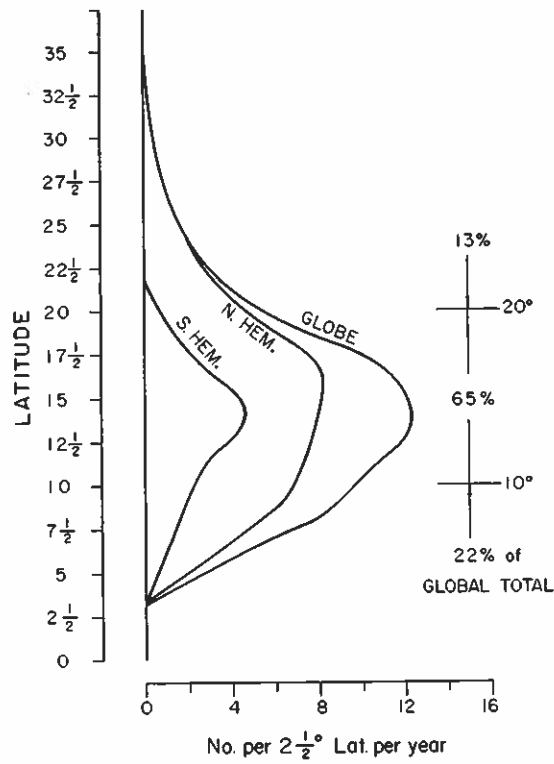


Figure 6. Latitude at which initial disturbances which later became tropical storms were first detected.

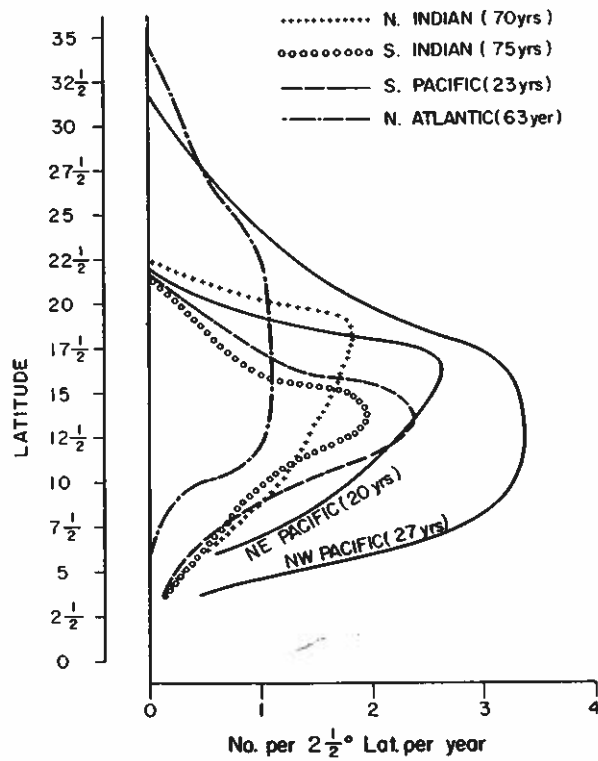


Figure 7. Latitude at which initial disturbances which later became tropical storms were first detected for the various development regions. Number of years in data average in parenthesis.

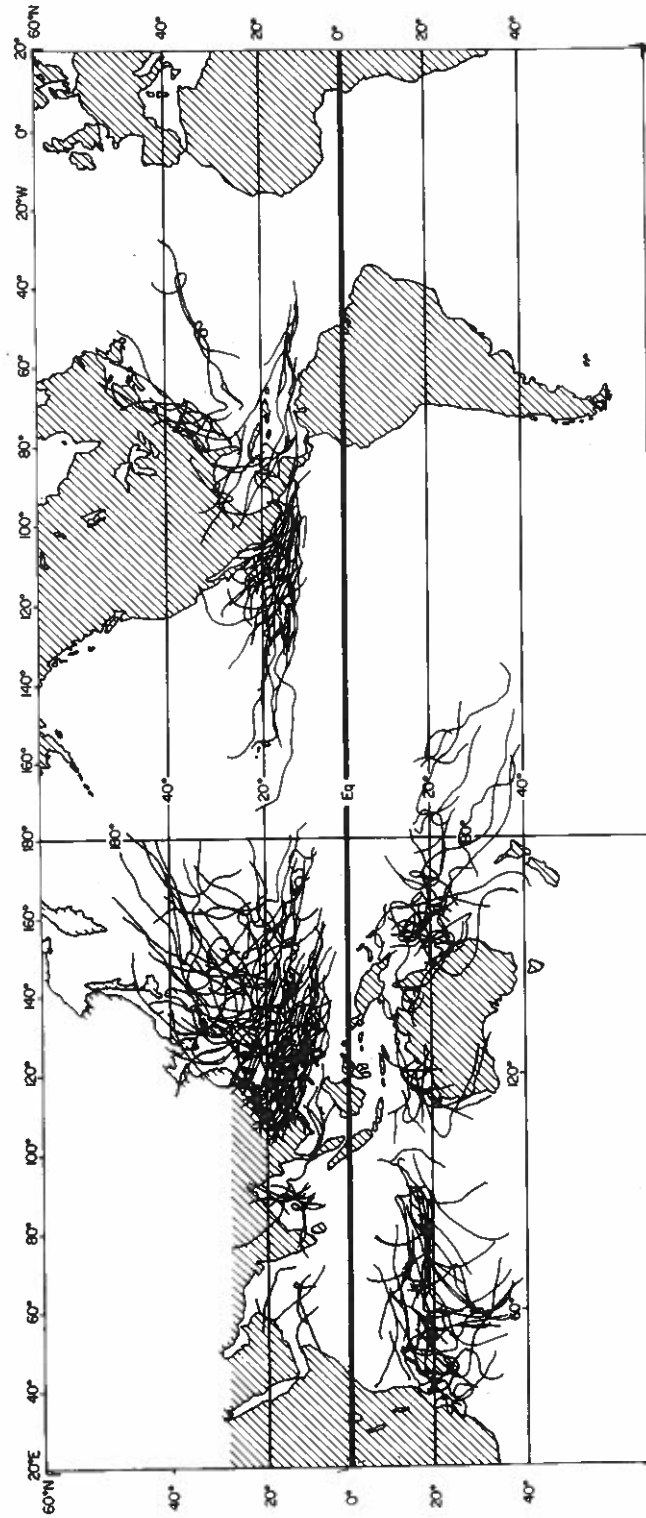


Figure 8. The tracks of tropical cyclones for a 3-year period.

d.

for

Figure 8 shows the tracks of tropical cyclones for a 3-year period. Note the wide variation of tracks. Also note that:

(1) Cyclones do not form within $4\text{--}5^\circ$ of the equator. Genesis is especially favoured in the latitude belts $5\text{--}15^\circ$. Genesis does not occur poleward of 22° latitude in the southern hemisphere. In the northern hemisphere genesis occurs at latitudes as high as $\sim 35\text{--}36^\circ$.

(2) Regions centred around 90°E , 140°E and 105°W are especially favoured for genesis.

(3) Although the majority of tropical cyclones form in the summer, genesis is possible in all seasons in the western North Pacific. This region has nearly one third of all tropical cyclones.

(4) There are two seasons of cyclone formation in the north Indian Ocean between $5\text{--}15^\circ$ latitude: a minor period in the spring associated with the onset of the southwest monsoon, and a major period in the autumn associated with its retreat.

(5) The southeast Pacific and the South Atlantic are devoid of cyclones.

(6) Cyclone genesis is especially favoured near the seasonal location of the ITCZ (Sadler 1967a; Gray 1968).

More statistical information will be portrayed in a forthcoming report of Gray and Frank (1979).

(a) *Clustering of cyclones in time*

Cyclones tend to cluster in time and space. One often observes 5–15 cyclones about the globe within 1–2 weeks, separated by 2–3-week periods when there is very little cyclone activity. This clustering in time for northern and southern hemisphere cyclones of the last 20 years is shown in Figs. 9 and 10. The active periods produce 2–6 times the number of cyclones that would otherwise be expected for that date. Similar time clustering of weaker tropical systems such as cloud clusters is much less evident. Cloud cluster systems exist most of the time and can occur in large-scale environmental situations not conducive to cyclone genesis. It appears that cyclones are a result of the larger-scale general circulation changes in the tropical atmosphere which occur on time scales of about 10 to 20 days. Unfavourable genesis situations can exist in some locations for weeks or months. These active genesis periods make up a quarter or a third of the hurricane–typhoon season yet they account for about two thirds to three quarters of the cyclones which form.

As previously discussed (Gray 1968), about 80–85% of tropical cyclones originate in or just on the poleward side of the inter-tropical convergence zone (ITCZ) or doldrum trough. Most of the remainder ($\sim 15\%$) form in the trade winds at a considerable distance from the ITCZ but usually in association with an upper tropospheric trough to their northwest (Sadler 1967a, 1967b, 1974).

There is another smaller class of subtropical or semi-tropical cyclones. These are anomalous warm core systems. They comprise about 3–5% of the global total of tropical cyclones. They form in subtropical latitudes in baroclinic regions within stagnant frontal zones or to the east of westerly upper troughs. Typically, they produce low intensity storms. The following discussion will not treat this mixed type of tropical–middle latitude cyclone. These subtropical formations are most prevalent in the northwest Atlantic and the northwest Pacific.

4. CLIMATOLOGICAL CONSIDERATIONS

The author (Gray 1968) has previously discussed the important roles which strong low-level relative vorticity and small vertical shear of the horizontal wind play in determin-

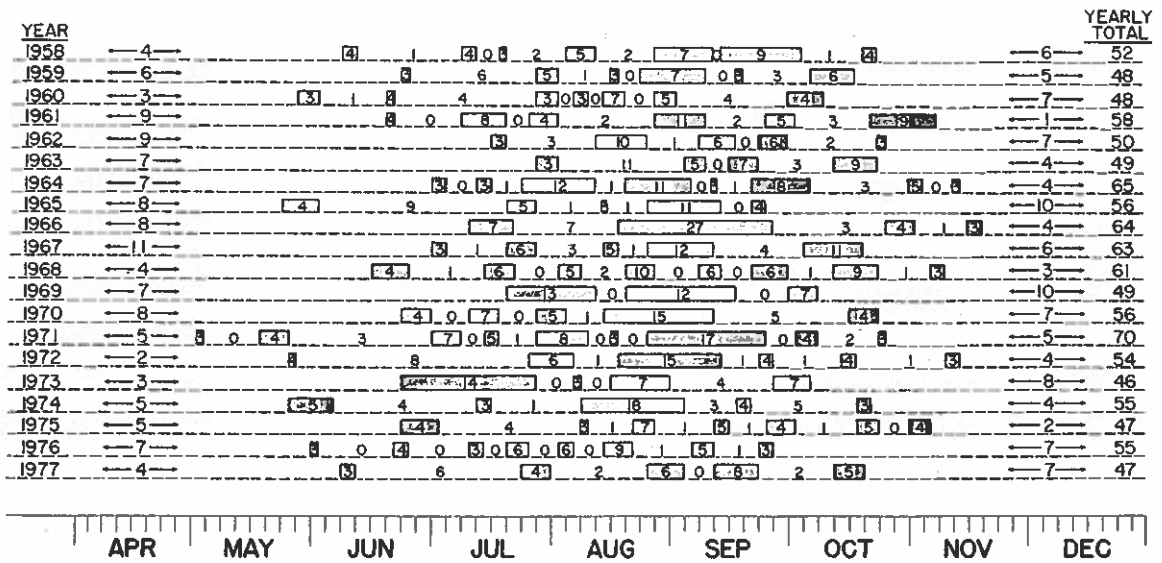


Figure 9. Time and space clustering of northern hemisphere cyclone genesis. Numbers in shaded areas give the numbers of tropical cyclone formations during active genesis periods. Numbers of formations during inactive periods are also shown in areas without shading. Numbers between arrows indicate the numbers of cyclone formations before and after the active genesis periods.

ing regions of high tropical cyclone genesis frequency. Genesis also requires other favourable conditions. A number of authors have discussed the very important role which sea surface temperature and ocean thermal energy play in tropical cyclone existence. The importance of thermal buoyancy from the surface to middle levels for Cb convection has been discussed by Palmén (1948, 1957) and a number of other researchers. Other authors have noted the lack of tropical cyclone development near the equator and have hypothesized the importance of the earth's rotation in the genesis process. The present author has observed a high frequency of cyclone genesis in regions where seasonal values of middle-level humidity are high.

It appears that seasonal tropical cyclone frequency can be directly related on a clima-

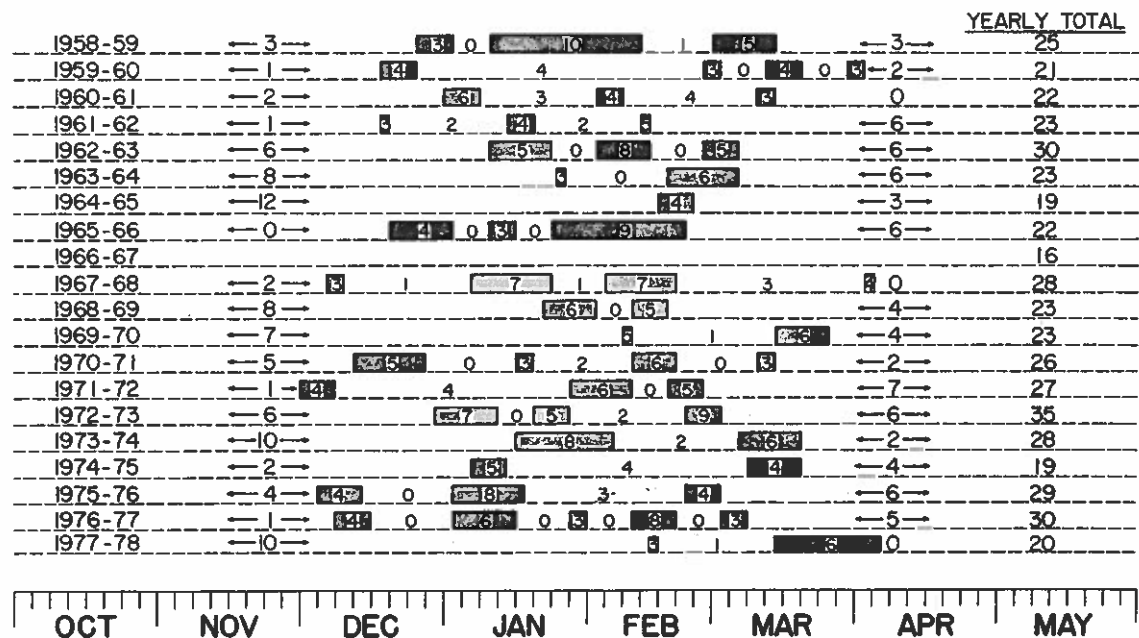


Figure 10. As Fig. 9 except for the southern hemisphere.

tological or seasonal basis to a combination of six physical parameters which will henceforth be referred to as primary climatological genesis parameters. These parameters are:

- (1) low-level relative vorticity (ζ_r),
- (2) Coriolis parameter (f),
- (3) the inverse of the vertical shear, S_z , of the horizontal wind between the lower and upper troposphere ($1/S_z$),
- (4) 'ocean thermal energy' – sea temperature excess above 26°C to a depth of 60 m (E),
- (5) vertical gradient of θ_e between the surface and 500 mb ($\partial\theta_e/\partial p$),
- (6) middle troposphere relative humidity (\overline{RH}).

(a) *Role of low-level relative vorticity*

Deep, surface to 400 mb, convergence exists with all classes of tropical disturbance (reference discussion below, or reports of Williams and Gray 1973; Ruprecht and Gray 1976a; Zehr 1976; McBride 1977). This inflow produces cyclonic spin-up in proportion to the existing environmental vorticity field. It is observed that tropical cyclones form only in regions of positive low-level vorticity (Gray 1968). The larger this low-level vorticity, the greater the potential for cyclone genesis. Other conditions being favourable and remaining constant seasonal cyclone genesis frequency should be directly related to the magnitude of the seasonal lower tropospheric relative vorticity.

(b) *Role of earth's rotation*

Cyclones do not form within 4–5° of the equator. The influence of the earth's rotation would thus appear to be of primary importance. A number of previous researchers have stressed this relationship. Note in Fig. 6 that cyclone genesis frequency increases almost linearly from 3° to 15° latitude. Except for places where strong meridional flow and import of momentum from higher latitudes is occurring, winds on the equator are very weak. Geostrophic considerations dictate that pressure gradients near the equator be very weak. Frictional dissipation is, however, independent of latitude. Wind acceleration is related to the magnitude of the pressure gradient and is thus latitude dependent. Disturbance intensification cannot occur if frictional dissipation is greater than generation. Other conditions being favourable and remaining constant, tropical cyclone genesis frequency should be directly related to the strength of the Coriolis parameter.

(c) *Role of tropospheric vertical wind shear and ventilation*

As previously discussed (Gray 1968, 1975), observational evidence clearly shows that tropical cyclones form under conditions of minimum vertical shear of horizontal wind between lower and upper troposphere. As shown in Fig. 11 the individual level zonal wind, u , may be quite different than the cluster or disturbance velocity, u_d . The magnitude of $u - u_d$ determines the extent to which the cluster is ventilated. If the cloud cluster ventilation is small, as in the third diagram from the left of Fig. 11, enthalpy and moisture increase can occur. This will lead to gradual surface pressure decrease and cyclone formation. If, however, tropospheric flow at any level, relative to the motion of the incipient disturbance, is large, as in the other three profiles of Fig. 11, then mass ventilation through the disturbance is too rapid to permit concentration and accumulation of enthalpy and moisture. Pressure falls will not occur. Other conditions being favourable and remaining constant, cyclone genesis frequency should be inversely related to the magnitude of seasonal values of tropospheric ventilation.

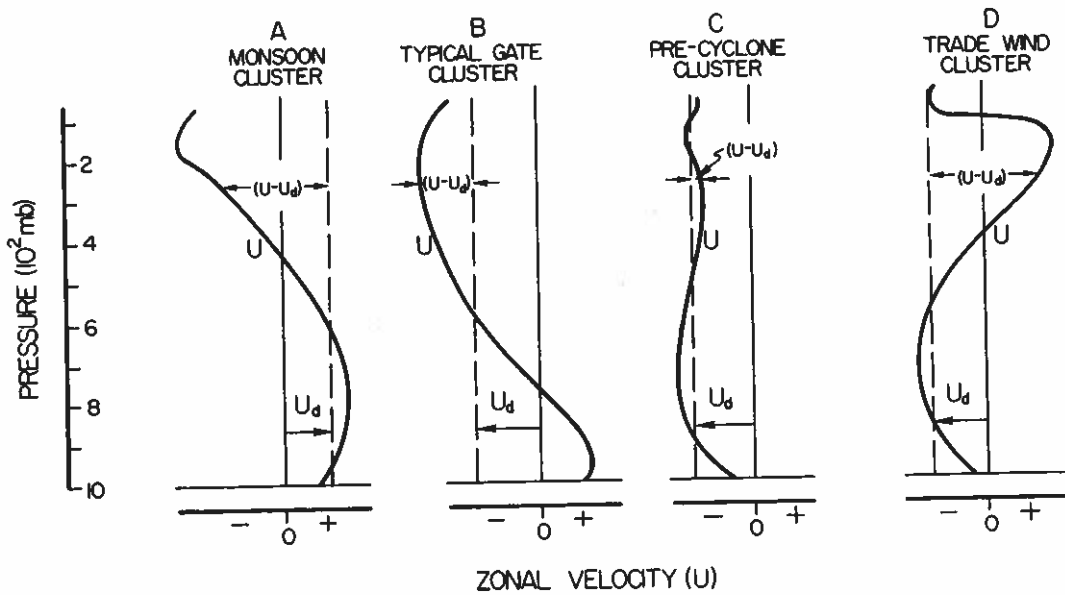
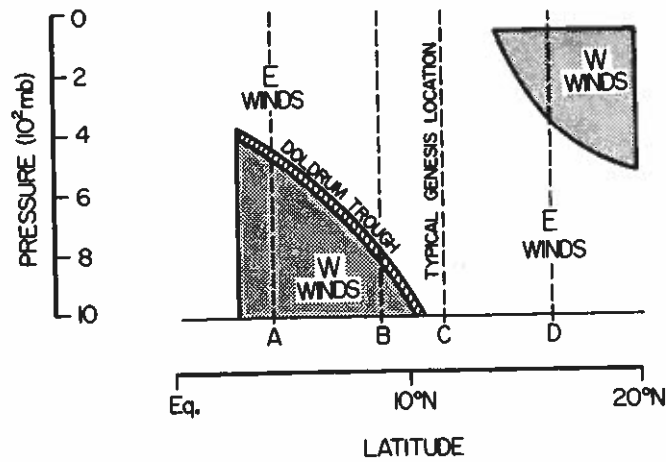


Figure 11. North-south cross-sections of the typical locations of various classes of tropical cloud clusters relative to the doldrum equatorial trough, and the usual zonal winds present with these systems (top diagram). The bottom diagram portrays the vertical distribution of typical zonal wind velocity, u , occurring with different, A to D, types of cloud cluster whose general location is specified in the top diagram. The usual zonal cluster velocity is designated u_d and the difference in cloud cluster and environmental wind velocity at any level is given by $u - u_d$.

(d) Role of ocean thermal energy

As previously discussed by Jordan (1964), Landis and Leipper (1968), Leipper (1967), Leipper and Jensen (1971), Leipper and Volgenau (1972), Heffernan (1972) and Perlroth (1967, 1969), tropical cyclones can have a profound influence on the temperature of the ocean over which they travel. The altered ocean temperature, in turn, can feed back and alter the character of the cyclone.

Leipper and his research group have indicated that the inner region (0-240 km) of the average hurricane consumes about $168 \times 10^6 \text{ J m}^{-2} \text{ d}^{-1}$ ($4000 \text{ cal cm}^{-2} \text{ d}^{-1}$) of ocean sensible and latent heat energy. In their study of the hurricane boundary layer Malkus and Riehl (1960) put the consumption at $130 \times 10^6 \text{ J m}^{-2} \text{ d}^{-1}$ ($3100 \text{ cal cm}^{-2} \text{ d}^{-1}$). Whitaker's (1967) calculations for hurricane Betsy indicate a value of about $154 \times 10^6 \text{ J m}^{-2} \text{ d}^{-1}$ ($3700 \text{ cal cm}^{-2} \text{ d}^{-1}$). Although these estimates are probably too high (as will be discussed later), they do indicate that the ocean energy source is quite important for tropical cyclone

maintenance. More recently W. Frank (1977b) has estimated from composited rawinsonde data that the magnitude of the sea to air flux of sensible plus latent heat in the average typhoon is about $62 \times 10^6 \text{ J m}^{-2} \text{ d}^{-1}$ ($1470 \text{ cal cm}^{-2} \text{ d}^{-1}$) in the inner 80 km. This large surface energy requirement of the hurricane precludes its existence over land or over the ocean if these transfers should somehow be suppressed. Brand (1971) has discussed how typhoons can weaken when they cross the track of a previous typhoon which has produced a lower sea surface temperature due to upwelling.

Both Leipper and Perlroth have indicated that the influence of hurricanes on the ocean underneath them can extend down to about 60 m. Given the well-established criterion of surface air temperature being above 26°C , then, following Leipper and Jensen (1971) and Leipper and Volgenau (1972), an ocean thermal energy potential, E , in units of cal cm^{-2} , can be defined to be the ocean thermal energy above 26°C down to a depth of 60 m, or

$$E = \int \rho_w c_w (T - 26) dz \quad (2)$$

where the integral is from the surface to 60 m, or to where $T = 26^\circ\text{C}$. ρ_w is ocean density, c_w the specific heat of water, and T the ocean temperature in $^\circ\text{C}$.

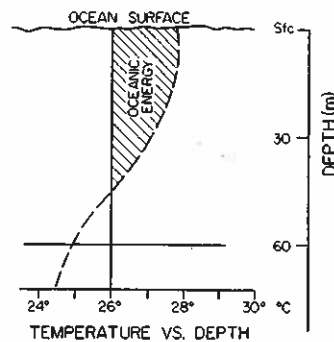


Figure 12. Cross-section view of the typical ocean temperature decrease with depth and how the ocean thermal energy, E , is defined (hatched) following Leipper and Volgenau (1972) as the area to the right of the 26°C isotherm to a depth of 60 m.

This energy is portrayed in Fig. 12. Other conditions being favourable and remaining constant, seasonal tropical cyclone genesis frequency should be directly related to the magnitude of E .

(e) Role of surface to middle troposphere θ_e gradient

Cyclones do not occur unless there is a well-established vertical coupling of the lower and upper tropospheric flow patterns. Cumulonimbus convection acts as the primary mechanism for this vertical coupling. Cb convection is typically associated with a substantial (10 K or more) decrease of θ_e between the boundary layer and the middle troposphere. For convenience, and following the author's previous paper (Gray 1968), θ_e gradients are taken between the surface and 500 mb; they typically range between 15 and 20 K. Except in subtropical latitudes in winter, values of this parameter are usually adequate for cyclone development. Daily parameter deviations are small and typically not well related to cyclone genesis potential. This parameter mainly helps to distinguish between summer and winter genesis.

Other conditions being favourable and remaining constant, seasonal cyclone genesis should be directly related to the seasonal averaged moist buoyancy potential or the seasonal magnitude of the boundary layer to middle troposphere difference of θ_e .

(f) Role of middle troposphere humidity

It is observed that tropical cyclones form only in regions where seasonally averaged values of middle-level humidity are high. Other factors being equal, an environment of high middle-level humidity is more conducive to deep cumulus convection and greater vertical coupling of the troposphere because entrainment of moist air into updraughts inhibits their growth less than entrainment of dry air. High middle-level humidity is also conducive to high cloud-precipitation efficiency.

It must be remembered that in cyclone genesis situations the oceanic boundary layer does not experience a diurnal surface warming cycle, as over land, and that tropospheric vertical wind shears are small. These conditions preclude the intense buoyant updraught and downdraught activity that is possible where large afternoon surface heating cycles and strong tropospheric wind shears are present over middle latitude land areas. Although deep and intense Cb convection occurs over middle latitude land areas in conditions of low middle-level relative humidity, Cb convection does not typically occur over ocean regions when middle-level humidity is less than 50–60%. Over tropical oceans high middle-level vapour content appears to be a strong enhancer rather than an inhibitor of deep cumulus convection.

It will be assumed that cyclone genesis is directly related to the seasonal average of 500 and 700 mb relative humidities. Seasonal values of middle-level humidity are related to a humidity parameter which is defined and is assumed to be associated with cyclone genesis: the parameter varies from 0 to 1; cyclone development is assumed not to be possible if the seasonal 500–700 mb humidity is less than 40%; the parameter then increases linearly to 1 for seasonal 700–500 mb humidity equal to or greater than 70% (i.e. humidity parameter = $(\overline{RH} - 40)/30$). Other conditions being favourable and remaining constant, seasonal tropical cyclone genesis frequency should be directly related to seasonal values of middle tropospheric humidity.

(g) Specification of seasonal genesis frequency

It is hypothesized that tropical cyclone formation will be most frequent in the regions and in the seasons when the product of the six primary genesis parameters just discussed is a maximum.

There is some difficulty with using these seasonal values directly. Seasonal values are not always a close measure of what daily parameter values can be. Thus, the seasonal relative vorticity in the western Atlantic is slightly negative. The seasonally determined genesis potential would not predict cyclone genesis in a region where it obviously occurs. When the seasonal values of $|\partial V/\partial p|$ are small, unreasonably large values of $1/S_z$ are obtained, which are not representative of the average of the daily values. Similarly, the seasonal values of $\partial\theta_e/\partial p$ between the surface and 500 mb could be zero or negative, but individual period values can be positive.

To cover the range of possible daily deviations of three of these parameters, arbitrary units were added to the seasonal values to simulate the average of the possible daily deviations of these values. Five units of 10^{-6}s^{-1} vorticity were added to all the seasonally measured values of this parameter and 5 K was added to all the seasonal values of $\partial\theta_e/\partial p$. To prevent unreasonably large values of the genesis frequency when $|\partial V/\partial p|$ approaches zero, 3 m s^{-1} was arbitrarily added to all the seasonal vertical shear values. The minimum value of the vertical shear parameter is thus 3 units.

A 'seasonal genesis parameter', s.g.p., is now defined by

$$\text{s.g.p.} = (\text{vorticity parameter})(\text{Coriolis parameter})(\text{vertical shear parameter}) \times (\text{ocean energy parameter})(\text{moist stability parameter})(\text{humidity parameter}) \quad (3)$$

where

$$\begin{aligned} \text{vorticity parameter} &= (\zeta_r + 5), \text{ where } \zeta_r \text{ is in units of } 10^{-6} \text{ s}^{-1}; \\ \text{Coriolis parameter} &= f; \\ \text{vertical shear parameter} &= 1/(S_z + 3) \text{ where } S_z = |\partial V/\partial p|, \text{ is in units of } \text{ms}^{-1} \text{ per } 750 \text{ mb}; \\ \text{ocean energy parameter} &= E \text{ as defined in Eq. (2). } E \text{ is in units of } 10^{-5} \text{ cal cm}^{-2} \text{ (0.42 J m}^{-2}\text{)}; \\ \text{moist stability parameter} &= \partial\theta_e/\partial p + 5, \text{ where } \partial\theta_e/\partial p \text{ is in K (500 mb)}^{-1}; \\ \text{humidity parameter} &= (\overline{RH} - 40)/30 \text{ where } \overline{RH} \text{ is the mean relative humidity between 500 and 700 mb, but zero for } \overline{RH} \leq 40, \text{ and 1 for } \overline{RH} \geq 70. \end{aligned}$$

This seasonal genesis parameter may also be thought of in the form:

$$\text{s.g.p.} = (\text{dynamic potential}) \times (\text{thermal potential}) \quad (4)$$

where

$$\begin{aligned} \text{dynamic potential} &= (f)(\zeta_r + 5)\{1/(S_z + 3)\} \\ \text{thermal potential} &= (E)(\partial\theta_e/\partial p + 5)(\overline{RH} \text{ parameter}). \end{aligned}$$

Dynamic potential is in units of $10^{-11} \text{ s}^{-2} ((\text{ms}^{-1})/(750 \text{ mb}))$, and thermal potential in units of $10^{-5} \text{ cal cm}^{-2} \text{ K (500 mb)}^{-1}$. Thermal potential may also be thought of as the potential for Cb convection.

The product of dynamic potential and thermal potential is defined as the 'seasonal genesis parameter', with units of $1.5 \times 10^{-8} \text{ cal K s}^{-1} \text{ cm}^{-3}$. When expressed in these units, the s.g.p. gives just the right value required to specify seasonal cyclone genesis frequency in number per 5° latitude-longitude square per 20 years.

Figures 13 to 25 have been arranged to portray all parameters in sequence for the season July-September. Seasonal genesis is expressed in number per 5° latitude-longitude square per 20 years. Note how well the s.g.p. predicts genesis frequency. Favourable comparisons are also found for the other three seasons. Annual values are shown in Figs. 26 and 27. See Gray (1975) for data on the other seasons.

(h) Discussion

The very close correspondence between predicted and observed seasonal cyclone frequency lends support to earlier arguments concerning the relevant physical genesis parameters. It was not expected that the agreement between predicted and observed genesis frequencies would be this close.

It is seen how closely the seasonal climatology of each area dictates the number of cyclones which form there even though the days of cyclone genesis (1-15 per 5° square per 20 years) make up but a very small percentage of the season. If it is assumed that cyclone genesis requires a favourable daily genesis potential to exist for three consecutive days over a 5° latitude-longitude square (or for 1-day periods in three adjacent upstream and downstream 5° squares one day apart), then the number of genesis days even in the regions of most active formation is no more than $2\frac{1}{2}\%$ of the number of non-genesis days. It is doubtful that these cyclones have a very large influence on the seasonal climatology. Seasonal clima-

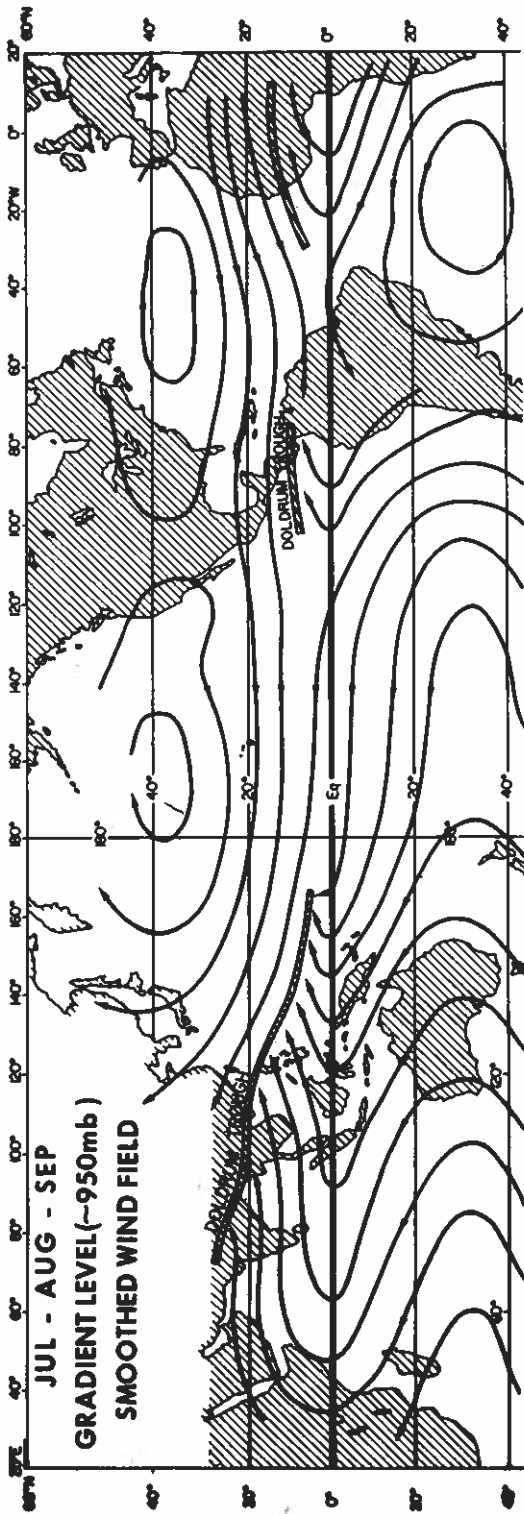


Figure 13.

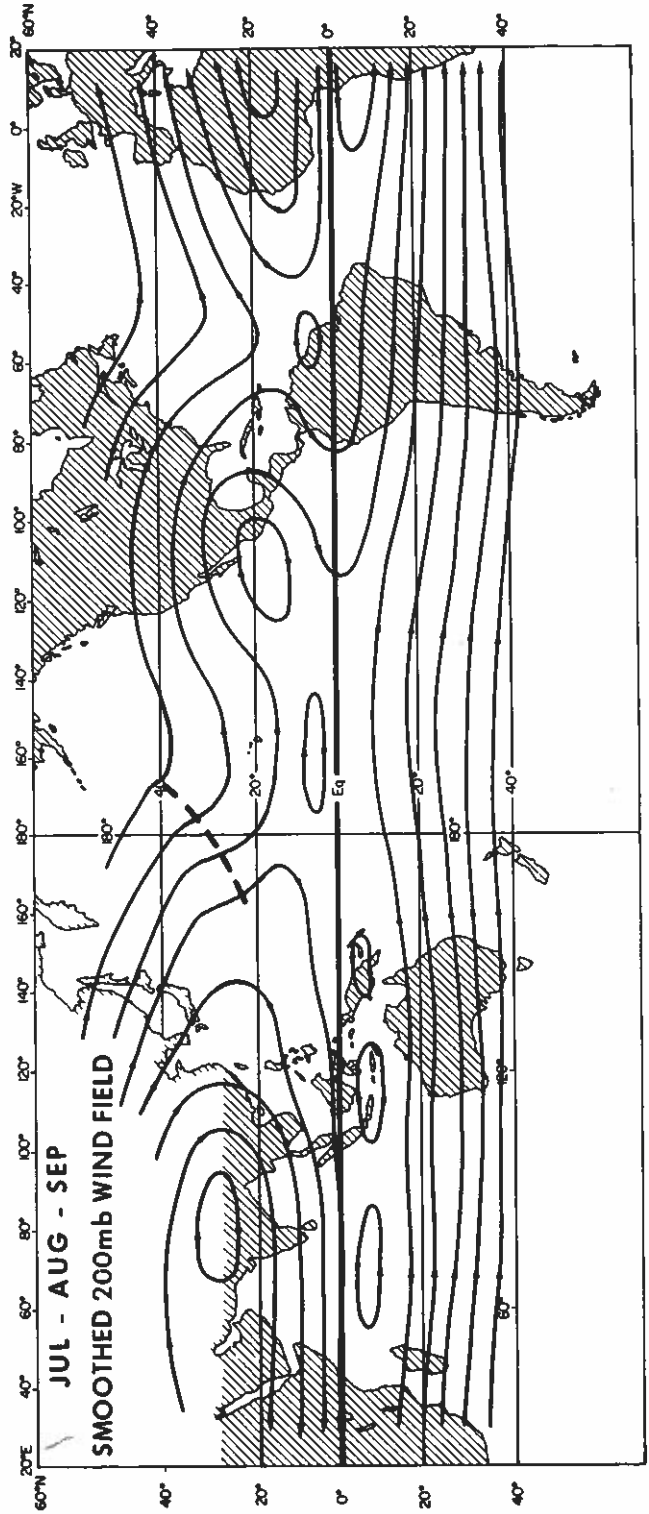


Figure 14.

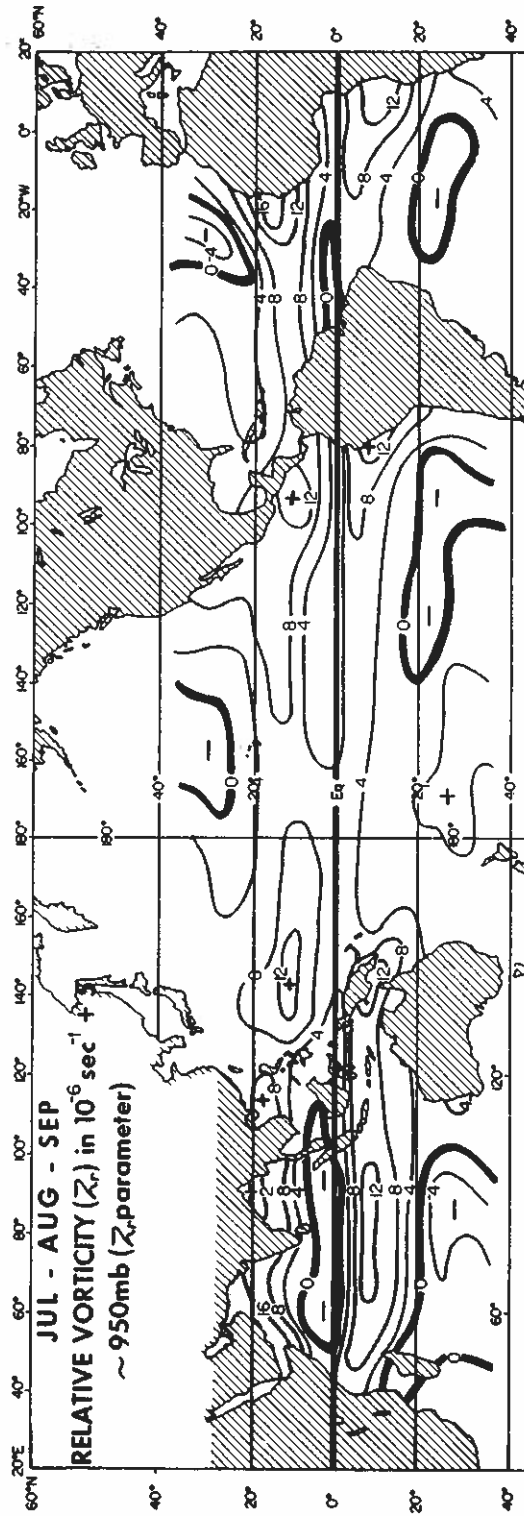


Figure 15.

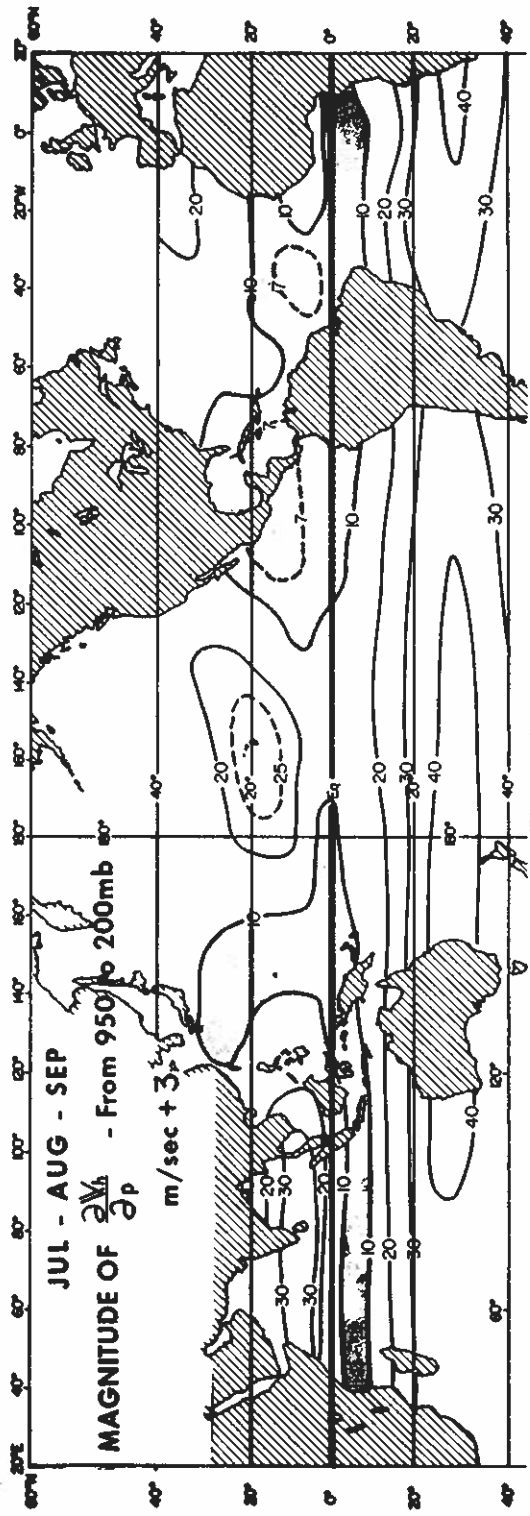


Figure 16.

Figure 16.

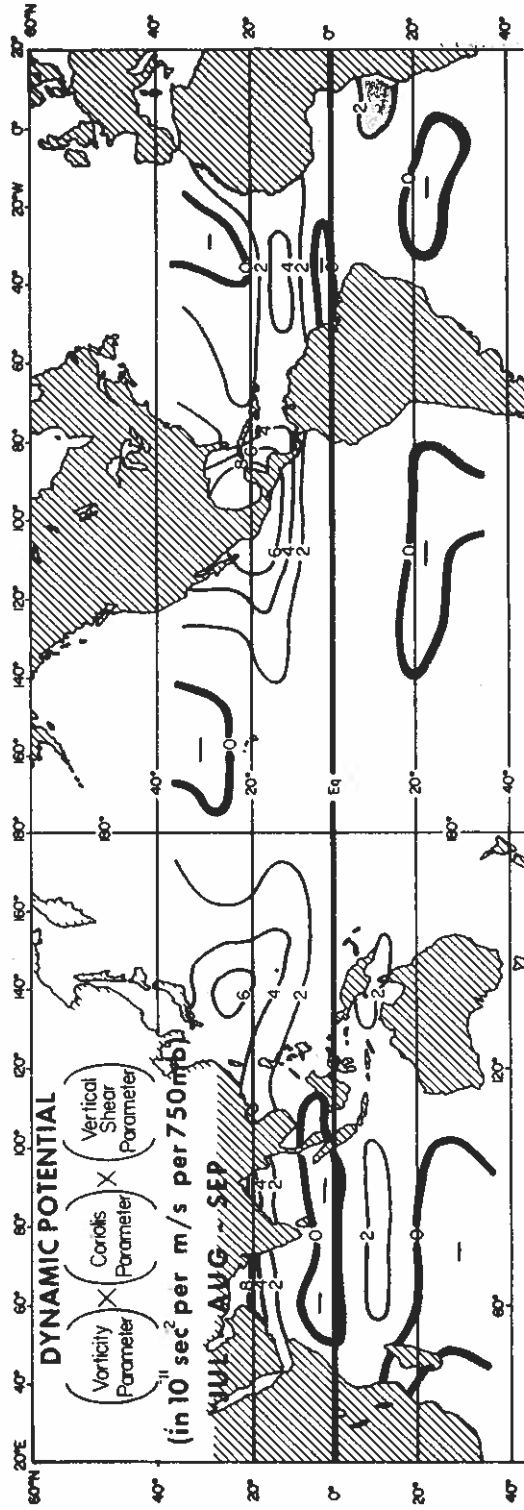


Figure 17.

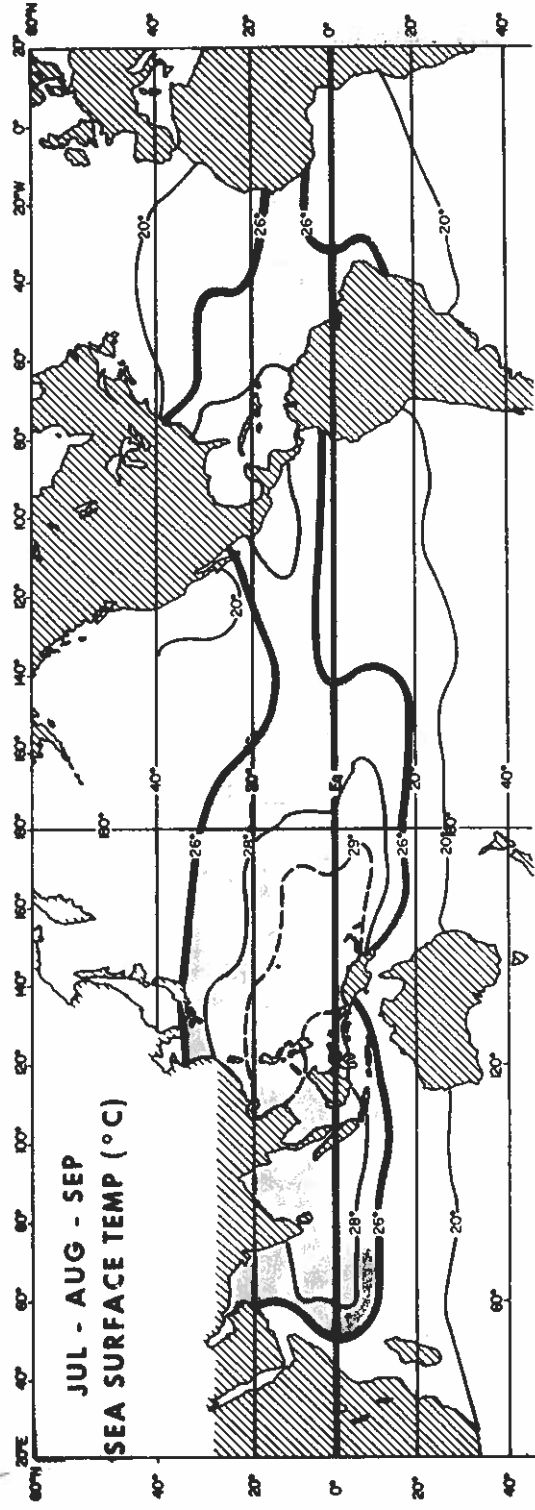


Figure 18.

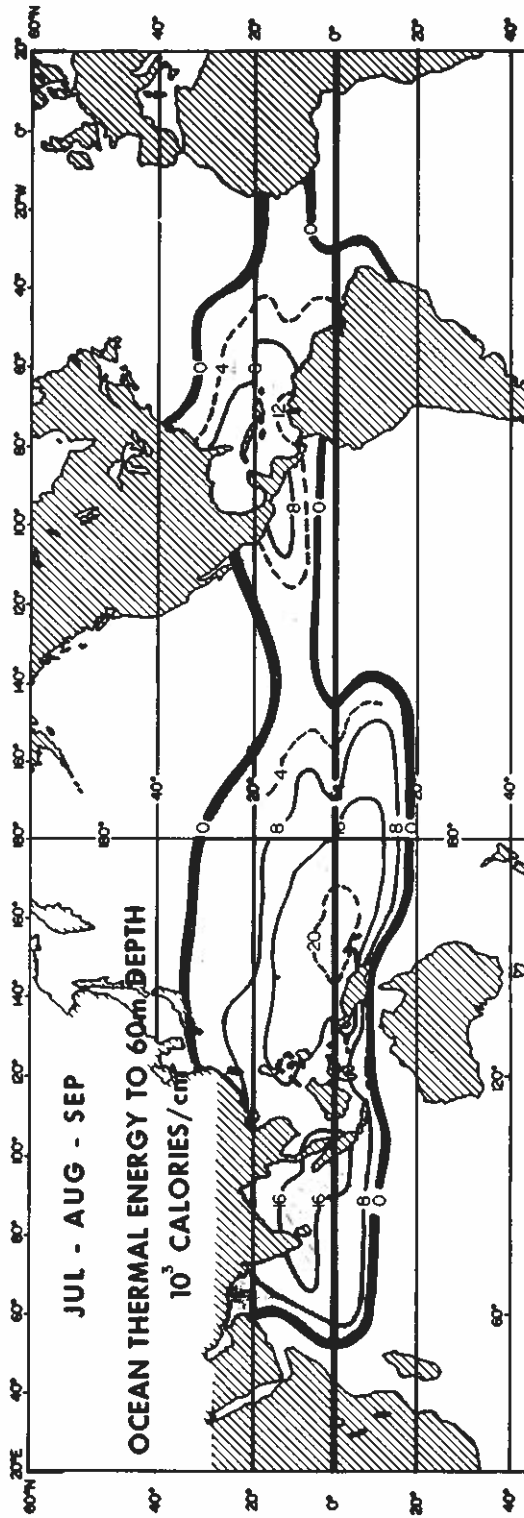


Figure 19.

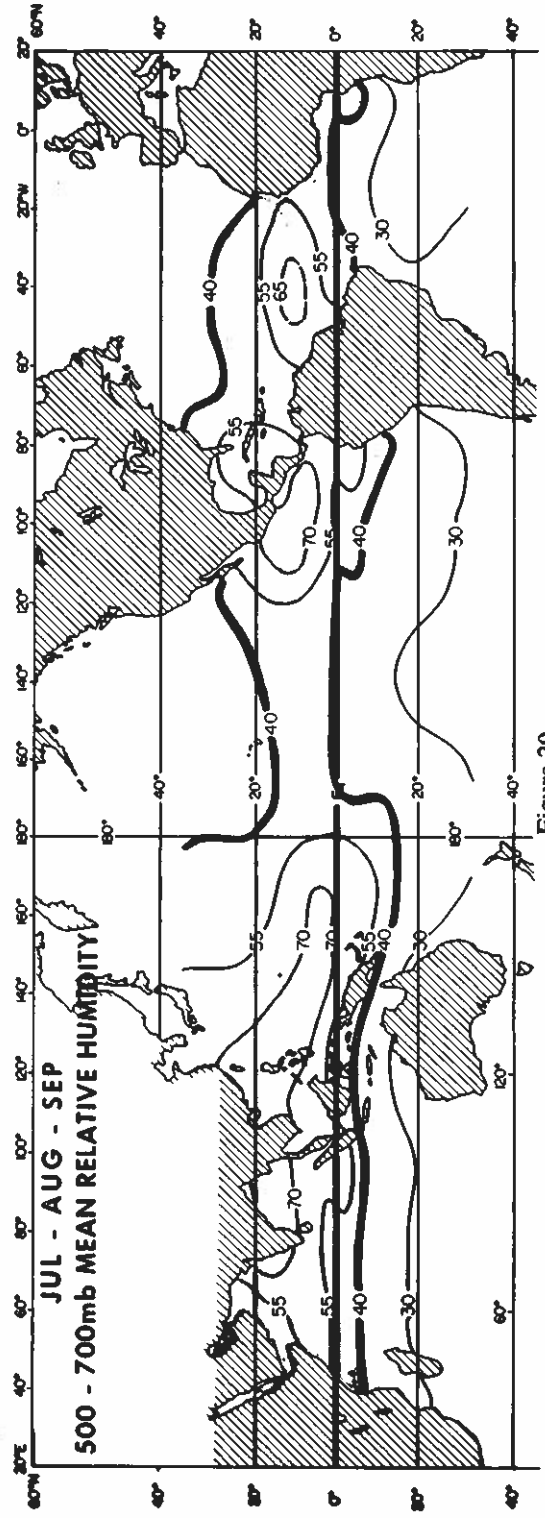


Figure 20.

Figure 20.

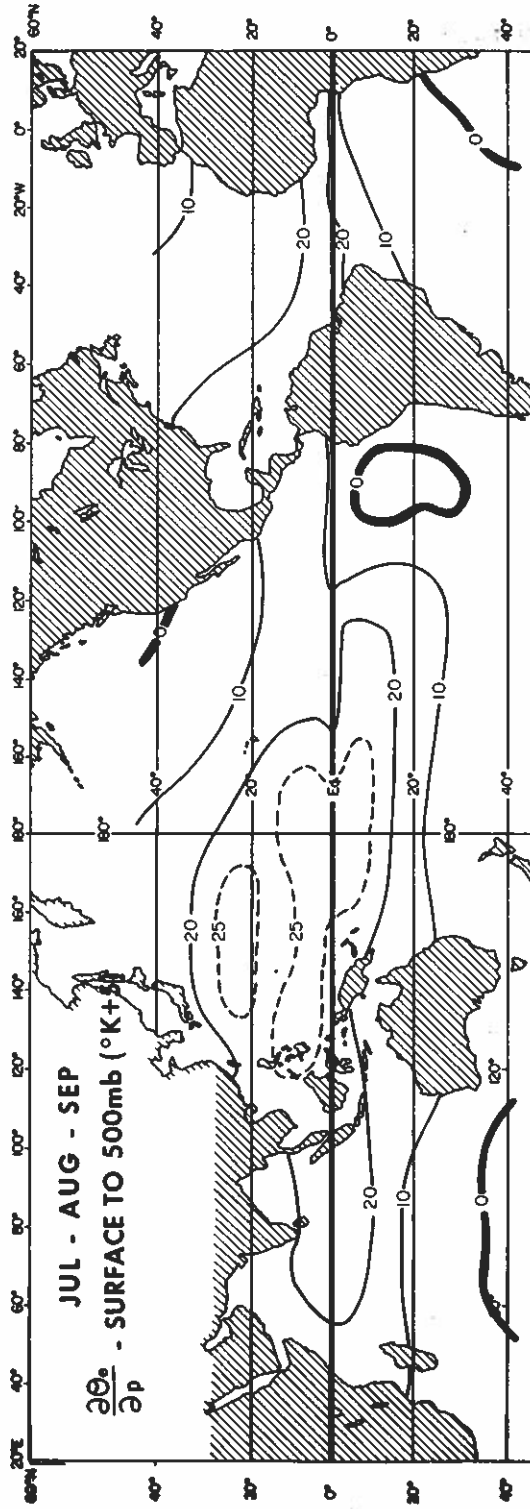


Figure 21.

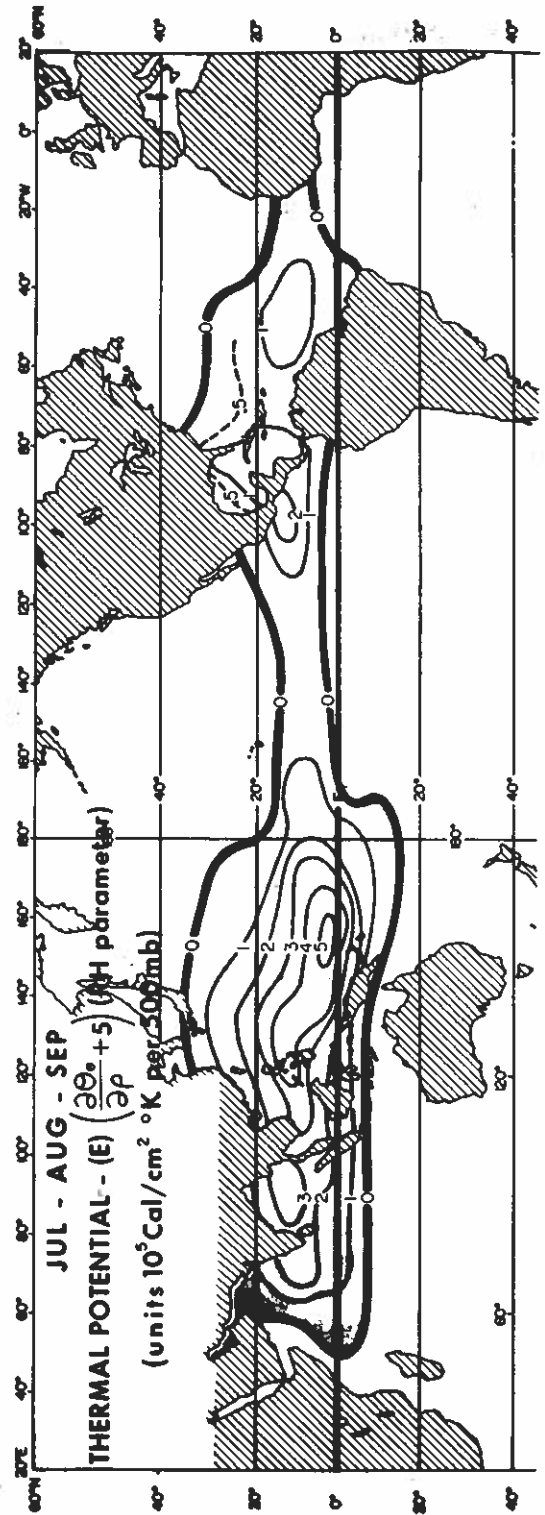


Figure 22.

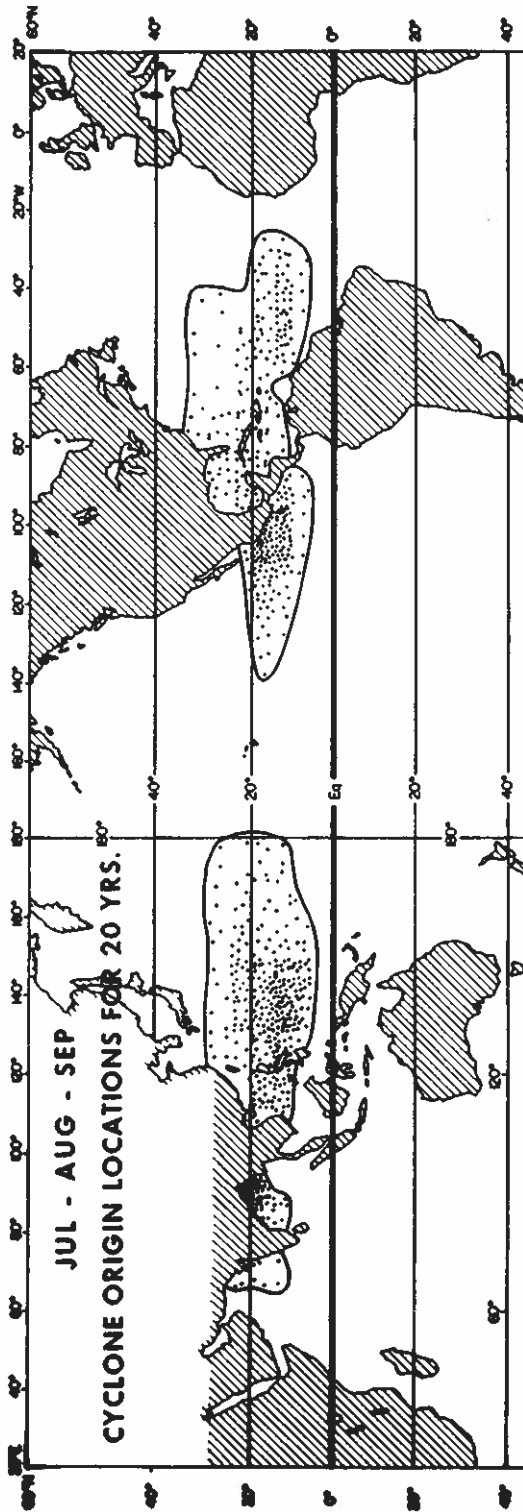


Figure 23.

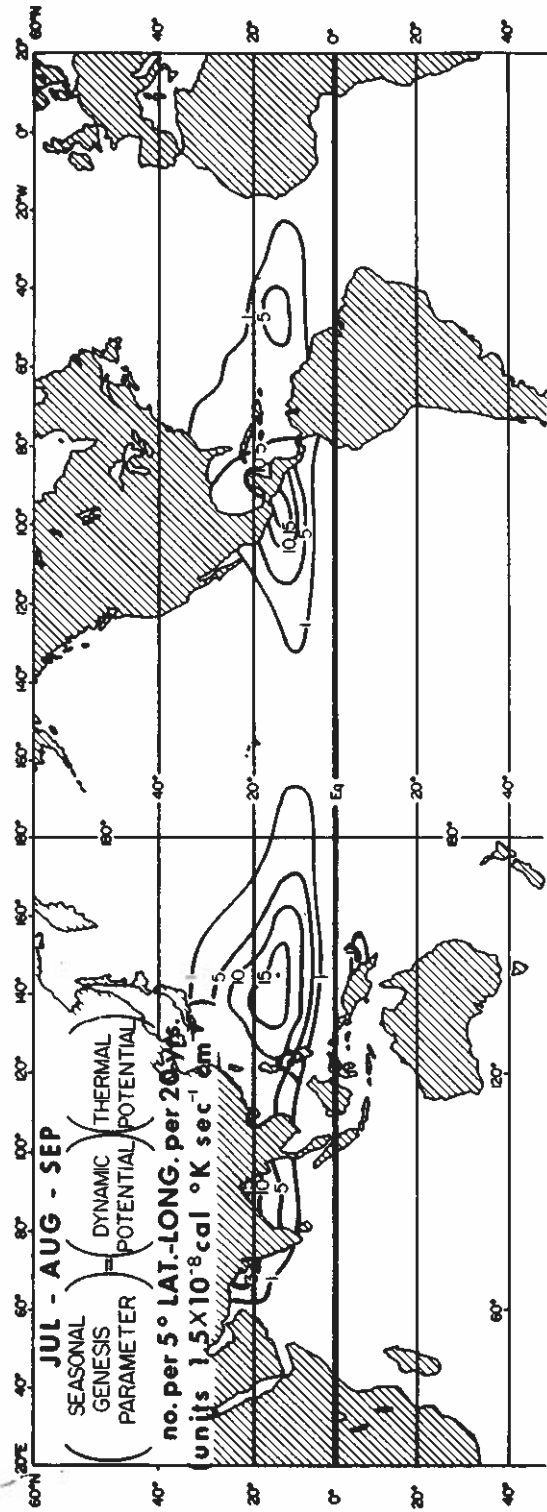


Figure 24.

Figure 24.

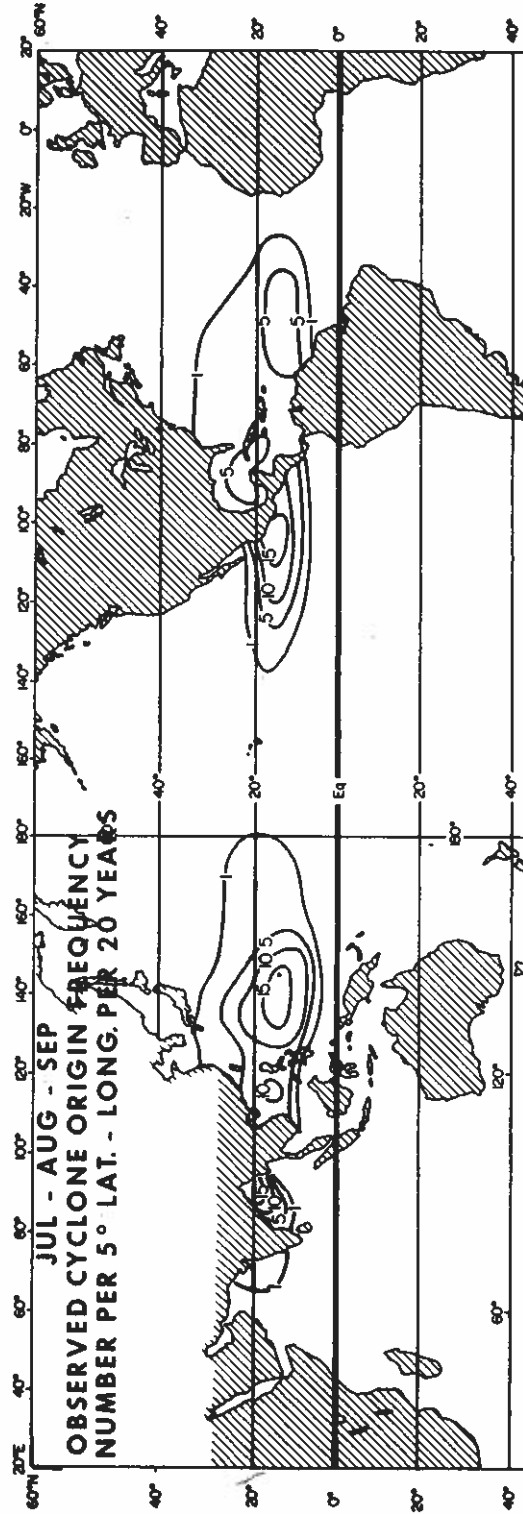


Figure 25.

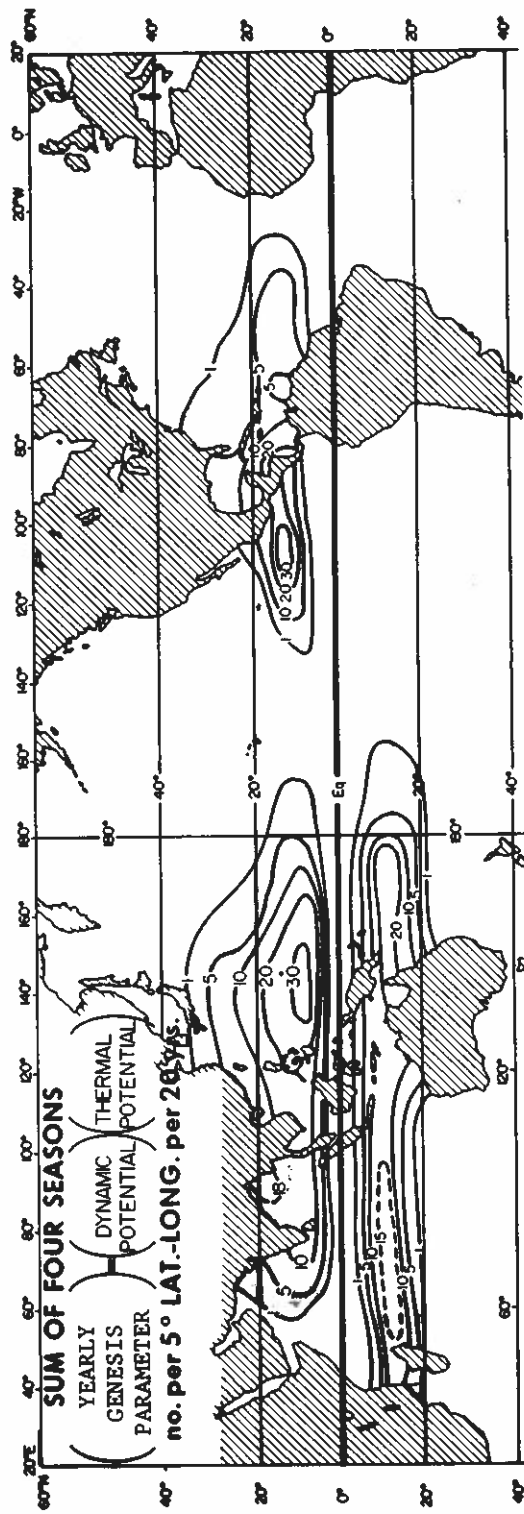


Figure 26.

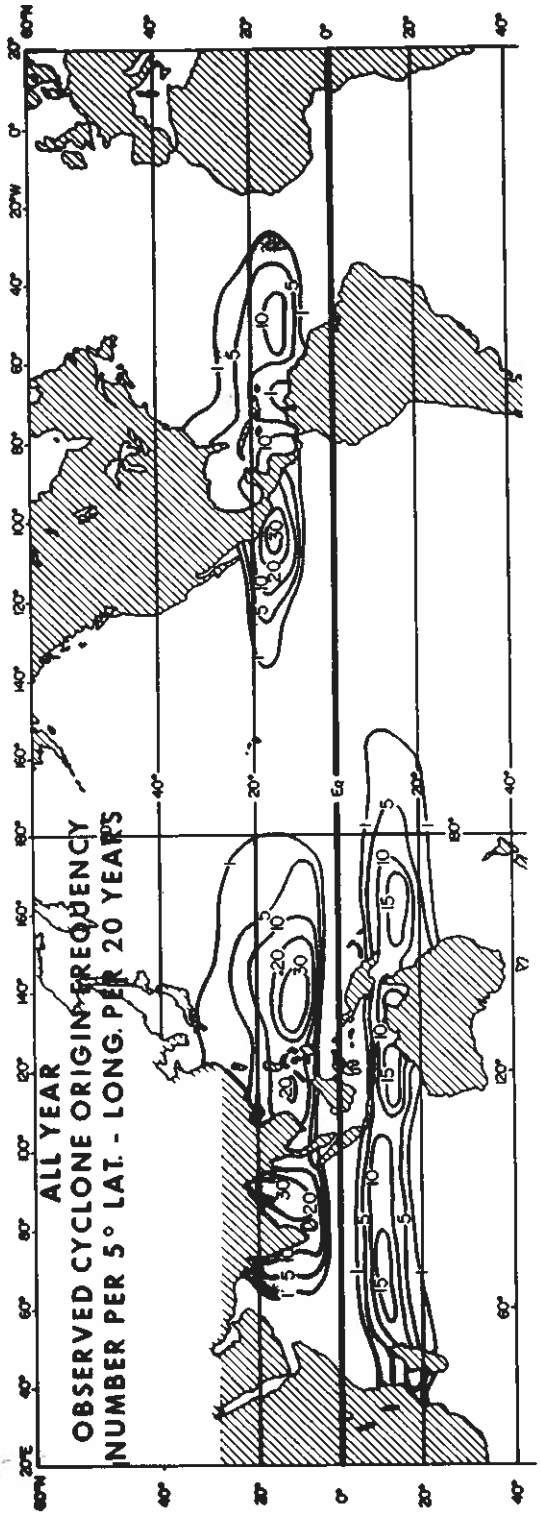


Figure 27.

tology parameters are, to a large extent, independent of the cyclones. The cyclones are, however, not independent of the climatology.

It is not just the correlation of the six seasonal parameters with genesis frequency which is noteworthy, but also the physical rationale concerning the effects of these parameters on genesis. It is possible that other climatological parameters can be found which are also related to cyclone frequency, but the author doubts whether these other parameters, if detected, can be as well related to the previously discussed physical requirements.

(i) *Relationship of seasonal to daily genesis potential*

Cyclone genesis requires a positive deviation of genesis potential from seasonal values. If one assumes that these short-term favourable deviations of genesis potential from the climatological potential are random and largely independent of location and season (which in a general sense they appear to be in tropical latitudes) then one can better understand why cyclone genesis frequency is related to the s.g.p. If one assumes that individual case genesis requires a genesis threshold potential of 30 units or more, and that short-period standard deviations from climatology are about 10 units, then one can see that the needed threshold values greater than 30 can occur on only a few days per season. Note how shifts in the s.g.p. from 1 to 5, 10 or 15 can increase the number of periods when the genesis potential is above 30 by a significant amount. Seasonal climatology thus plays a fundamental role in specifying the number of short periods in which the required genesis potential can be large enough to activate individual cyclone formation. It is seen that cyclone frequency, although occurring on only a very few days per season, is, nevertheless, directly related to the large-scale and long-term shifts in the tropical general circulation. Genesis does not occur in the tropical southeast Pacific and south Atlantic because the background seasonal climatology is so unfavourable. Although short-period positive deviations of genesis potential may be as large at these locations as elsewhere, they can never overcome their strongly unfavourable climatological background.

5. INDIVIDUAL DAY CYCLONE GENESIS

Since tropical cyclones form over tropical oceans where upper air observations are rare, definitive descriptions of the genesis characteristics of 'individual' tropical cyclones are grossly deficient. In order to do any quantitative analysis of cyclone formation processes one is obliged to composite, or average, many cases of genesis together. If the physical processes of genesis are basically similar for all cyclones (as the author believes, at present we have no physical or observational reasons for thinking otherwise), then some meaningful insight may be gained.

At locations and in seasons in which genesis regularly occurs, such as around Guam during the summer, the thermal potential (ocean depth of warm water, θ_e gradient in lower troposphere, middle-level humidity) is always positive and large. This parameter is not a significant factor in determining individual day genesis potential. Consideration must be given to dynamic factors. New individual case data sets of developing and non-developing disturbances have to be constructed to try to understand better the day by day factors which control cyclone genesis. To understand cyclone genesis one must explain not just the processes which bring about genesis, but also the conditions which, in the majority of cases, inhibit genesis. These new data sets have been extensively discussed in the reports of Zehr (1976), Erickson (1977), Arnold (1977) and McBride (1977).

(a) *Data sets*

(i) *Zehr (1976)*. Ten years (1961–1970) and 130 cases of western North Pacific cyclone genesis (designated data set 2) are treated. Over 600 rawinsonde reports are contained within 4° radius of the centres of these developing cases. A greater rawinsonde sample is available at larger radii. Positioning is by the Guam Annual Typhoon Reports best track analysis, combined since 1966 with satellite positions.

Two sets of non-developing disturbances are used for comparison. All these are equatorwards of 18°N . One sample is of 87 non-developing cloud cluster disturbances during the summers (June until September) of 1967 and 1968 (designated sample 00), with a regional restriction (Fig. 28). The other is a larger data sample of approximately 400 cases of non-developing cloud cluster disturbances through the years 1967–1968 including disturbance clusters over a broader area (designated sample 0). The non-developing cases were positioned by satellite. Non-developing data samples 00 and 0 have 391 and 1903 rawinsonde reports within 4° of their centres. Approximately twice as many rawinsonde reports are contained within $4\text{--}6^\circ$ radius of these systems.

(ii) *Erickson (1977)*. All cases are in the western Pacific within the latitude belt $3\text{--}19^\circ\text{N}$, longitude $125\text{--}178^\circ\text{W}$, during the years 1971–1975. This data sample contains 53 cases of developing disturbance clusters (designated early stage 1 or ES1) and 49 cases of prominent non-developing disturbance cluster systems. The non-developing systems (designated data set 00') were tracked with the direct readout military satellite pictures from Guam. All systems were tracked for at least one day. The average period of tracking was $2\frac{1}{2}$ to 3 days. The number of rawinsonde reports contained within 4° and 6° radius of the centre for each of these two classes of systems is about 200 and 400 respectively.

(iii) *McBride (1977)*. McBride has more extensively analysed Zehr's Pacific data samples 00 and 2 plus Zehr's Pacific intensifying cyclone data sample which treats early cyclone genesis up to the point where the cyclone has maximum sustained winds of 50 knots. He has also assembled five additional data sets for the western Atlantic – West Indies region which are further designated by 'D' for developing and 'N' for non-developing.

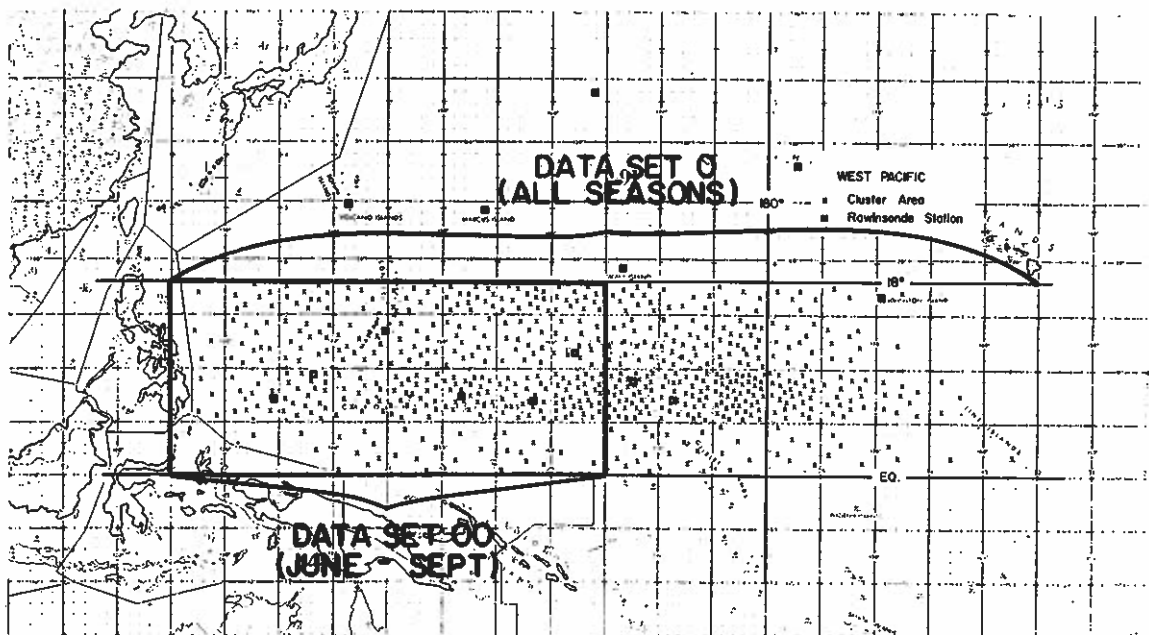


Figure 28. Crosses mark positions of the clusters included in the non-developing cluster data set, stage 0. Clusters were included which existed during all seasons. Non-developing cluster data set, stage 00, included clusters only in the enclosed region and only during the months of June until September.

These data sets include:

N4 – Atlantic depression: Western Atlantic depressions which do not develop into tropical storms. Positions are from the annual reports *Atlantic Tropical Systems* of 1967–76 by staff of the National Hurricane Center published in *Monthly Weather Review*. Mean latitude is $\sim 21^{\circ}\text{N}$; longitude 81°W ; $V_{\max} \sim 30$ kt.

D5 – Atlantic prehurricane depression: Positions for this data set and for data set D6 are from the official best tracks of the National Hurricane Center (NHC). Data set D5 consists of all 12-hourly positions (up to a maximum of six positions per storm) immediately preceding data set D6. It represents the depression before it begins significant intensification. Latitude is 21°N ; longitude 75°W ; $V_{\max} \sim 30$ kt.

D6 – Atlantic intensifying cyclone: This data set is made up of that portion of each storm's track such that:

- (1) $35 \text{ kt} < \text{estimated maximum sustained winds} \leq 70 \text{ kt}$;
- (2) the last position where $V_{\max} \leq 35 \text{ kt}$ is included in the data set; and
- (3) V_{\max} increases with every time period (12 hours) within the data set.

This data set is thus the portion of the track when the system is actually intensifying through the tropical storm stage. Mean latitude is $\sim 22^{\circ}\text{N}$; longitude $\sim 78^{\circ}\text{W}$; $V_{\max} \sim 40$ kt.

N7 – Atlantic cluster: In collaboration with V. Dvorak of NOAA/NESS Applications Group, positions were obtained from satellite pictures of tropical weather systems which subjectively looked to have potential for development into tropical storms. If a circulation centre for the disturbance was visible, it was taken as the position of the system; otherwise the centre of mass of the cloud area was used. The mean latitude is $\sim 20^{\circ}\text{N}$; longitude $\sim 82^{\circ}\text{W}$; $V_{\max} \sim 15$ kt or less.

N8 – Atlantic easterly wave: N. Frank, director of the NHC, has tracked the movement of Atlantic easterly waves since 1968. Using his tracks in the Caribbean for the years 1968–1974 a composite was made relative to the centres of these wave disturbances. Only wave systems which had a significant amount of cluster-type convection associated with them were composited. The centre of each system was defined such that the longitude was that of Frank's trough axis, and the latitude was the central latitude of convective activity as determined from geostationary satellite pictures. Mean latitude is $\sim 16^{\circ}\text{N}$; longitude $\sim 72^{\circ}\text{W}$; $V_{\max} \sim 15$ kt or less.

To retain the ability to make meaningful comparisons between systems which develop into storms and those which do not, no positions were included in non-developing data sets when the system centre was within 1° latitude of land within the following 24 hours.

The number of rawinsonde reports contained within each of these eight independent data sets is shown in Table 5 by radial belt.

TABLE 5. NUMBER OF RAWINSONDE OBSERVATIONS INCLUDED BETWEEN $1\text{--}3^{\circ}$, $3\text{--}5^{\circ}$ AND $5\text{--}7^{\circ}$ LATITUDE DISTANCE FROM THE CENTRE OF EACH COMPOSITE SYSTEM

	2°	4°	6°
00 Pacific cluster ($V_{\max} \sim 15$ kt)	142	224	283
0 Pacific pre-typhoon cluster ($V_{\max} \sim 25$ kt)	151	281	352
4 Pacific intensifying cyclone ($V_{\max} \sim 40$ kt)	135	272	358
N4 Atlantic depression ($V_{\max} \sim 30$ kt)	46	75	137
D5 Atlantic pre-hurricane depression ($V_{\max} \sim 30$ kt)	113	179	267
D6 Atlantic intensifying cyclone ($V_{\max} \sim 40$ kt)	111	227	299
N7 Atlantic cluster ($V_{\max} \sim 15$ kt)	170	393	548
N8 Atlantic easterly wave ($V_{\max} \sim 15$ kt)	186	344	447

(b) *Vertical motion and disturbance cloudiness as related to cyclone genesis potential*

Our research project has spent much effort in determining whether significant convective and vertical motion differences exist between tropical disturbances which develop into cyclones and those which do not. Our studies show, in general, that the primary distinguishing parameters of disturbance cyclone genesis potential are not well related to the magnitude of cumulus convection and vertical motion or to disturbance moisture and temperature differences. The primary feature distinguishing genesis appears to be lower and upper tropospheric vorticity values at large radii ($\sim 6^\circ$).

Figure 29 compares the average divergence within 4° radius of the centre of Zehr's developing west Pacific disturbances (data set 2) with those of his non-developing cluster systems (data sets 0 and 00). Note the small differences between the two classes of systems. Figures 30 and 31 are from Erickson's independent data sample. They show mean divergences of his early stage one (ES1) genesis disturbances compared with those of his prominent cluster non-developing systems (00'), for areas inside 4° and 6° radius. Note again the small differences in average divergence between these two classes of systems.

Using US Defense Military Satellite Program satellite (DMSP) data, Erickson investigated many other individual day cloud features of his two disturbance classes. In general, individual day disturbance movement, cloud amounts, and other cloud characteristics do not well differentiate developing and non-developing systems.

The primary cloud difference in these systems was the percentage of time that anti-cyclonic cirrus outflow was seen at outer radii on the poleward side of the developing systems. Cloud amount and areal extent were not significantly related to development potential.

Of equal importance in making the case against amount of convection as a distinguishing characteristic of genesis is the large case by case variability of deep penetrative convec-

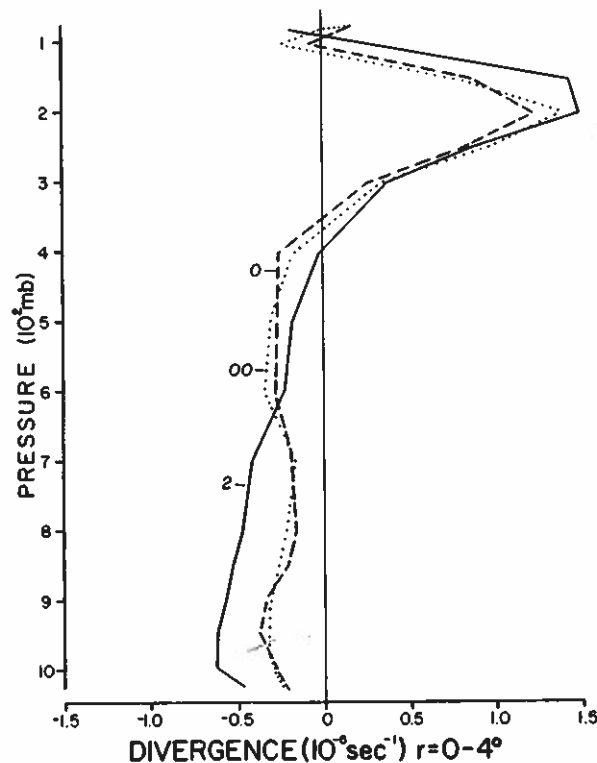


Figure 29. Mean divergence within the $r = 0-4^\circ$ area for the average pre-typhoon cloud cluster (2) and for two classes of non-developing cloud clusters (0) and (00) as reported by Zehr (1976).

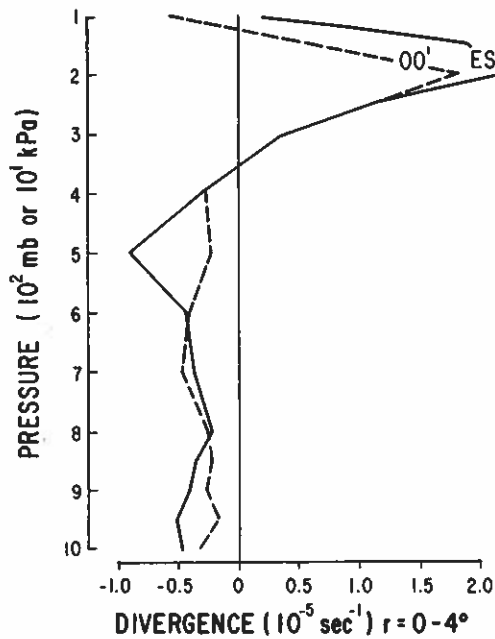


Figure 30. Mean divergence within the area $r = 0-4^\circ$ for the developing (ES1) and non-developing (OO') disturbances (from Erickson 1977).

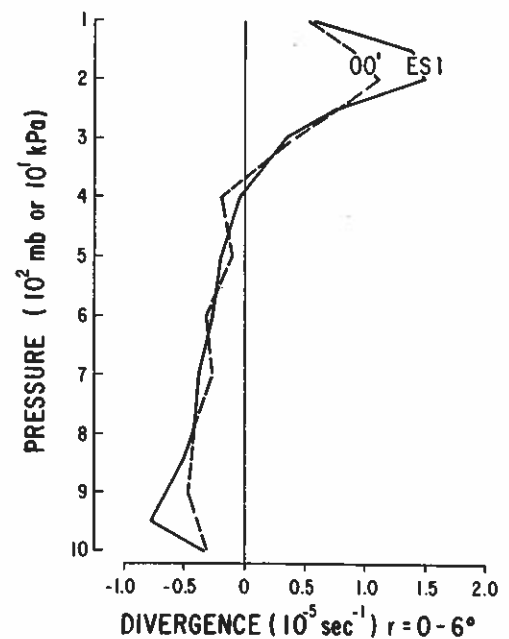


Figure 31. As Fig. 30 except for $r = 0-6^\circ$ (from Erickson 1977).

tion and of area of total cirrus cover. *Individual case variability of penetrative convection is very large for both classes of disturbances.* A similar variability also occurs in cirrus coverage. Developing systems often have smaller amounts of deep penetrative convection and/or area of cirrus shield than do non-developing systems. Some non-developing disturbance systems can have massive amounts of deep convection and cirrus. Thus, for both the average and for individual cases, the amount of deep convection and area of cloudiness are not good determining parameters of genesis potential. This is, of course, not surprising to satellite meteorologists such as V. Dvorak (1975). His skill at forecasting genesis from satellite cloud pictures is dependent primarily on cloud configuration and shape, not on cloud amount and intensity.

Our recent studies are showing that the primary factors differentiating the few tropical disturbances which become cyclones from the majority which do not are the relative vorticities at 900 and 200 mb averaged within 6° radius of the disturbance centre and the meridional gradient of 900 to 200 mb vertical wind shear across the disturbance, $(\partial/\partial y)(-\partial u/\partial p)$. The tropospheric vertical shear of zonal wind at the disturbance centre should be small and change sign. For genesis to occur shear should be positive to the poleward side and negative to the equatorward side of the disturbance, as seen in Fig. 32. It is important that the line of zero zonal vertical shear cross near the centre of the disturbance, as in this figure. This change in sign of zonal vertical shear applies very well for genesis in other regions. All our composite genesis cases fit this general pattern. McBride (1979) is also investigating individual cases of genesis and he finds that this general shear pattern (as the data can best be interpreted) is valid for the majority of individual genesis cases.

A contrasting example for a non-developing cluster disturbance is shown in Fig. 33. Although vertical shear is also not large near the centre of these non-developing cases, the N-S gradient of shear is much smaller than those of the developing cases.

The east to west gradient of 900 to 200 mb meridional vertical wind shear, $(\partial/\partial x)(\partial v/\partial p)$, can also contribute to genesis, but typically is smaller than the N-S shear gradient.

ant convec-
develop into
distinguish-
: magnitude
emperature
and upper

e of Zehr's
ping cluster
of systems.
mean diver-
f his promi-
te again the

son investi-
In general,
teristics do

e that anti-
developing
development

distinguish-
tive convec-

uster (2) and
76).

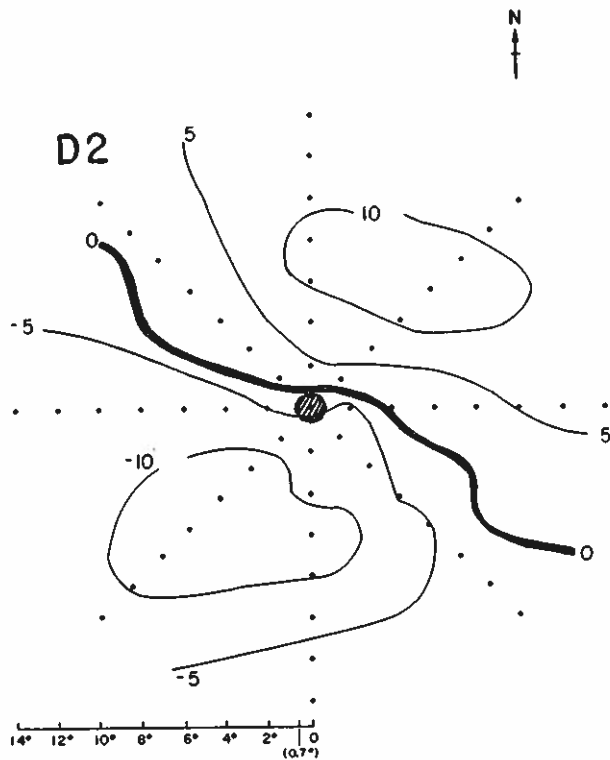


Figure 32. Plan view of zonal shear, $u_{200} - u_{900}$ (m s^{-1}), for the Pacific pre-typhoon cluster, D2.

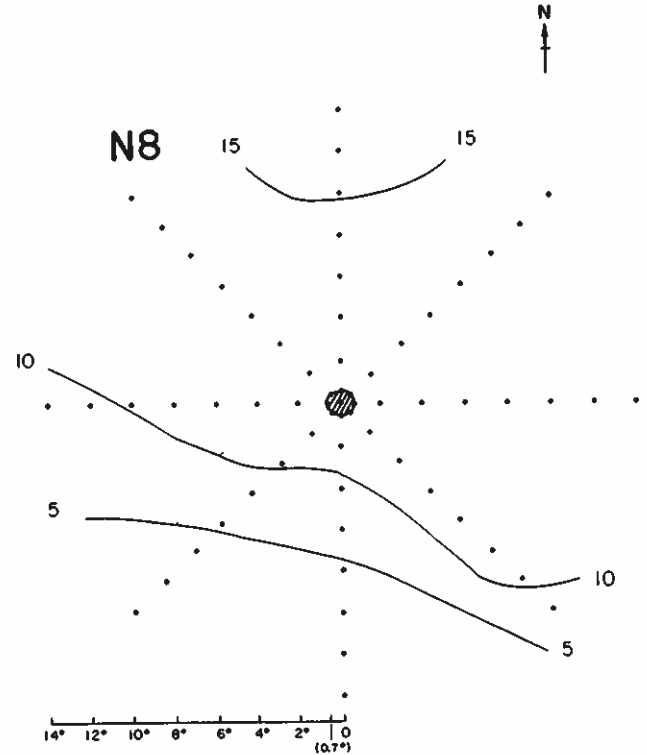


Figure 33. As Fig. 32 but for non-developing Atlantic easterly wave, N8.

These shear gradients may also be thought of in terms of differences in lower and upper tropospheric vorticity. Thus, genesis is favoured by the largest possible values of $(\partial/\partial y)(-\partial u/\partial p) + (\partial/\partial x)(\partial v/\partial p)$, or $(\partial/\partial p)(\partial v/\partial x - \partial u/\partial y)$, or $\partial \zeta_r / \partial p$, where ζ_r is the relative vorticity. The daily cyclone genesis potential (g.p.) for an individual disturbance may be estimated from the magnitude of $(\zeta_r)_{900} - (\zeta_r)_{200}$ averaged within an appropriate radius.

Erickson (1977) has calculated these upper and lower tropospheric vorticity differences by different radial bands for his developing (ES1) and non-developing (00') disturbances. Results are shown in Table 6. The best results are found for radial intervals between 0 and 6°. Differences are 3 to 1. Ratios for other parameter differences, moisture, temperature, wind speed, cloudiness, vertical motion, etc., are nowhere near this large.

TABLE 6. MEAN RELATIVE VORTICITY ($\bar{\zeta}_r$) DIFFERENCES BETWEEN 900 AND 200 mb FOR DEVELOPING (ES1) AND NON-DEVELOPING (00') DISTURBANCES (FROM ERICKSON 1977)

Radial area	$(\bar{\zeta}_r)_{900} - (\bar{\zeta}_r)_{200} (10^{-5} \text{s}^{-1})$	
	Developing (ES1)	Non-developing (00')
0-2°	5.9	3.4
0-4°	3.6	1.3
2-4°	2.8	0.6
0-6°	3.0	1.0
4-6°	2.5	0.8

McBride (1977) has also tested the vorticity differences for Zehr's three Pacific stratifications and for his five recently composited Atlantic developing and non-developing systems. Values of daily g.p. for developing systems (2, 4, D5, D6) are significantly larger (by about 3 to 1) than for non-developing systems (00, N4, N7, N8) (Table 7). As with the Erickson

TABLE 7. DAILY GENESIS POTENTIAL (g.p.). MEAN RELATIVE VORTICITY DIFFERENCES BETWEEN 900 AND 200 mb FOR EACH COMPOSITE DATA SET. DEVELOPING SYSTEMS ARE IN ITALICS (FROM McBRIDE 1977)

		$(\bar{\zeta}_r)_{900} - (\bar{\zeta}_r)_{200} (10^{-5} s^{-1})$		
		0-2°	0-4°	0-6°
00	Pacific cluster	2.0	1.6	0.7
2	Pacific pre-typhoon cluster	4.9	3.1	2.4
4	Pacific intensifying cyclone	8.6	4.7	3.0
N4	Atlantic depression	5.5	2.0	1.0
D5	Atlantic pre-hurricane depression	5.2	2.8	1.8
D6	Atlantic intensifying cyclone	9.8	4.2	2.8
N7	Atlantic cluster	-0.5	0.4	0.7
N8	Atlantic easterly wave	1.9	0.5	0.3

TABLE 8. DAILY GENESIS POTENTIAL (g.p.) - AVERAGE OF DEVELOPING AND NON-DEVELOPING DATA SETS ($10^{-5} s^{-1}$)

	0-2°	0-4°	0-6°
Average non-developing (N1, N4, N7, N8)	2.2	1.1	0.7
Average developing - weak systems (D2, D5)	5.1	3.0	2.1
Average developing - all systems (D2, D5, D6)	7.1	3.7	2.5

study, other parameter differences were much smaller. Comparing the developing and non-developing systems, one obtains daily g.p. ratios of three to one or more (see Table 8).

Vertical cross-sections of mean vorticity inside 6° radius for the two independent data samples of Zehr and Erickson are shown in Figs. 34 and 35. There can be no doubt but that significant vorticity differences exist in the two classes of surrounding disturbance wind fields. Note that these vorticity differences are concentrated in the lower and upper tropo-

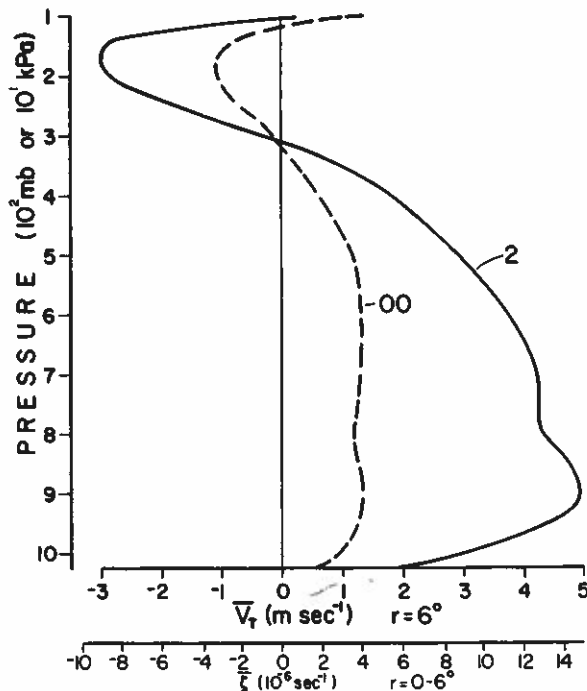


Figure 34. Mean relative vorticity within the area $r = 0-6^\circ$ (equivalent to mean tangential winds in $r = 5-7^\circ$ band) from Zehr's (1976) developing (stage 2) and non-developing (stage 00) disturbances.

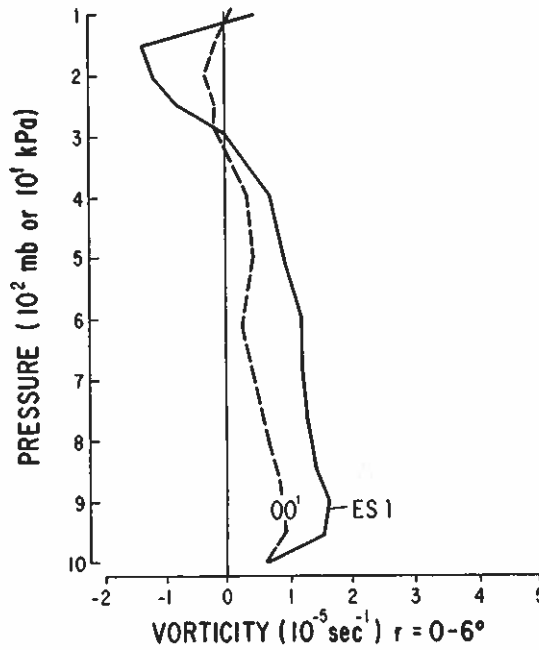


Figure 35. Mean relative vorticity within the area $r = 0-6^\circ$ for Erickson's (1977) developing (ES1) and non-developing (00') disturbances.

sphere. As the lower and upper troposphere are the primary analysis levels in the tropics and since the geostationary satellite will often be able to furnish winds at these levels, a quantitative evaluation of this daily genesis parameter can probably be made in many future potential genesis cases.

(c) Discussion

It appears that cyclone genesis is dependent not upon the magnitude of tropical disturbance convergence and rainfall but rather upon the strengths of the surrounding low-level cyclonic circulation and upper tropospheric anticyclonic circulation.

Genesis might be thought of from the point of view of conditions which lead to an increase of absolute angular momentum, m_a , within a cylindrical area of the disturbance region out to 6° radius. Thus,

$$\int (\partial m_a / \partial t) \delta M = - \int_{100\text{mb}}^{Sfc} \int_0^{2\pi} (m_a V_r / g) \delta \theta \delta p + \int r F_\theta \delta M \quad (5)$$

(1)	(2)	(3)
Mean rate of change of momentum within disturbance region	Import of angular momentum at the 6° radius boundary	Dissipation of angular momentum within the disturbance region

where $m_a = rV_\theta + \frac{1}{2}fr^2$,

$$\int \delta M = \int_{100\text{mb}}^{Sfc} \int_0^{2\pi} \int_0^{6^\circ} r \delta r \delta \theta (\delta p / g),$$

V_r, V_θ = radial and tangential winds, and F_θ = tangential friction.

Cyclone genesis requires positive values of term (1) {term (2) significantly larger than term (3)}. The observational data of Zehr (1976), Erickson (1977) and McBride (1977) allow us to calculate these terms at 6° radius for the various developing and non-developing disturbance data sets. Results indicate sizeable differences in the inward angular momentum

transport between these two classes of disturbances. Developing systems have much stronger inward transport of momentum. This subject is now being more extensively investigated by J. McBride. Kinetic energy and other budgets are also being made.

The large-scale positioning of the disturbance's surrounding lower and upper tropospheric flow patterns thus appear to be a crucial factor in the specification of cyclone genesis. Sadler (1967a,b, 1974, 1976a,b) has presented much evidence of the importance for genesis of the positioning of a surrounding upper tropospheric trough to the northwest of pre-cyclone disturbances. H. Riehl (1975)* has often noted that many cases of Gulf of Mexico cyclone formation are associated with the passage of an upper-level westerly wind trough to the north of an incipient disturbance. Riehl has consistently emphasized the importance for genesis of favourable subtropical or middle latitude upper tropospheric flow features. Yanai (1961)† has also emphasized the role of favourable large-scale surrounding flow features as a requirement of genesis.

The favourable positioning of surrounding wind fields is not well related to the amount of disturbance convection. This is consistent with the observation that heavily raining tropical disturbances often do not form cyclones while other less intense disturbance systems often do. Thus, it would appear that cyclone genesis can never be realistically modelled through schemes which deal only with differences in disturbance convection. It is necessary that the influences of the surrounding wind fields be understood and properly modelled.

6. DISCUSSION OF THE PHYSICAL PROCESSES OF GENESIS

To explain differences in cloud cluster genesis potential one must look for typically distinguishing features other than those of condensation energy release. The primary determinant for cluster growth appears to be the existence of environmental flow patterns which allow the accumulation of water vapour, enthalpy, and momentum spin up from converging air within a moderately strong large-scale vorticity field.

One of the primary determinants for cloud cluster growth to cyclone strength rests with the characteristics of the horizontal heat and moisture dispersion processes. Only rarely do the wind conditions relative to the moving cloud cluster act to inhibit horizontal dispersion of these quantities and thereby allow enthalpy and vapour accumulation within the moving system.

Disturbance blow-through, or ventilation, is defined (see Zehr 1976) as the non-divergent relative wind which blows through the disturbance. Composited rawinsonde data allow this feature to be measured. We have evaluated blow-through components for a large number of intensifying and non-intensifying tropical disturbances. We find significantly more blow-through in non-developing disturbances. The vorticity patterns implicit in the favourable vertical shear pattern of Fig. 32 possess minimum ventilation and allow energy accumulation within its centre much more readily than do the non-developing wind patterns. The character of the large-scale surrounding upper- and lower-level wind fields are thus crucial to cyclone genesis.

(a) Numerical modelling

Following the initial studies of Ooyama (1964), Charney and Eliassen (1964), Ogura (1964) and Kuo (1965), several numerical modellers have simulated the intensification process of moderately intense tropical cyclones which extend through the depth of the

* And personal communications 1957-1962.

† And personal communications 1962-1970.

troposphere. These modelling efforts have simulated cyclone intensification. They have not dealt with the question of cyclone genesis, however. Table 9 gives the observed low-level wind strengths of various classes of tropical disturbances as measured by our rawinsonde compositing studies. Note how weak the early stage disturbances are in comparison with the initial cyclone strength assumed by numerical modellers, as shown in Table 10. The transformation of a disturbance to a cyclone has yet to be realistically modelled.

Most cyclone intensification models have been based on the theory of conditional instability of the second kind (CISK) first formulated by Ooyama (1964) and Charney and Eliassen (1964). This theory appears to offer a satisfactory explanation for the later stage

TABLE 9. COMPARISON OF OBSERVED WESTERN PACIFIC DISTURBANCES WITH REGARD TO THEIR AVERAGE RADIUS OF MAXIMUM TANGENTIAL WIND, MAXIMUM TANGENTIAL WIND VELOCITY, AND RESULTING RELATIVE VORTICITY (FROM ZEHR 1976)

Weather system	Radius of maximum tangential wind about the disturbance (km)	Average 900 mb tangential wind about disturbance centre at radius of maximum wind (m s^{-1})	Mean relative vorticity inside the radius of maximum tangential wind (10^{-6}s^{-1})
Typical tropical disturbance (summer)	~400	1.6	8
Average tropical disturbance (all seasons)	~500	2.5	10
Pre-cyclone disturbance in early intensification stage	~400	5.3	26
Intensifying cyclone	~200	10.1	107
Mean assumed initial vortex of modellers*	172	12.2	142

* Based on the numerical models listed in Table 10 excluding Carrier (1971) model.

TABLE 10. RECENT NUMERICAL MODELLING PAPERS ON TROPICAL CYCLONE INTENSIFICATION AND THEIR ASSUMED INITIAL LOWER TROPOSPHERIC CYCLONE STRENGTH

Modellers	Assumed initial maximum wind velocity and radius of maximum wind (m s^{-1}) (km)	Vortex vorticity inside the radius of maximum winds (10^{-6}s^{-1})	Type of vortex
Kuo (1965)	10 141	142	Symmetrical
Yamasaki (1968)	4.7 100	94	Symmetrical
Ooyama (1969)	10 50	400	Symmetrical
Miller (1969)	10 200	100	Real vortex
Rosenthal (1970)	7 250	56	Symmetrical
Sundqvist (1970)	15 200	150	Symmetrical
Carrier (1971)	21 50	840	Symmetrical
Anthes <i>et al.</i> (1971a,b)	18 240	150	Asymmetrical
Anthes (1972)	18 240	150	Asymmetrical
Mathur (1972)	15 200	150	Asymmetrical
Harrison (1973)	~10 ~120*	~170	Asymmetrical
Kurihara and Tuleya (1974)	12 200	120	Symmetrical
Ceselski (1974)	17 ~100-150	~200	Real vortex
Kurihara (1975)	12 200	120	Symmetrical
Anthes (1977)	18 240	150	Symmetrical
Rosenthal (1978)	7.2 220	65	Symmetrical

Typical pre-cyclone cloud cluster vorticity is $\sim 10-15 \times 10^{-6}\text{s}^{-1}$.

* Estimated from initial height field.

and inner-core region intensification of already developed cyclones but appears to be deficient in other regards. These numerical modelling efforts have not dealt with the pivotal question of specifying how the deep tropical cyclone from which integrations are started is itself formed. Cyclones of the strength and vertical depth assumed initially by most modelers are rare. The majority of naturally occurring cyclones of such intensity reach hurricane strength. In addition, most of these modelling efforts have yet to incorporate the large outer radius horizontal eddy processes occurring in the tropical cyclone.

(b) Divergence in tropical disturbances and the CISK hypothesis

Figure 36 shows vertical profiles of divergence inside 4° radius for two classes of non-intensifying tropical disturbances (0 and 00) and for six progressive stages of cyclone development (see reports of Zehr 1976 and Frank 1976). Table 11 describes these classification stages. Note the deep inflow through 400 mb in all the early genesis stages. Only a small fraction of the mass converging into the disturbance can result from boundary layer (\sim surface to 900 mb) frictional processes.

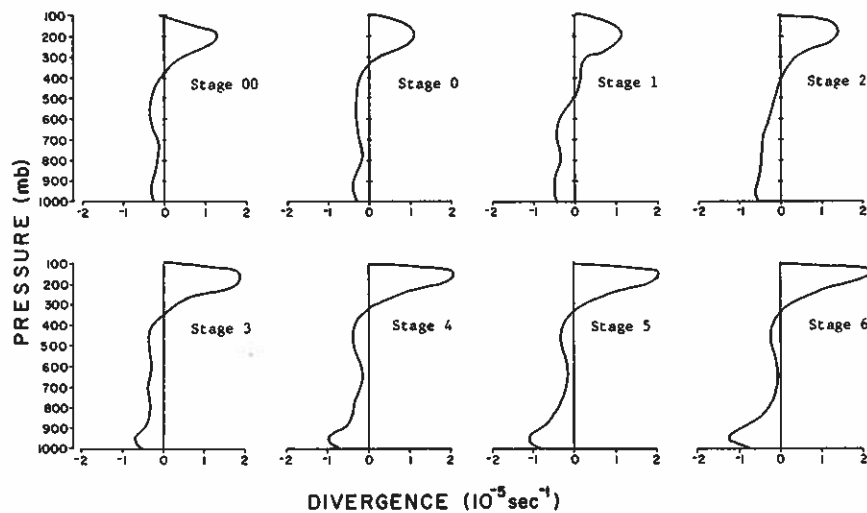


Figure 36. Mean divergence within the $r = 0-4^\circ$ area for all data sets. Stage 5 has been interpolated.

TABLE 11. TROPICAL DISTURBANCE CLASSIFICATION STAGES AND SURFACE PRESSURE AND WIND ESTIMATES AT THESE VARIOUS STAGES. TWO CLASSES OF NON-INTENSIFYING DISTURBANCE AND SIX STAGES OF DISTURBANCE-TO-CYCLONE INTENSIFICATION ARE SHOWN

Disturbance classification	Stage	Estimated minimum sea level pressure (mb)	Estimate of maximum sustained surface winds ($m s^{-1}$)
General class of non-developing disturbances	0	1008	8
Non-developing disturbances of summer in cyclone genesis region	00	1008	8
Initial cluster	1	1007	8
Pre-typhoon cluster	2	1005	10
Genesis	3	1003	12
Intensifying	4	1000	18
Tropical storm (980-1000 mb)	5	990	25
Typhoon (950-980 mb)	6	965	40

Gray (1973) and Gray and Mendenhall (1974) statistically analysed pibal and rawinsonde wind data over the tropical oceans. They showed that, after the thermal wind effect had been eliminated, the typical veering of the surface wind relative to the wind at the top of the boundary layer (or layer of mechanically driven gust scale turbulence, ~900 mb) is about 12°. These results have been verified with the GATE data. It is assumed that this veering is due to mechanical friction processes. It is emphasized that the veering angle referred to is that between the surface wind and the wind at the top of this layer (~900 mb), not that between the surface wind and the surface isobars – in the low latitude tropics the latter angle may be much larger, typically 25–30°. The author (Gray 1972) has also observed that over tropical oceans the decrease of wind speed from the top of the boundary layer to the surface is small. This is demonstrated in Fig. 37.

A schematic of the wind at the top of the boundary layer at a distance r from the centre of the disturbance is shown in Fig. 38. The convergence at the top of the boundary layer is equal to $\tan \beta$ times the vorticity at this level (or ζ_1). If it is assumed that the tangential wind maintains its strength through the boundary layer, and that the boundary layer frictional processes bring about a further 12° turning of the wind, then the convergence at the surface

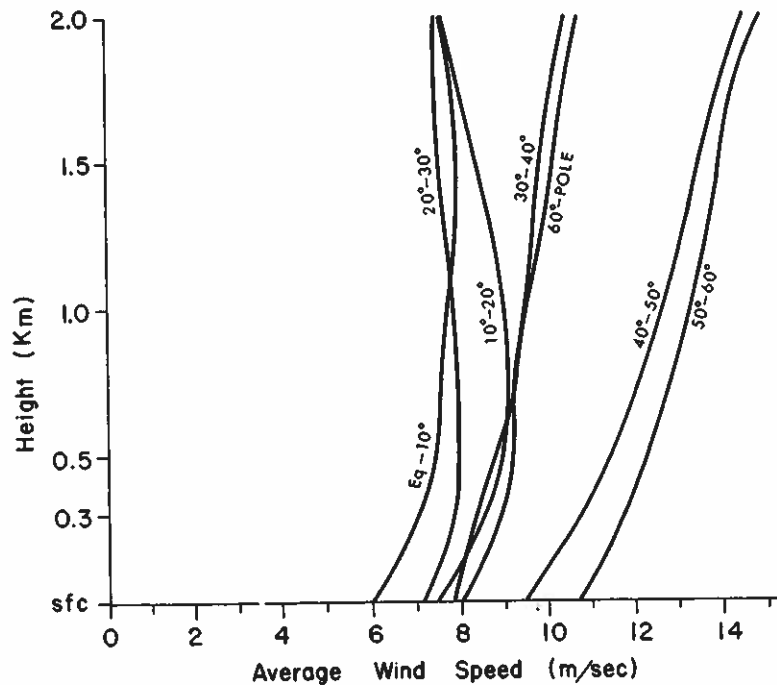


Figure 37. Variation of wind speed in the lowest 2 km – from Gray (1972).

is equal to $\tan(\beta + 12^\circ) \times \zeta_1$. Thus, if the veering varies linearly with height, the average convergence in the boundary layer is $\frac{1}{2} \zeta_1 \times (\tan \beta + \tan(\beta + 12^\circ))$. Defining C_F as the additional convergence due to the frictional turning of the wind, or

$$C_F = (\text{observed boundary layer convergence}) - (\text{convergence at the top of the boundary layer}),$$

then

$$\begin{aligned} C_F &= \frac{1}{2} \zeta_1 (\tan \beta + \tan(\beta + 12^\circ)) - \zeta_1 \tan \beta \\ &\approx \frac{1}{2} \zeta_1 \tan 12^\circ \\ &\approx 0.1 \zeta_1 \end{aligned} \quad (6)$$

Assuming that the planetary boundary layer extends to approximately 900 mb, Table 12 was constructed using Eq. (6) and the measured 0 to 4° radius convergences shown in

TABLE 12. OBSERVED MASS CONVERGENCE AND CALCULATED FRICTIONAL CONVERGENCE, C_F , IN $g\text{cm}^{-2}\text{day}^{-1}$ FOR TWO CLASSES OF NON-INTENSIFYING DISTURBANCES AND SIX STAGES OF DISTURBANCE-TO-CYCLONE INTENSIFICATION. THE LEVEL OF NON-DIVERGENCE (LND) IS ALWAYS BETWEEN 300 AND 400 mb. CONVERGENCE VALUES ARE CALCULATED BETWEEN 0-4° RADIUS. DATA OF STAGE 5 HAVE BEEN INTERPOLATED

Data	(1)	(2)	(3)	(4)		(5)		(6)	
	Observed convergence sfc. to LND	Observed convergence sfc. to 900 mb	$0.1\bar{C}_t$ or C_F	Observed	C_F	Observed (sfc.-LND)	C_F	Observed (sfc.-900)	Observed (sfc.-LND)
Stage 00	140	30	7	0.2	0.2	0.1	0.1	0.2	0.2
Stage 0	130	30	9	0.3	0.3	0.1	0.1	0.2	0.2
Stage 1	165	45	17	0.4	0.4	0.1	0.1	0.3	0.3
Stage 2	190	55	22	0.4	0.4	0.1	0.1	0.3	0.3
Stage 3	200	60	31	0.5	0.5	0.2	0.2	0.3	0.3
Stage 4	195	70	38	0.5	0.5	0.2	0.2	0.4	0.4
Stage 5	200	85	46	0.5	0.5	0.3	0.3	0.5	0.5
Stage 6	210	100	55	0.6	0.6	0.3	0.3	0.5	0.5

The first column is the total observed convergence to the LND (~350 mb).
 The second column is the observed convergence from the surface to 900 mb.
 The third column is the calculated convergence due to frictional veering, designated C_F .
 The fourth column is the ratio of C_F to the actual boundary layer convergence.
 The fifth column is the ratio of C_F to the total convergence.
 The sixth column is the ratio of the observed boundary layer convergence to the total surface to LND convergence.

rawin-
 effect
 top of
 mb) is
 at this
 angle
 0 mb),
 ics the
 served
 tyer to

centre
 ayer is
 d wind
 xional
 surface

verage
 : addi-

(6)
 Table
 own in

Fig. 38. From this table it is seen that frictional convergence, C_F , is not the dominant mechanism importing mass into the developing tropical disturbance and cyclone. Most of the inward mass transport occurs above 900 mb. C_F makes up only 15–20% of the observed surface to level of non-divergence (LND) mass convergence occurring in the early stages of both intensifying and non-intensifying disturbances. For the intensifying cyclone (stage 4 and higher), C_F accounts for progressively more of the total convergence, but still no more than 30–35%.

From the last column of this table one must conclude that in all stages of cyclone development there is a large down-pressure-gradient flow above the boundary layer. Even in stage 6 (typhoon) about 50% of the mass inflow at 4° radius occurs above 900 mb. Thus, there is substantially more mass inflow into tropical disturbances and cyclones than can be explained from boundary layer frictional processes.

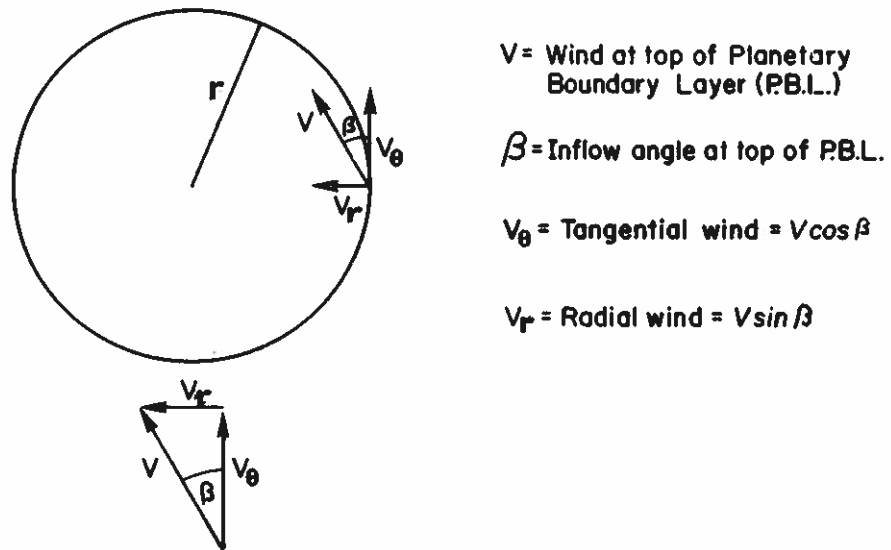


Figure 38. Schematic depiction of the wind field at the top of the boundary layer at the radius r . The vorticity averaged over the circle is $2V_\theta/r$ or ξ_1 . The convergence averaged over the circle is $\tan \beta \cdot 2V_\theta/r$ or $\tan \beta \cdot \xi_1$.

Disturbance v , surrounding area height gradients (not shown) support this deep layer of mass convergence to 400–500 mb. These deep layer inward height gradients extend over a horizontal scale significantly larger than the disturbance convective region and are probably the driving mechanism for the deep inflow. They must be produced by disturbance and surrounding region diabatic heating differences maintained by processes operating on a scale larger than the disturbance cloud region.

(c) *Radiational characteristics of the tropical disturbance and its environment*

Figure 39 portrays estimated values of the daily average radiation-induced temperature change within a typical summertime tropical disturbance with a thick cirrus shield and within the surrounding cloud-free regions, as derived by the author from discussions with S. Cox and from information in his and his colleagues' radiation papers (Cox 1969, 1971a, 1971b; Albrecht and Cox 1975). Note the sizeable differences in radiation-induced energy changes at all levels between the disturbance with thick cirrus and the surrounding clear regions.

Cox indicates that the layered upper clouds of organized weather systems are largely opaque to infrared (IR) energy penetration. They prevent upward IR energy loss from lower

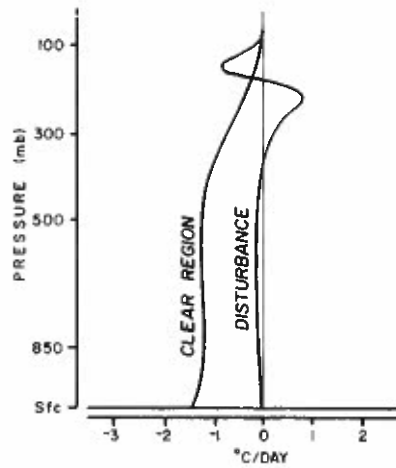


Figure 39. Comparison of typical rate of net radiation-induced temperature changes in a tropical disturbance with an opaque high cloud cover and in a tropical clear region, from information supplied by S. Cox and from other quoted radiation papers.

layers and produce a net flux convergence of IR energy in the layers underneath the cloud tops. By contrast, the upper levels of the surrounding cloud-free regions are not able to inhibit IR energy loss from lower levels. These upper-level cloud-free areas radiatively cool through IR energy loss at rates significantly greater than at levels of the disturbance underneath the cloud shield. Absorption of solar energy is also greatly altered by the presence or absence of disturbance upper-level cloud shields. Much solar energy is absorbed in the upper levels of the disturbance. Note that radiation acts to increase the upper-level enthalpy in the tropical disturbance.

If these disturbance and surrounding region radiation values are realistic, then one must ascribe a significant role to radiation as a fundamental mechanism to the maintenance of the tropical disturbance. The deep inflow of the tropical disturbance (Fig. 36) is more likely to be due to radiation influences than to the influences of boundary layer friction or cumulus convection.

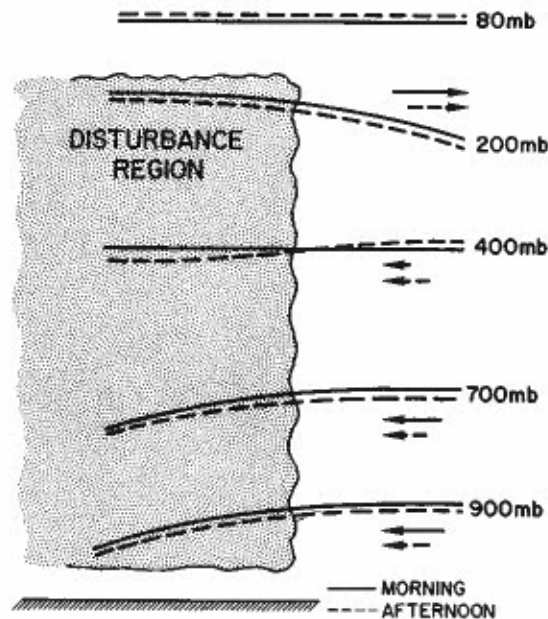


Figure 40. Hypothesized slope of pressure surfaces in the typical tropical disturbance, and the magnitude of the usual inflow (arrows).

ian-
ard
e to
oth
and
han

one
ven
rus,
1 be

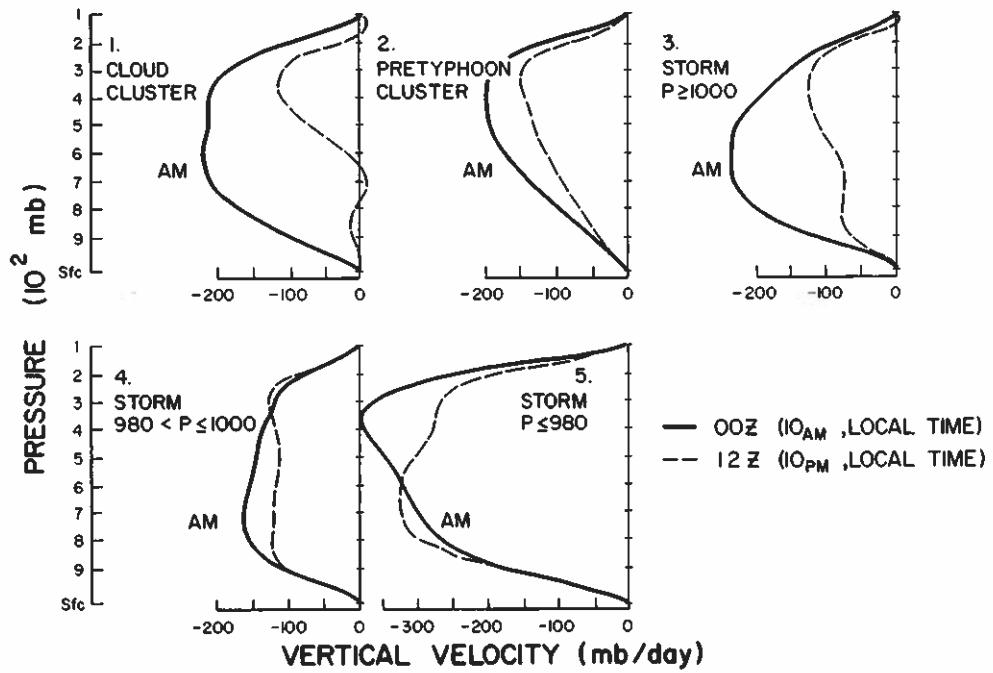
The
/r or

r of
er a
ibly
and
n a

ure
and
vith
71a,
rgy
lear

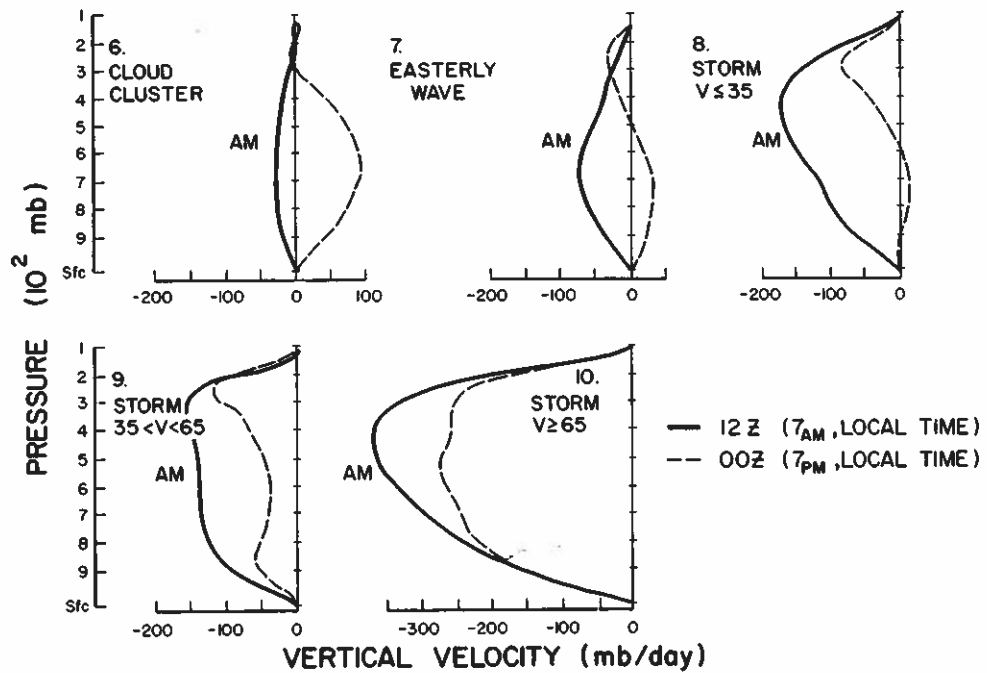
gely
wer

WESTERN PACIFIC VERTICAL VELOCITY



(a)

WESTERN ATLANTIC VERTICAL VELOCITY



(b)

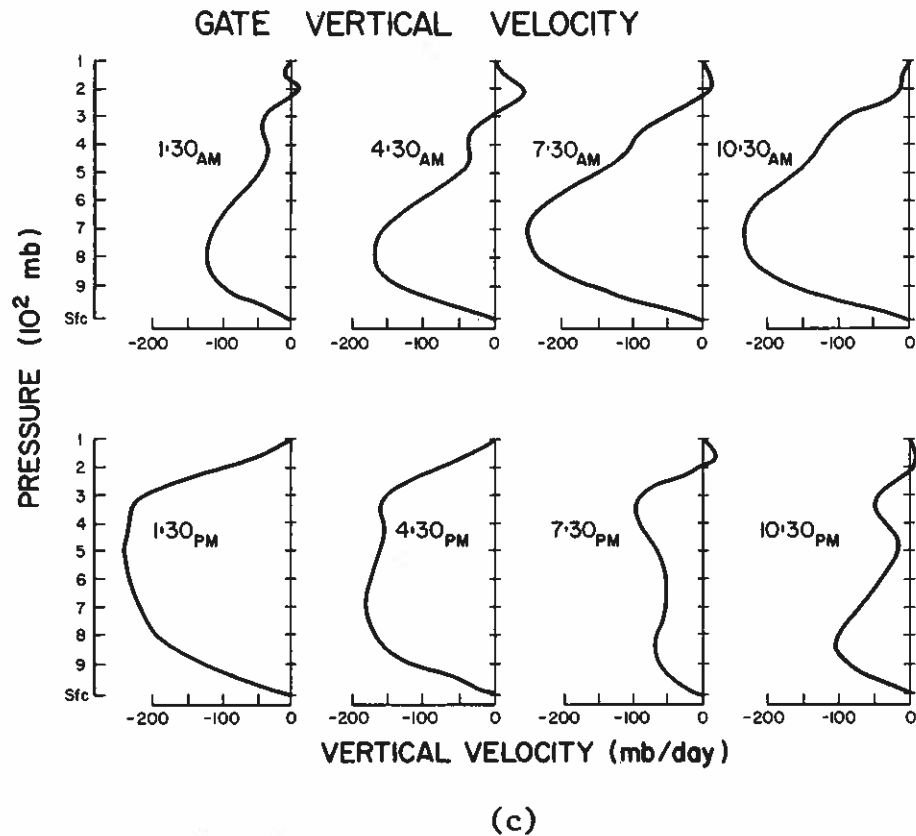


Figure 41(a)–(c). Mean vertical velocity within the $r = 0\text{--}3^\circ$ area for: (a) the five western Pacific composite systems; (b) the Western Atlantic composite systems; and (c) GATE A/B array mean vertical motion for the 10 most active convective days in GATE.

The atmosphere surrounding the tropical disturbance is hypothesized to adjust to its larger radiational cooling with extra subsidence. This surrounding region subsidence results in convergence into the adjacent disturbance region. At upper levels the cloud regions radiationally cool more than their environment. This acts in a complementary fashion with conditions at lower levels to establish the disturbance and surrounding region pressure slope and convergence profiles as idealized in Fig. 40. The winds respond to these radiation-induced pressure gradients and develop a deep layer of convergence. Winds at low latitudes can be quite ageostrophic with large down-gradient crossing angles. This type of radiation response can occur most readily in organized conservative cloud cluster systems of dimensions $5\text{--}6^\circ$ width, which are typical of the pre-cyclone disturbance.

The observed diurnal variation of the tropical disturbance's deep convergence layer and heavy rainfall as reported by Ruprecht and Gray (1976b), Gray and Jacobson (1977), Gray and McBride (1978) is further evidence of the likely important role of disturbance minus surrounding region radiation differences. Figures 41(a)–(c) show the diurnal variation of the kinematically determined vertical motion for eleven independent composite data sets from three regions. Values are obtained from a vertical integration of divergence. Divergence is calculated by a line integration of the normal component of the wind and represents the average divergence over a 3° latitude radius circle in the western oceans and over the A/B array ($\sim 3\text{--}8^\circ$ latitude radius) in the GATE region. Note that morning vertical motion greatly predominates over afternoon–evening values in all cases except for developed tropical cyclones where it is to be expected that boundary layer frictional convergence is more dominant. The numerical modelling results of Fingerhut (1978) also lend support to the influence of day v. night disturbance and surrounding region radiation differences as a

primary cause of the large observed diurnal divergence modulation of these systems. If day v. night radiation differences can so modulate the tropical disturbance's divergence profile, then it is likely that radiation is an important physical parameter in the maintenance of the disturbance. It also implies that the disturbance's convergence does not occur primarily in response to the disturbance's cumulus convection.

(d) *Condensation-produced enthalpy changes*

Our CSU observational studies (particularly the reports by Lopez 1968, 1973a, 1973b; Gray 1973; and Grube 1978) indicate that the latent heat released from cumulus clouds (both precipitating and non-precipitating) goes primarily into potential energy gain and increasing the temperature of the rising parcel relative to that of the environment. Other studies support these observations. The small extra (above environment) temperature increase of 1–2 degC of the rising Cu or Cb parcel, which is required for buoyancy, does not warm the environment unless it directly mixes out from the cloud at a higher temperature. It appears that the rising cumulus parcels typically continue rising until they lose their buoyancy and temperature excess. They then mix with their environment at temperatures little different (or even lower) than that of the environment. This does not directly warm the environment. Any heat transport from the rising cloud is overcome by evaporation of the residual liquid water particles as the cloud dies. Although heavy rainfall may have occurred, there is typically no local region warming; instead, there is often a local cooling of the immediate environment. As far as direct temperature change is concerned, a 'cooling tower' as opposed to a 'hot tower' concept may be more valid. This is not to say that Cb convection is not indirectly responsible for most of the vertical energy exchange occurring in the tropical environment as a whole, as hypothesized by Riehl and Malkus (1958).

Cumulus-cloud-induced enthalpy changes occur primarily as a result of the cloud's return flow subsidence and adiabatic compression. Cumulus convection typically produces positive enthalpy changes only in the upper troposphere where subsidence warming is always greater than cloud reevaporational cooling. At lower levels cloud reevaporation is typically as large as or larger than subsidence warming and small enthalpy decreases usually occur. For many years Riehl (1954, 1967) has emphasized the 500–900 mb cold core structure of most tropical disturbances.

Vertical mass recycling within the tropical disturbance typically leads to small upper tropospheric warming and a small lower tropospheric cooling, or neutral enthalpy change. The rates of enthalpy increase due to condensation in the upper layers of the disturbance relative to its surroundings are at most only 0–1.0 degC day⁻¹ (as we have been best able to infer from a variety of observational approaches). These enthalpy changes make up only a very small percentage (0–3%) of the cloud-released condensation energy.

Calculations of rates of condensation energy release of 8–12 degC day⁻¹ and compensating adiabatic cooling rates of the same magnitude have little practical meaning as regards enthalpy changes. These processes very closely balance each other. It is important to distinguish between 'condensation heating' and 'enthalpy change'. The latter is not necessarily related to the former.

Condensation-produced enthalpy change in cloud clusters is also not well related to the vertical motion at the top of the boundary layer or to boundary layer moisture convergence (as assumed by the many CISK and wave-CISK modellers). It appears that this warming cannot be realistically modelled by direct convective temperature adjustments needed to maintain lapse rates or by warming due to cumulus parcel minus environmental temperature differences; or by assuming that enthalpy change is proportional to total disturbance moisture convergence.

The nature of the processes which cause the upper tropospheric enthalpy increase required for disturbance-to-cyclone transformation is difficult to specify. These changes probably require special large-scale flow configurations and wind pressure imbalances which concentrate and enhance the subsidence warming processes.

There appear to be two primary types of condensation-produced enthalpy increase. Both result from compensating subsidence. They are:

(1) *Enthalpy increases on a time and space scale of cumulus convection from subsidence warming around the sides of the cumulus updraughts.* This surrounding cumulus subsidence is a small fraction of the updraught mass flux (Lopez 1973a) and is largely compensated for by evaporation of cloud water. Cb convection produces small enthalpy increase in the upper troposphere where cloud liquid water reevaporation is not sufficient to overcome the subsidence warming. At lower levels, cumulus convection typically produces no enthalpy increase. Often small negative enthalpy changes occur because cloud reevaporation is equal to or larger than the surrounding subsidence warming.

(2) *Enthalpy changes on a mesoscale resulting from dynamically forced subsidence due to upper-level convergence.* Examples are the dynamically driven subsidence of the hurricane eye (Gray and Shea 1973) or the mechanically forced subsidence in advance of middle latitude squall lines (Hoxit *et al.* 1976). On a different scale, there are strong lower stratospheric subsidence-induced enthalpy increases accompanying middle latitude cyclogenesis. Such dynamically forced subsidence can apparently be quite strong in selective situations occurring in the tropics. Large rates of upper-level positive enthalpy increase ($\sim 0.2\text{--}0.5 \text{ degC h}^{-1}$) and corresponding surface pressure decrease ($\sim 0.5\text{--}1.0 \text{ mb h}^{-1}$) over small regions of 50–100 km diameter can result for short periods of a few hours, as occur with tropical cyclone centre formation. This type of subsidence requires a favourable positioning of upper-level converging wind systems or special wind–pressure imbalances. It forces subsidence warming and compensating divergence underneath the converging layer. This type of mechanically driven subsidence typically occurs in clear or partly cloudy areas adjacent to regions of deep convection. If sustained in conditions of weak tropospheric vertical wind shears for periods of 3–6 hours, it can result in significant concentrated local warming and pressure decrease. This type of dynamically driven subsidence should be distinguished from the considerably weaker subsidence occurring over clear and partly cloudy regions in response to radiational cooling. This latter type of subsidence warming is nearly cancelled by radiational cooling and produces no significant enthalpy changes.

It appears that process (1) is too weak to allow for significant disturbance enthalpy increase and concentration such that a tropical cyclone can result. Observational evidence indicates that cyclone formation requires some type of dynamically forced subsidence mechanism such as (2).

A large body of satellite information is now available for both the western Atlantic and the Pacific to indicate that the location of the centre of a newly forming tropical cyclone is not typically within the disturbance's active convective region (Fett 1966; Oliver and Anderson 1969; Dvorak 1975; Wright 1976; Arnold 1977; Erickson 1977; plus personal communications from Fett (1965) and Hubert (1968) and other data). Instead the centre occurs:

- (1) within the clear region just to the west or northwest of the cluster, as seen in Fig. 42(a);
- (2) in the clear region between two different disturbance clusters, as seen in Fig. 42(b);
- or
- (3) between active convective regions in the same cluster, as seen in Fig. 42(c).

The dotted areas of these figures show typical regions of concentrated warming due to dynamically forced subsidence. These locations are places where the disturbance's upper-level outflow impinges upon the circulation of an upper-level trough, the outflow from

another cluster, or the outflow from different cloud groups within the disturbance. The outflows merge and cause a mechanically forced downward motion. It is hypothesized that it is only at locations where dynamically forced subsidence occurs that enthalpy increase can be of sufficient magnitude to initiate a cyclone. More supporting evidence of this linkage has been given in reports by Arnold (1977) and Erickson (1977). Similar types of warming are also being observed with the GATE data by Grube (1978).

In a detailed analysis of the initial development of a tropical disturbance which later became hurricane Alma of 1962, Yanai (1968) also found the initial warming and pressure drop to occur away from the disturbance cloudiness.

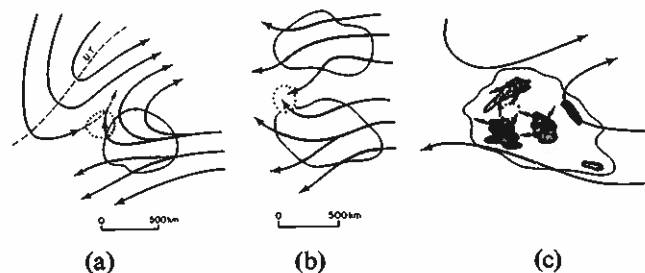


Figure 42. (a) Idealized portrayal of 200 mb flow features associated with intensifying tropical disturbance where the initial cyclone centre occurs in the dotted region adjacent to the cloud area (shaded) and an upper trough (UT) is present to the northwest. (b) Schematic of how the outflow from two disturbances could produce large flow convergence in the dotted region between the disturbances. (c) Conditions where dynamically forced subsidence occurs within the disturbance cirrus shield (light shading) but between active convective elements (heavy shading). The cirrus-level outflows from the convective areas meet in the dotted circle region.

The importance of the disturbance's convective region in the cyclone formation process appears to be not that of producing a direct enthalpy increase from the release of condensation energy in the cumulus but rather that of acting as a strong and concentrated source of upper-level mass outflow for adjacent region convergence and dynamically forced subsidence. Recent geostationary satellite measurements of tropical cloud cluster cirrus outflow by Martin *et al.* (1977) indicate that quite intense ($4 \times 10^{-5} \text{ s}^{-1}$) upper-level convergence can exist on the sides of tropical cloud clusters.

It appears that the rate of enthalpy change occurring within the typical pre-cyclone disturbance from direct condensation energy release is too small to produce the warming required for initial cyclone formation. Some type of dynamically forced subsidence at the side of or between the deep convective groups appears to be a necessary genesis requirement. The strong upper-level outflow from the deep convective areas appears to act as the mass source for this dynamically forced subsidence. A favourable superposition of surrounding upper-level flow features such as an upper tropospheric trough to the northwest or an adjacent disturbance outflow, can probably enhance the dynamical subsidence. This favourable positioning of surrounding wind fields is not well related to the amount of disturbance convection.

It appears that no cumulus parameterization scheme which directly relates condensation energy release with enthalpy increase will ever be able to simulate realistically the disturbance-to-cyclone transformation. Most of the cumulus parameterization schemes so far proposed have yet to include the linkage of convection with the surrounding large-scale wind fields and the implications to enthalpy change of dynamic subsidence produced by wind-pressure imbalances. It appears that this must be done.

(e) *Fundamental role of large-scale influences on tropical cyclone formation*

Tropical cyclones form only from pre-existing mesoscale systems that occur in very selective large-scale environments. It appears that the unique feature to specifying time and location of genesis is not so much the characteristic of the individual mesoscale systems themselves. These systems are common and occur in all seasons and at most locations.

Once the climatological conditions of genesis are met, it appears that favourable 10–15-day timescale changes in the large-scale tropical general circulation is the primary factor dictating whether the often present individual organized mesoscale systems will intensify or not. It appears that genesis occurs when an organized tropical cloud cluster moves into a favourable large-scale environment. Similar ideas have been advanced by Shapiro (1977a, 1977b).

The clustering of cyclones in time and space has been discussed in section 2. The hemispheric periods of 1–3 weeks of active and inactive tropical cyclone activity as indicated in Figs. 9 and 10 for northern and southern hemispheres are believed indicative of basic 1–3-week period alternations of the tropical general circulation. Cyclone genesis frequency thus appears to be primarily a slave to the large-scale 1–3-week shifts in the tropical general circulation. By contrast, the population of mesoscale cloud clusters from which cyclones originate does not appear to undergo such periodic variations, neither do easterly waves. Extensive easterly wave activity can occur at times and in regions where cyclones do not form (Frank and Clark 1977).

(f) *Tropical disturbance and cyclone energy budget*

Moist-static energy, h , can increase or decrease in the typical tropical disturbance through transfer from the sea by latent and sensible exchange, E_s , by radiation, R , or through horizontal transport on the boundaries, $\nabla \cdot Vh$. This energy balance may be expressed as:

$$\partial h / \partial t = E_s + R - \nabla \cdot Vh \quad (7)$$

where $h = gz + c_p T + Lq$. Each term has been integrated through the depth of the troposphere. Estimates of E_s and R for the inner 4° radius of tropical systems indicate that $E_s + R$ is slightly positive in weak disturbances but strongly positive in hurricanes, where large sea

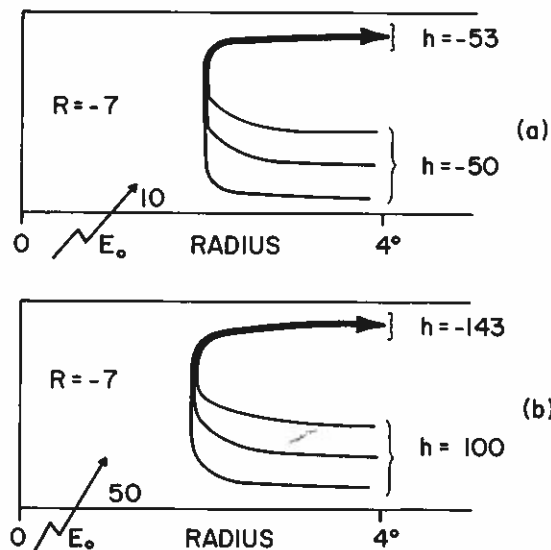


Figure 43. Schematic representation of the typical h budget within 4° radius of the steady-state cloud cluster, (a), and of the steady-state hurricane, (b). Units are arbitrary.

surface energy input occurs. Steady-state, $\partial h/\partial t = 0$, hurricanes export large amounts of energy. They accomplish this through radial export of potential energy in their upper-level outflows. Idealized h budgets for the steady-state cloud cluster and hurricane are portrayed in Fig. 43.

It is seen that the usual vertical circulations through the organized tropical weather system or cyclone typically produce an energy depletion of the system. The tropical system maintains itself only through energy received from the ocean. It is observed that most tropical systems weaken or die when this ocean energy source is cut off.

Cumulus parameterization schemes which show energy accumulation depending on the magnitude of the mean upward circulation appear quite invalid. Energy received from the low-level inflow goes to enhance deep Cb convection. These Cb rise to great heights and induce outflow at levels (~ 12 – 14 km) where h is larger than that of the inflow air. *Thus, the transverse circulation of the tropical disturbance and cyclone is typically acting to decrease the energy of the system.* Any process which acts to reduce this mean circulation is likely to lead to energy accumulation within the system and intensity increase. Conversely, any process leading to an enhancement of the radial circulation will lead to energy loss and system weakening. This idea is quite at variance with the long-held and prevailing view that increase in intensity of the mean radial circulation is positively related to increased intensity. Our data sets show that this is definitely not the case. Intense and intensifying cyclones do not have stronger transverse circulations than do weak and filling systems. It should also be realized that frictional dissipation is a slowly acting process and that the momentum field of the tropical system will be only slowly influenced by a temporary lessening of the transverse circulation's cross-contour flow. Energy accumulation will increase the system pressure gradients and will help re-establish the magnitude of cross-contour flow even though the inflow–outflow angles may be reduced somewhat.

(g) *Role of surrounding regional vertical wind shear patterns for tropical system intensity change*

Our rawinsonde compositing information is beginning to indicate that there are significant differences in the gradient wind balances between intensifying and filling cyclones and also between intensifying and non-intensifying tropical disturbances. Intensifying systems are observed to have more supergradient or less subgradient winds at lower and upper tropospheric levels than steady or filling systems. Accelerations differ by about 20–30%.

Supergradient winds (or winds less subgradient than average) at upper and lower tropospheric levels are believed favourable for genesis and cyclone intensification because such accelerations are likely to lead to a small inhibiting of the transverse circulation through the system and thus allow more inner system energy accumulation from the sea. The primary radial circulation of the cyclone is driven by friction, radiation and condensation acting on a quasi-balanced wind–pressure field. Subgradient or supergradient winds enhance or restrict this mass circulation.

If this evaluation is correct, then one may better understand the likely role which Cb convection and the surrounding system vertical wind shears play in disturbance and cyclone intensification if one can agree to the likely relevance of the Cb cloud model that has been proposed by Imperial College scientists (Green and Pearce 1962; Ludlam 1963, 1966; Moncrieff and Green 1972; Moncrieff and Miller 1976).

This cloud model hypothesizes that Cb convection can act in an 'up-gradient' mode to increase the vertical wind shear between upper and lower tropospheric levels. This Cb

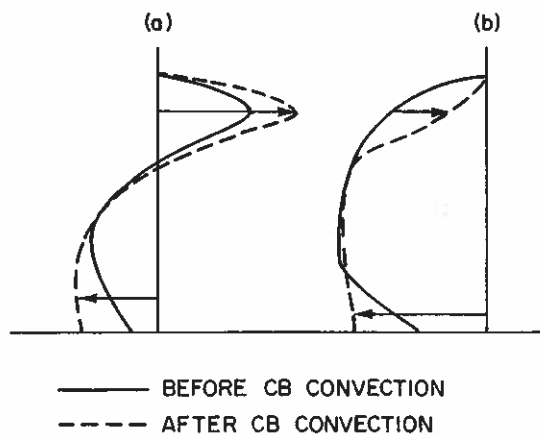


Figure 44. Idealized picture of how Cb convection acts to increase the tropospheric vertical wind shear. For further explanation see text.

model (as the author understands it) acts to convert vertical updraught and downdraught kinetic energy (KE) into horizontal kinetic energy at upper and lower tropospheric levels. When the wind blows in opposite directions at upper and lower tropospheric levels (see Fig. 44(a)), Cb convection acts to enhance the vertical wind shear by increasing both lower- and upper-level winds. It is just this type of wind shear pattern which exists around developing cloud clusters, that is, low-level trade winds and upper-level westerlies to the poleward side, low-level westerlies and upper-level easterlies on the equatorward side (see information of section 4 and also Fig. 32). The shear pattern of (b) is indicative of conditions at closer-in radii.

When wind does not change direction with height, the evidence indicates that the Cb act in the usually envisaged 'down-gradient' sense to decrease the vertical wind shear, as previously discussed by the author (Gray 1967) for hurricane eye-wall convection. Thus, when the wind is from the same direction throughout the troposphere an increase in KE at upper and lower levels will act to suppress the vertical shear (see Fig. 44(b)).

Another mechanism by which the Cb may act to increase the upper tropospheric winds is through absorption of gravity waves. This is likely only in special vertical shear conditions

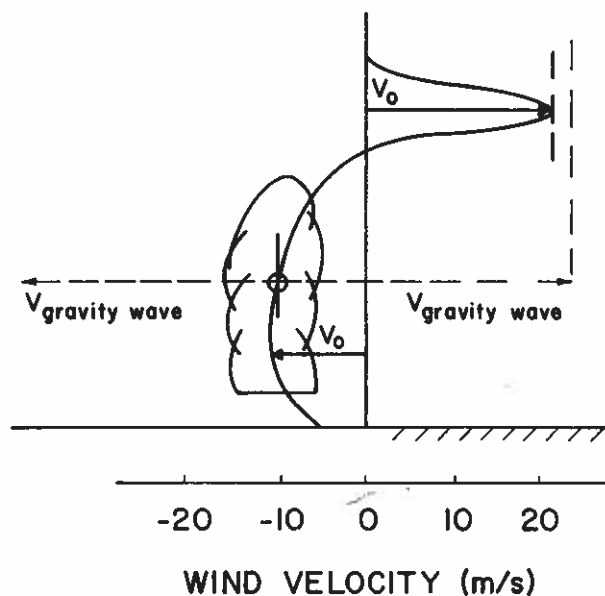


Figure 45. Idealized picture of how dispersionary gravity waves ($V \sim 25-30 \text{ ms}^{-1}$) from Cb convection in the lower troposphere could have velocities similar to upper tropospheric winds with vertical shear pattern as shown in Fig. 44(a).

where the magnitude of the vector difference between the lower and upper tropospheric winds is near the speed of the Cb-induced gravity waves, as indicated in Fig. 45. If Cb-generated gravity waves at lower and middle tropospheric levels were to travel outwards at velocities of $\sim 25\text{--}30\text{ m s}^{-1}$, the velocity difference between these gravity waves and the upper-level winds would be quite small. Absorption of these gravity waves would lead to a momentum increase at upper levels. Other vertical shearing patterns would not permit such absorption. This topic needs more exploration. It is, nevertheless, interesting to note again that this is the type of vertical wind shear pattern existing about tropical systems undergoing intensification. It is also of interest to note that wind speeds within the tropics typically show quite a strong upper tropospheric velocity concentration near 125 to 175 mb. Why are high wind speeds concentrated at these levels?

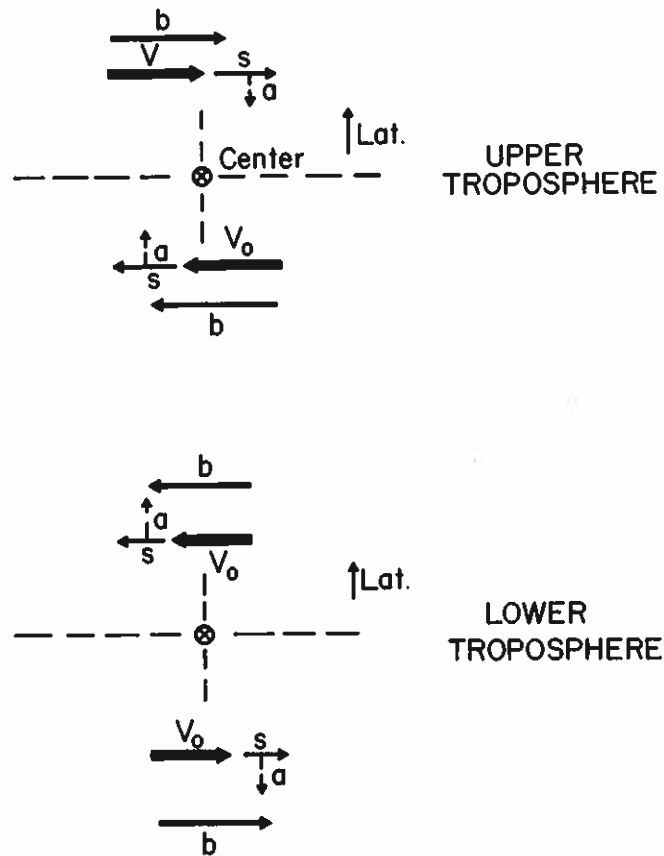


Figure 46. Idealized view of how initial winds, V_0 , poleward and equatorward of the developing disturbance are increased by amount s due to Cb convection, the direction of the resulting unbalanced acceleration a , and the magnitude of the resulting balanced wind b when wind and pressure come into adjustment.

Regardless of the relevant mechanisms and their likely physical explanation, it appears that Cb convection can act (in special vertical shear situations) to increase the momentum at upper and lower tropospheric levels and increase the ratio of wind to pressure acceleration. The role of Cb squall lines in increasing the boundary layer winds is better understood.

Accepting that Cb convection acts to increase winds at lower and upper tropospheric levels, one can hypothesize that Cb clouds can act to change the wind–pressure acceleration balance and bring about supergradient (or less subgradient) winds at upper and lower levels. This should act to cause a reduction in the cyclone or disturbance's transverse circulation and lead to a consequent energy accumulation and system intensification. This adjustment is schematically represented in Fig. 46 where it is assumed that the initial balanced wind, V_0 , is increased by Cb convection to $V_0 + s$ and a resulting outward

acceleration, a , takes place to cause a reduction in the mean upper-level divergence and lower-level convergence. These radial wind alterations act to reduce the transverse circulation and bring about an adjustment of the wind-pressure fields. When the wind and pressure come into balance, the resulting wind is represented by b . Intensification may be thought of as a gradual step by step wind-pressure unbalancing and then wind-pressure adjustment to this unbalancing.

When vertical shear patterns do not permit the Cb convection to act in this manner, wind-pressure balances are not favourably altered and transverse circulation decreases and intensification does not occur. System weakening occurs when the wind-pressure ratio is one causing substantial subgradient winds.

Thus, the role which the strong surrounding vertical wind shear patterns of growing disturbances play may be that of allowing the outer radii Cb convection (often in the form of squall lines) to act to increase the lower and upper tropospheric wind-pressure ratios which, in turn, act to inhibit the system's transverse circulation. By previous reasoning this should lead to intensification.

7. LARGE-SCALE ASPECTS OF HURRICANE STRUCTURE

For a thorough discussion of our recent typhoon and hurricane structure studies, the reader is referred to Shea and Gray (1973), Gray and Shea (1973, 1976), W. Frank (1976, 1977a, b, c, d) Arnold (1977) and Núñez and Gray (1977). Space allows only a brief summary of some of the most relevant results on the large-scale aspects of the cyclone. Information on storm inner-core characteristics will not be presented. Much of the information in this section can also be found in the W. Frank papers.

(a) Radial winds

Two-dimensional cross-sections of radial wind, V_r , for the typhoon and the hurricane are shown in Figs. 47 and 48. These winds have been adjusted to achieve mass balance. The

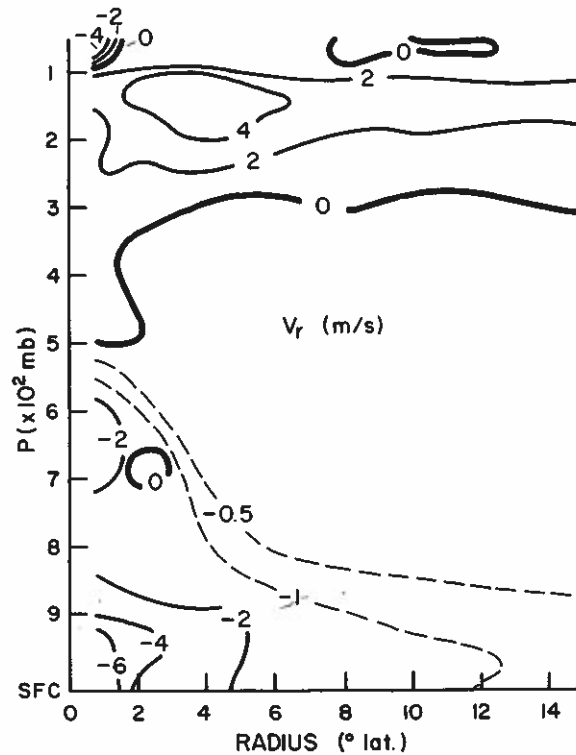


Figure 47. Two-dimensional cross-section of radial winds, V_r , for the mean steady-state typhoon.

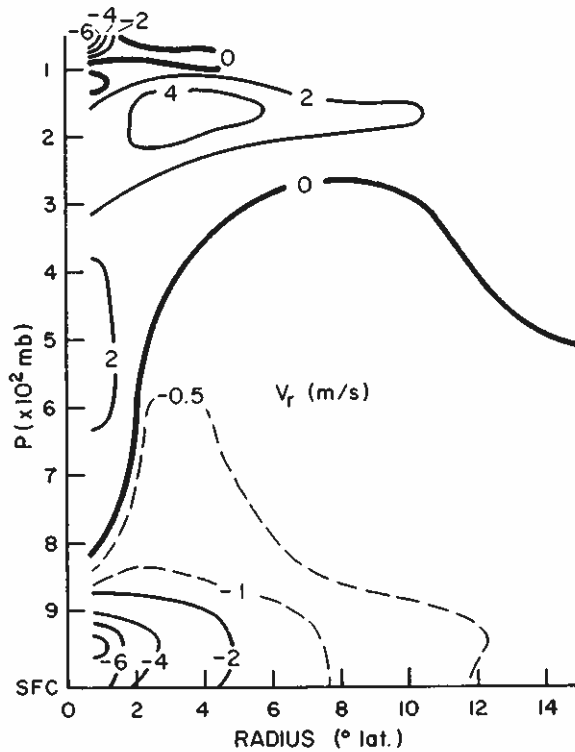


Figure 48. As Fig. 47 but for the mean steady-state hurricane.

magnitude of this adjustment is usually very small. Maximum inflow occurs at 950 mb for both systems. Note the generally high level of the inflow to nearly 300 mb for data beyond 2° radius. This upper-level inflow is unlikely to result from boundary layer frictional influences. The outflow layer is centred near 150 mb and extends farther out for the typhoon, which is typically of larger areal size than the hurricane. The outflow has a large asymmetry with maximum outflow to the northeast in the hurricane and northeast and southwest in the typhoon.

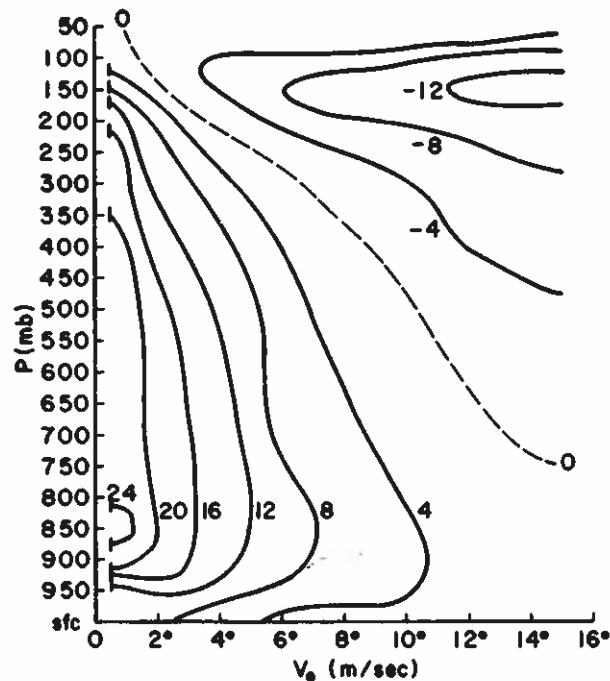


Figure 49. Two-dimensional cross-section of tangential winds, V_θ , for the mean typhoon (central pressure < 980 mb).

(b) Tangential winds

Mean tangential wind, V_θ , cross-sections for both systems are shown in Figs. 49 and 50. Maximum cyclonic flow is found in both cases to be at 850 mb, where the effective top of the frictional boundary layer is located. Surface winds are lower than those to be expected over the oceans. Cyclonic rotation extends through the depth of the troposphere only inside the 2° radius. The magnitude of the tangential wind at any radius is smaller for the hurricane system, reflecting the smaller average size of Atlantic storms. Tangential wind speeds show no significant diurnal variation.

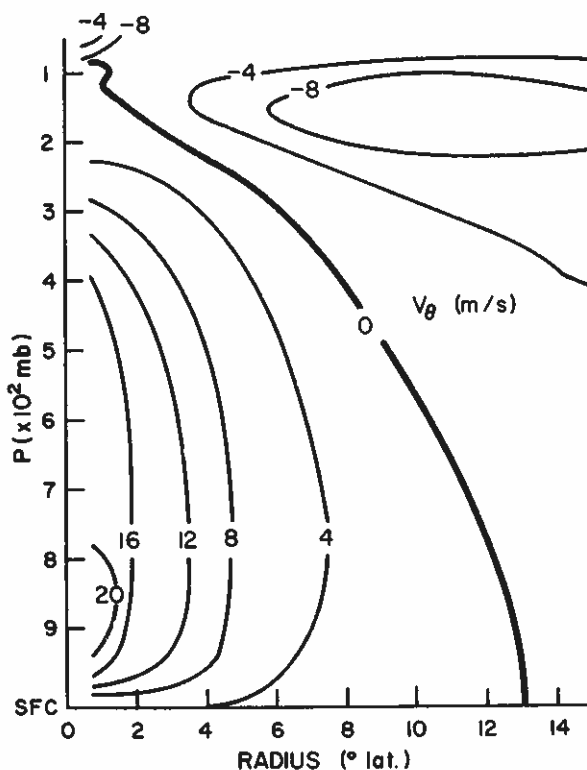


Figure 50. As Fig. 49 but for the mean hurricane ($V_{max} > 65$ kt).

The anticyclonic maximum occurs around 150 mb in both tropical cyclone systems. The $V_\theta = 0$ line serves as a boundary between cyclonic and anticyclonic circulation. These large-scale flow features are largely independent of the inner core strength of the cyclone. Intense and weak eye circulations can occur with near-similar outer region flow regimes.

(c) Hurricane rainfall and sea surface energy fluxes

Tropical cyclones converge large quantities of water vapour. They also evaporate much sea water due to their high surface winds. The equation for conservation of water vapour integrated over a cylindrical volume extending from the surface to 100 mb is

$$\int \partial(\bar{\rho}q)/\partial t = - \int \bar{\nabla} \cdot \bar{\rho} \nabla q + E - P \quad (8)$$

where E is evaporation from sea surface and P is precipitation.

Analyses of all rawinsondes surrounding cyclones with central pressures ≤ 980 mb and/or maximum sustained winds > 65 kt have been made. A steady state is assumed. The term on the left of this equation is thus zero. The first term on the right is the total horizontal

transport of water vapour into the volume, which is measured. The second and third terms are evaporation from the sea and precipitation. Rainfall measurements from Miller (1958) and Frank (1976) are used for the precipitation estimate (Fig. 51). Evaporation is solved as a residual. The water budget is shown in Fig. 52.

About 75% of the observed 0–2° precipitation results from inward water vapour advection. Nearly 65% of the 0–6° precipitation, however, may be attributed to evaporation within that area. The area-weighted evaporation from 0–6° is about 1.5 cm day⁻¹. Since mean typhoon season evaporation is about equal to the seasonal precipitation (~0.5 to

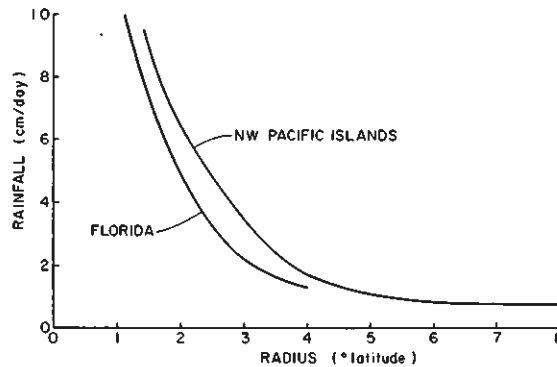


Figure 51. Observed precipitation around tropical cyclones from Florida (Miller 1958) and from NW Pacific islands (Frank 1976).

	WATER BUDGET (cm/day)					
CONVERGENCE OF q	6.7	1.2	-0.7	0.1	-0.1	-0.1
PRECIPITATION	9.0	2.3	0.7	0.7	0.7	0.7
REQUIRED EVAPORATION	12.3	11.1	11.4	10.6	10.8	10.8
	0°	2°	4°	6°	8°	10°

Figure 52. Water budget for 0–12° region. Evaporation values shown are the amounts required to achieve balance (from Frank 1976).

0.7 cm day⁻¹), approximately 60–70% of the total 0–6° evaporation may be assumed to result from the increased wind speeds associated with tropical cyclones. About 60% of the 0–6° storm precipitation is due to this anomalous sea surface evaporation. The important role of the sea surface in the storm's water budget and hence in its energetics is obvious. This phenomenon helps explain the rapid decay of tropical cyclones as they move over land.

These evaporation determinations agree with estimates using the bulk aerodynamic formula, $E = \rho C_E V (q_s - q)$, when C_E is taken to be $1.5 - 2.0 \times 10^{-3}$ and 900 mb winds are used for V . See Frank (1976) for more discussion.

(d) Sea surface energy fluxes

It is generally accepted that tropical cyclones require a warm sea surface layer of significant depth to maintain their intensity. Climatological studies by Palmén (1948, 1957) and Gray (1968, 1975) have shown that tropical cyclone genesis occurs only in regions where the sea surface temperature is above about 26°C and where the depth of the 26°C isotherm is 60 m or more. Ooyama's (1969) and Rosenthal's (1971) modelling experiments have shown that surface fluxes of moisture and sensible heat are critical in achieving realistic storm intensifications.

Frank (1977b) has calculated typhoon total sea-surface to air fluxes of h from vertically

integrated h budgets assuming Bowen ratios of 0.1 and 0.2. Values range from about $62 \times 10^6 \text{ J m}^{-2} \text{ d}^{-1}$ ($1472 \text{ cal cm}^{-2} \text{ d}^{-1}$) inside 1° radius to $\sim 20 \times 10^6 \text{ J m}^{-2} \text{ d}^{-1}$ ($470 \text{ cal cm}^{-2} \text{ d}^{-1}$) at radius of $6-8^\circ$. Some previous researchers have estimated sea to air energy fluxes 3-4 times larger than the values calculated by Frank. Estimates of Leipper (1967) are especially high, $174 \times 10^6 \text{ J m}^{-2} \text{ d}^{-1}$ ($4160 \text{ cal cm}^{-2} \text{ d}^{-1}$) for the inner 240 km radius of hurricane Hilda (1964).

Previous ideas held that θ_e of the low-level inflowing air must increase enormously to allow buoyant convection in the strong warm core environment near the storm centre (Malkus and Riehl 1960). Adiabatic expansion would predict surface temperature drops of 3-9 degC. This observation led Malkus and Riehl to estimate sea to air sensible heat fluxes of $131 \times 10^6 \text{ J m}^{-2} \text{ d}^{-1}$ ($3140 \text{ cal cm}^{-2} \text{ d}^{-1}$) inside 90 km for a fairly strong hurricane. The results of Frank's recent study indicate a mean sea to air sensible heat flux which is only about 20-35% of the Malkus and Riehl estimate. Malkus and Riehl assumed an idealized boundary layer inflow into the hurricane. Our recent calculations indicate that about 60% of the inflow at 2° radius is above 950 mb. Since cloud base is typically at or below 950 mb, it is safe to say that no more than a third of the inflow inside 2° is occurring in the sub-cloud layer. In addition, analysis of vertical h fluxes at cloud base shows that the cloud base mass flux in the inner cyclone region is typically 4-5 times larger than the mean vertical motion at cloud base (Frank 1977c). The result is that air does not simply flow in and expand adiabatically, go up in the eyewall, and depart. There is an enormous amount of mass recycling in the lower levels at all radii which results in liberation of the latent heat of condensation and warming from environmental subsidence. Adiabatic assumptions are invalid above cloud base. Subcloud air may be vertically recycled several times before reaching the eyewall.

(e) Angular momentum budgets

The conservation of relative angular momentum in cylindrical stationary coordinates may be expressed as

$$dm/dt = -rfV_r - (1/\rho)(\partial p/\partial \theta) + rF_\theta \quad (9)$$

where $m = V_\theta r$ is the relative angular momentum, F_θ is tangential friction, and the other symbols are standard.

Steady state is assumed, and terms involving $\partial/\partial \theta$ drop out when integrated around a circle. Vertical flux terms also integrate to zero assuming no flux at 100 mb. Therefore, the large-scale vertically integrated angular momentum balance is

$$\overline{\nabla \cdot \mathbf{V}_r V_\theta r} = -\overline{frV_r} + \overline{F_\theta r} \quad (10)$$

The term on the left is the convergence of m due to the radial circulation. This flux is estimated by compositing individual values of $\overline{V_\theta V_r}$ (overbar represents time and space averaging). By subtracting the flux due to the mean circulation, $\overline{V_r} \cdot \overline{V_\theta}$, it is possible to estimate the horizontal eddy flux. As noted by Riehl (1961), horizontal momentum fluxes near the centre can be well estimated from the mean circulation. At greater radii, however, the transport becomes increasingly dominated by eddy fluxes. About 60% of the total momentum import at 10° radius in the typhoon is accomplished by eddy fluxes resulting primarily from strongly divergent anticyclonic flow in the upper-level outflow (Fig. 53) jets. Similar large inward upper troposphere eddy transport is required at 8° and 12° radius. Eddy fluxes at 2° and 4° radius are negligible, however.

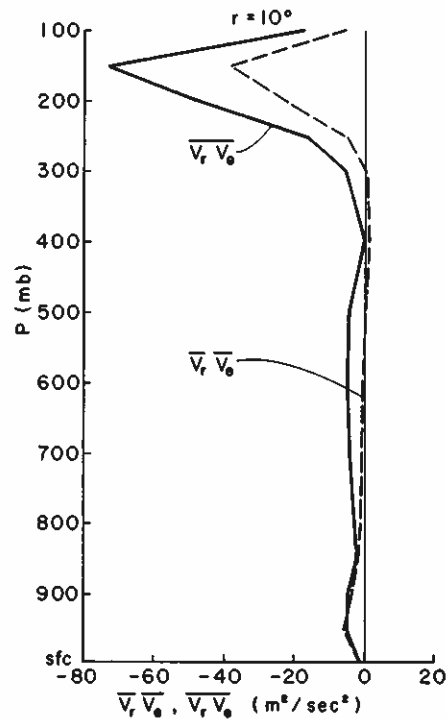


Figure 53. Total horizontal flux of relative angular momentum divided by radius, $\overline{V_r V_\theta}$, and flux by mean circulation, $\overline{V_r} \overline{V_\theta}$, at $r = 10^\circ$. The difference between the curves is the horizontal eddy flux.

(f) Kinetic energy budgets

Our rawinsonde compositing of typhoons and hurricanes also indicates that eddy kinetic energy processes are of great importance in the overall energetics of tropical cyclones and their surrounding environments. The outer storm circulation region exhibits substantial net generation and export of kinetic energy. This results primarily from transient eddy processes at upper levels. Previous empirical studies of tropical cyclone kinetic energy have implied that eddy horizontal transports and generation of kinetic energy were generally not of major importance to the storm energy budgets. Numerical modelling studies have reinforced this view. But most of these previous studies have primarily treated the inner areas of the hurricane where eddy processes are of less importance. As yet few studies have been made of the tropical cyclone's outer circulation.

The equation of conservation of kinetic energy is

$$\partial \overline{K} / \partial t = -\nabla \cdot \mathbf{V} K - \overline{\partial(\omega K) / \partial p} - \mathbf{V} \cdot \nabla \phi + \mathbf{V} \cdot \mathbf{F} \quad (11)$$

where K is kinetic energy per unit mass, $\phi = gz$ is potential energy, \mathbf{F} represents frictional processes, and other symbols as normally defined.

The term on the left of Eq. (11) is the local rate of change of kinetic energy and is zero for a steady-state hurricane. The first term on the right is the horizontal flux divergence of kinetic energy. The second term is the vertical flux divergence of K , and the third term is the generation of kinetic energy by down-gradient flow. The last term is the frictional dissipation.

West Pacific storms export large quantities of kinetic energy, and eddies become the dominant export mode at large radii (Fig. 54). Transport and eddy fluxes occur almost entirely in the upper troposphere (Fig. 55) and reflect the presence of the outflow jets. Frank (1977d) has estimated west Pacific storms to generate (and export) an excess of about 4.8 W m^{-2} averaged over their inner $0-10^\circ$ radius region. West Atlantic storms are observed

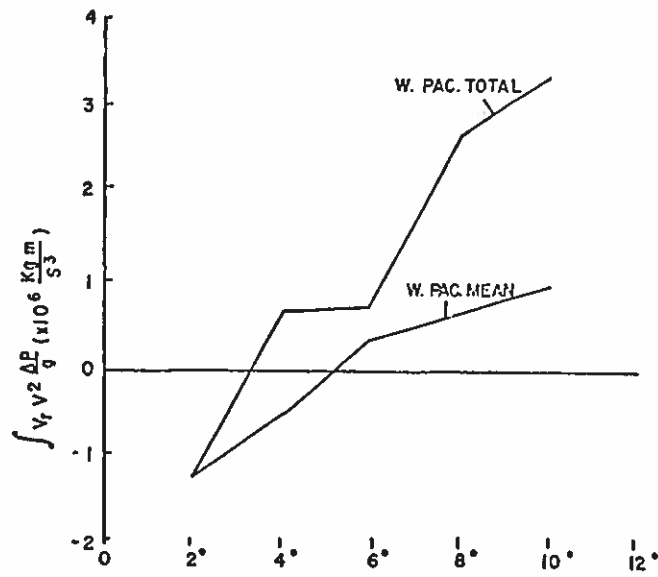


Figure 54. Total vertically integrated horizontal flux of kinetic energy times two, $(\overline{V_r V^2})$, and flux by mean circulation $(\overline{V_r} \overline{V^2})$, for west Pacific typhoons (from Frank 1977d).

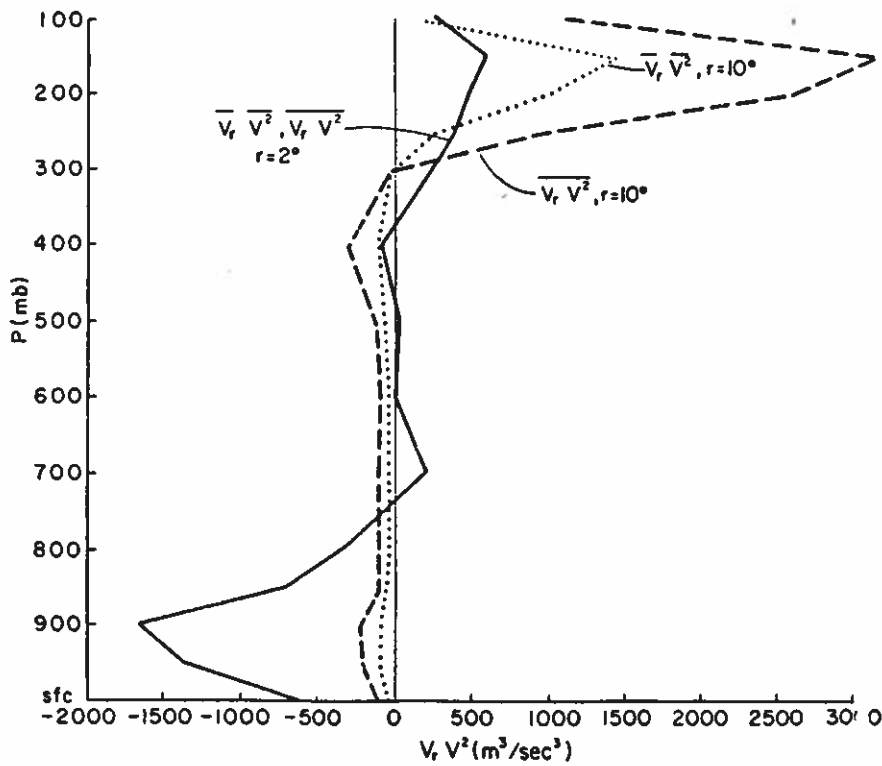


Figure 55. Total flux of kinetic energy times two, $(\overline{V_r V^2})$, and flux by mean circulation, $(\overline{V_r} \overline{V^2})$, at $r = 10^\circ$ in west Pacific typhoons (from Frank 1977d).

to export less kinetic energy ($\sim 1.7 \text{ W m}^{-2}$) in their upper-level outflow channels at 10° radius. Total transports are only slightly greater than the mean circulation fluxes.

Eddy processes thus appear to be fundamentally important in the angular momentum and kinetic energy balances of tropical cyclones. Tropical cyclones are net sources of kinetic energy, largely due to strong generation of energy by transient eddy processes in the upper troposphere. As discussed by Frank (1976, 1977d) eddy generation and internal

dissipation of kinetic energy are probably at least as important as generation and dissipation by the mean circulation.

Due to the importance of asymmetric storm features in the overall momentum and kinetic energy balances, it seems doubtful that two-dimensional model theory can provide very realistic simulations of the tropical cyclone in its large-scale outer environment.

(g) *Cyclone influence on the large-scale general circulation*

Accepting the fact that the globe's convective rainfall occurs primarily as an up-moist and down-dry warming response to balance the troposphere's radiational cooling, one can ask: to what extent does tropical cyclone rainfall contribute to the global balancing of this radiational loss? One may also enquire about the extent to which the tropical cyclone's exported kinetic energy contributes to the maintenance of the kinetic energy balance of the globe.

Tropical cyclones are least frequent during April and May when the sensible heat transport from Eurasian and North American continental areas is at a maximum. Global surface to air latent heat transport and rainfall is reduced during this period. Cyclone activity is at a maximum in August and September when land to air sensible heat transport is reduced, and lapse-rate stability over land is reduced due to the seasonal lag of upper air temperature behind surface land temperature. Overland rainfall is reduced in late summer and autumn. More of the global rainfall must come from organized weather systems such as tropical cyclones. It is interesting that tropical cyclone activity is maximum at this time.

Frank (1976) has estimated that the mean precipitation within 6° radius of the average west Pacific cyclone whose central pressure is <980 mb is $\sim 2.3 \text{ cm d}^{-1}$ (see Fig. 52). Most cyclone precipitation occurs within 6° radius. As west Pacific cyclones are typically larger, and produce more rainfall than those of other regions, it will be assumed that the average global tropical cyclone (0 – 6° radius) has a mean precipitation of about two thirds of this amount, or $\sim 1.5 \text{ cm d}^{-1}$.

Assuming that the global average annual precipitation is $\sim 1 \text{ m yr}^{-1}$, that the average cyclone maintains its rainfall for about one week, and that there are about 75 cyclones per year (conservative estimate from Table 1), one can estimate that tropical cyclones account for about $(1.5 \text{ cm d}^{-1})(7 \text{ d})(75)(A_{\text{cyclone}}/(100 \text{ cm } A_{\text{globe}})) \sim 2\%$ of the global annual precipitation. During August and September they probably account for about 4–5% of the global precipitation while during April and May only about $\frac{1}{2}$ to 1%. During especially active 10–20-day periods in August and September, tropical cyclones may account for as much as 10–15% of the global precipitation and 20–30% of northern hemisphere precipitation. Thus, at selective times of the year, the influence of the tropical cyclone is likely to be a significant component of the day to day maintenance of the general circulation. For a local area, of course, the occurrence of one cyclone can cause a major alteration to that region's water budget. From the long-term point of view, however, the condensation energy contribution of tropical cyclones does not appear to be a primary component of the tropospheric water budget.

As previously discussed, the average export of kinetic energy from a 10° radius tropical cyclone in the west Pacific and west Atlantic is 4.8 and 1.7 W m^{-2} respectively. We might assume that the average annual export from 10° radius of the globe's approximately 75 tropical cyclones is about half that of the west Pacific and west Atlantic hurricane-typhoons, or about 2.3 W m^{-2} . Again assuming that the mean tropical cyclone exists in its average intensity state for about a week and that the average global dissipation of kinetic energy is about 1.0 to 1.5 W m^{-2} (estimated from various references), then tropical cyclones contribute about 2% of the global kinetic energy which is dissipated outside the cyclone areas. This

agrees with the cyclone's global contribution of condensation. The northern hemisphere contribution of KE between August and October may amount to 10–15%. During especially active 10–20-day cyclone periods, this KE contribution to northern hemisphere KE dissipation occurring outside the cyclone may go as high as 20–30%.

Much of the tropical cyclone's KE export goes into middle latitudes. Erickson and Winston (1972) have composited information on 14 autumn typhoons which showed evidence through cloud streaks of strong KE export to middle latitudes. They concluded that the cloud band connections are visible manifestations of large KE injections from tropical cyclones into middle latitudes, and that these energy injections contribute to the autumnal build-up of the hemispheric circulation.

Thus, although tropical cyclones account for only about 2% of the global annual rainfall and excess KE, they appear to be able, over short periods when cyclone activity is high, to contribute significantly to a hemisphere's general circulation. Energy-wise, tropical cyclones thus appear not to be a fundamental mechanism to the establishment and maintenance of the tropical general circulation. Their feedback to the general circulation is significant at the times and places where they exist but probably not to the long-term global condensation and kinetic energy budgets of the troposphere. The tropical cyclones' contribution to the globe's mass, moisture and energy budget could probably be accomplished (were their formation not to occur) by a greater number of weaker tropical disturbances existing in their place.

8. FUTURE RESEARCH

It is important that the 5–15-day bursts of hemispheric tropical cyclone activity be studied and compared with the 10–20-day inactive cyclone periods. To what extent can these active and inactive periods be associated with middle latitude and/or opposite hemisphere large-scale circulation features?

The recent technical advances of global data tape storage and retrieval and the archiving of daily upper air data sets makes such research possible. The author and certain other meteorologists believe that large-scale general circulation changes are indeed related to hemispheric periods of active and inactive cyclone activity. If this can be demonstrated, then some degree of improvement in genesis forecast skill may be forthcoming.

A second important research need is for more numerical modelling studies into the processes related to cloud cluster to cyclone transformation. This subject has yet to be satisfactorily treated. Models should be initialized with intensity conditions similar to that of the cloud cluster disturbance and not those of the already developed weak cyclone. More three-dimensional modelling of the outer hurricane circulation has to be accomplished so that the significance of the outer region horizontal eddy transport can be better understood. More numerical modelling should be accomplished into the significance of unbalanced pressure gradients resulting from Cb-induced momentum changes.

New and fresh ideas are needed as to the physical processes involved with tropical cyclone genesis. The easterly wave, CISK, wave-CISK, baroclinic and barotropic instability ideas, etc., so far proposed to explain cyclone formation, all appear inadequate. We need to look more at the observational data which have already been collected. Only this is likely to lead to an adequate theory of genesis. This has yet to be done.

Less attention should perhaps be given to the various cumulus heating and parameterization schemes and more to other physical processes such as radiation, Cb-induced momentum change, influence on tropical cyclones of different larger-scale surrounding flow patterns, etc. Cumulus-induced enthalpy change appears to be more related to the character of surrounding disturbance large-scale flow patterns than to the amount and intensity of

cumulus convection itself. The influence of large-scale wind–pressure imbalance on cyclone genesis and intensity change needs much study.

It is important that tropical cyclones be treated on a global rather than a local basis. Not enough exchange of ideas is occurring between the various countries which are affected by these storms.

It is important that an international data bank for tropical cyclone study be established so that maximum research on these systems can be made.

It is also important that more meteorologists take up seriously the study of tropical cyclones. To date, very few research meteorologists have devoted many years or a high percentage of their time to the study of these systems. Tropical cyclones are surely as worthy of study relative to their impact on the global population as other subjects under intensive investigation.

ACKNOWLEDGMENTS

The author would like to acknowledge the many discussions he has had on this subject over the last decade with his former and current graduate students. These include Raúl E. López, William M. Frank, William A. Fingerhut, John L. McBride, Raymond M. Zehr, Charles P. Arnold, Edwin Núñez and Steven Erickson.

The author is much indebted to Edwin Buzzell who, over the last eight years, has made most of the data tape runs necessary for this analysis. He is also appreciative of the manuscript assistance provided by Mrs Barbara Brumit and Mrs Dianne Schmitz.

This research has been supported by a continuing grant from the US National Science Foundation with supplementary support from the US National Oceanic and Atmospheric Administration and the US Navy Environmental Prediction Research Facility.

REFERENCES

- | | | |
|--|-------|---|
| Albrecht, B. and Cox, S. K. | 1975 | The large-scale reponse of the tropical atmosphere to cloud-modulated infrared heating, <i>J. Atmos. Sci.</i> , 32 , 16–24. |
| Anthes, R. A. | 1972 | Development of asymmetries in a three-dimensional numerical model of the tropical cyclone, <i>Mon. Weath. Rev.</i> , 100 , 461–476. |
| | 1977 | Hurricane model experiments with a new cumulus parameterization scheme, <i>Ibid.</i> , 105 , 287–300. |
| Anthes, R. A., Rosenthal, S. L. and Trout, J. W. | 1971a | Preliminary results from an asymmetric model of the tropical cyclone, <i>Mon. Weath. Rev.</i> , 99 , 744–758. |
| | 1971b | Comparisons of tropical cyclone simulations with and without the assumption of circular symmetry, <i>Ibid.</i> , 99 , 759–766. |
| Arnold, C. A. | 1977 | Tropical cyclone cloud and intensity relationships, <i>Atmos. Sci. Paper No. 277</i> , Colorado State Univ., Ft. Collins, Colorado. |
| Brand, S. | 1971 | The effects on a tropical cyclone of colder surface waters due to upwelling and mixing produced by a prior tropical cyclone, <i>J. Appl. Met.</i> , 10 , 865–874. |
| Carrier, G. F. | 1971 | The intensification of hurricanes, <i>J. Fluid Mech.</i> , 49 , 145–158. |
| Ceselski, B. F. | 1974 | Cumulus convection in weak and strong tropical disturbances, <i>J. Atmos. Sci.</i> , 31 , 1241–1255. |
| Charney, J. C. and Eliassen, A. | 1964 | On the growth of the hurricane depression, <i>Ibid.</i> , 21 , 68–75. |
| Cox, S. K. | 1969 | Radiation models of mid-latitude synoptic features, <i>Mon. Weath. Rev.</i> , 97 , 637–651. |
| | 1971a | Infrared radiation models for the tropics, <i>Proceedings of the Miami Workshop on Remote Sensing</i> , NOAA, Boulder, Colorado, 161–178. (Available from NOAA ERL, Boulder, Colorado.) |
| | 1971b | Cirrus clouds and the climate, <i>J. Atmos. Sci.</i> , 28 , 1513–1515. |

- Dewart, J. 1978 The diurnal variability of the atmosphere in the GATE region. M.S. thesis, Colorado State Univ., Atmos. Sci. Dept., Ft. Collins, Colorado.
- Dvorak, V. F. 1975 Tropical cyclone intensity analysis and forecasting from satellite imagery, *Mon. Weath. Rev.*, **103**, 420-430.
- Erickson, C. O. and Winston, J. S. 1972 Tropical storms, mid-latitude cloud-band connections and the autumnal buildup of the planetary circulation, *J. Appl. Met.*, **11**, 23-36.
- Erickson, S. 1977 Comparison of developing v. non-developing tropical disturbances, *Atmos. Sci. Paper No. 274*, Colorado State Univ., Ft. Collins, Colorado.
- Fett, R. W. 1966 Upper-level structure of the formative tropical cyclone, *Mon. Weath. Rev.*, **94**, 9-18.
- Fingerhut, W. A. 1978 A numerical model of a diurnally varying tropical cloud cluster disturbance, *Ibid.*, **106**, 255-264.
- Frank, N. and Clark, G. 1977 Atlantic tropical systems of 1976, *Ibid.*, **105**, 676-683.
- Frank, W. M. 1976 The structure and energetics of the tropical cyclone, *Dept. of Atmos. Sci. Paper No. 258*, Colorado State Univ., Ft. Collins, Colorado. (Available from Dept. of Atmos. Sci., CSU.)
- 1977a The structure and energetics of the tropical cyclone, Paper I: Storm structure, *Mon. Weath. Rev.*, **105**, 1119-1135.
- 1977b The structure and energetics of the tropical cyclone, Paper II: Dynamics and energetics, *Ibid.*, **105**, 1136-1150.
- 1977c Convective fluxes in tropical cyclones, *J. Atmos. Sci.*, **34**, 10, 1553-1568.
- 1977d Momentum and kinetic energy processes in the tropical cyclone, Paper prepared for the *11th Technical Conference on Hurricanes and Tropical Meteorology*, Dec. 13-16, Miami Beach, FL, 535-542.
- Gray, W. M. 1962 On the balance of forces and radial accelerations in hurricanes, *Quart. J. R. Met. Soc.*, **88**, 430-458.
- 1965 Calculations of cumulus vertical draft velocities in hurricanes from aircraft observations, *J. Appl. Met.*, **4**, 463-474.
- 1966 On the scales of motion and internal stress characteristics of the hurricane, *J. Atmos. Sci.*, **23**, 278-288.
- 1967 The mutual variation of wind, shear and baroclinicity in the cumulus convection atmosphere of the hurricane, *Mon. Weath. Rev.*, **95**, 55-73.
- 1968 Global view of the origin of tropical disturbances and storms, *Ibid.*, **96**, 669-700.
- 1972 A diagnostic study of the planetary boundary layer over the oceans, *Dept. of Atmos. Sci. Paper No. 179*, Colorado State Univ., Ft. Collins, Colorado. (Available from Dept. of Atmos. Sci., CSU.)
- 1973 Cumulus convection and large-scale circulations Part I: Broad-scale and meso-scale interactions, *Mon. Weath. Rev.*, **101**, 839-855.
- 1975 Tropical cyclone genesis, *Dept. of Atmos. Sci. Paper No. 234*, Colorado State Univ., Ft. Collins, Colorado. (Available from Dept. of Atmos. Sci., CSU.)
- Gray, W. M. and Mendenhall, B. 1974 A statistical analysis of factors influencing the wind veering in the planetary boundary layer, *Climatological Research*, The Hermann Flohn 60th Anniversary Vol., 167-194.
- Gray, W. M. and Shea, D. J. 1973 The hurricane's inner core region. II: Thermal stability and dynamic characteristics, *J. Atmos. Sci.*, **8**, 1565-1576.
- 1976 Data summary of NOAA's hurricane inner-core radial leg flight penetrations 1957-1967, and 1969, *Atmos. Sci. Paper No. 257*, Colorado State Univ., Ft. Collins, Colorado.
- Gray, W. M. and Jacobson, R. W. Jr. 1977 Diurnal variation of deep cumulus convection, *Mon. Weath. Rev.*, **105**, 1171-1188.

- Gray, W. M. and McBride, J. 1978 Influence of cloud and cloud-free radiational differences on tropical disturbance maintenance and diurnal modulation. Paper prepared for the 3rd Conference on Atmospheric Radiation, American Meteorological Society, June 28-30, Davis, CA.
- Gray, W. M. and Frank, W. M. 1979 Recent advances in tropical cyclone meteorology, Report being prepared for WMO.
- Green, J. S. A. and Pearce, R. P. 1962 Cumulonimbus convection in shear, *Tech. Note 12*, Dept. Met. Imperial College, London.
- Grube, P. 1978 Influence of GATE deep cumulus convection on tropospheric temperature change, *Dept. of Atmos. Sci. paper No. 305*, Colorado State Univ., Ft. Collins, Colorado. (Available from Dept. of Atmos. Sci., CSU.)
- Harrison, E. J. 1973 Three-dimensional numerical simulations of tropical storms utilizing nested finite grids, *J. Atmos. Sci.*, **30**, 1528-1543.
- Hawkins, H. F. and Rubsam, D. T. 1968 Hurricane Hilda, 1964: II. Structure and budgets of the hurricane on October 1, 1964, *Mon. Weath. Rev.*, **96**, 617-636.
- Hawkins, H. F. and Imbembo, S. M. 1976 The structure of a small intense hurricane - Inez, 1966, *Ibid.*, **104**, 418-442.
- Heffernan, R. F. 1972 Hurricane heat potential of the North Atlantic and North Pacific Oceans, M.S. thesis of the Naval Postgraduate School, Monterey, CA.
- Hoxit, L. R., Chappell, C. and Fritsch, M. 1976 Formation of pressure troughs in advance of cumulonimbus clouds, *Mon. Weath. Rev.*, **104**, 11, 1419-1428.
- Jordan, C. L. 1964 On the influence of tropical cyclones on the sea surface temperature field, *Proc. Symp. Tropical Meteorology*, Wellington, New Zealand Meteor. Service, 614-622.
- Kuo, H. L. 1965 On the formation and intensification of tropical cyclones, through latent heat release by cumulus convection, *J. Atmos. Sci.*, **22**, 40-63.
- Kurihara, Y. 1975 Budget analysis of a tropical cyclone simulated in an axisymmetric numerical model, *Ibid.*, **32**, 25-59.
- Kurihara, Y. and Tuleya, R. E. 1974 Structure of a tropical cyclone developed in a three-dimensional numerical simulation model, *Ibid.*, **31**, 893-919.
- Landis, R. C. and Leipper, D. F. 1968 Effects of hurricane Betsy upon Atlantic ocean temperature, based upon radio-transmitted data, *J. Appl. Met.*, **7**, 544-562.
- LaSeur, N. E. and Hawkins, H. F. 1963 An analysis of hurricane Cleo (1958) based on data from research reconnaissance aircraft, *Mon. Weath. Rev.*, **91**, 694-709.
- Leipper, D. F. 1967 Observed ocean conditions and hurricane Hilda, 1964, *J. Atmos. Sci.*, **24**, 182-196.
- Leipper, D. F. and Jensen, J. 1971 Changes in energy input from the sea into hurricanes, *Bull. Amer. Met. Soc.*, **52**, 9-28.
- Leipper, D. F. and Volgenau, D. 1972 Hurricane heat potential of the Gulf of Mexico, *J. Phy. Ocean.*, **2**, 218-224.
- Lopez, R. E. 1968 Investigation of the importance of cumulus convection and ventilation in early tropical storm development, *Atmos. Sci. Paper No. 124*, Colorado State Univ., Ft. Collins, Colorado.
- 1973a Cumulus convection and larger-scale circulations Part II: Cumulus and mesoscale interactions, *Mon. Weath. Rev.*, **101**, 856-870.
- 1973b A parametric model of cumulus convection, *J. Atmos. Sci.*, **30**, 1345-1373.
- Ludlam, F. H. 1963 Severe local storms: A review, *Met. Mon.*, Amer. Met. Soc.
- 1966 Cumulus and cumulonimbus convection, *Tellus*, **18**, 687-698.
- McBride, J. L. 1977 Observational analysis of the differences between developing and non-developing tropical disturbances. Paper prepared for the 11th Technical Conference on Hurricanes and Tropical Meteorology, Dec. 13-16, Miami Beach, FL, 260-267.
- 1979 Forthcoming Ph.D. thesis on tropical cyclone genesis from Colorado State Univ., Ft. Collins, Colorado.

- Malkus, J. S. and Riehl, H. 1960 On the dynamics and energy transformation in steady-state hurricanes, *Tellus*, **12**, 1-20.
- Martin, D., Suchman, D. and Sikdar, D. 1977 Deep convective mass transport - Two estimates from geostationary satellites, *Mon. Weath. Rev.*, **105**, 943-955.
- Mathur, M. B. 1972 Simulation of an asymmetric hurricane with a fine mesh multiple grid primitive equation model. Ph.D. dissertation, Florida State University, Tallahassee, Florida.
- Miller, B. I. 1958 Rainfall rates in Florida hurricanes, *Mon. Weath. Rev.*, **86**, 258-264.
- 1962 On the momentum and energy balance of hurricane Helene (1958). *NHRP Rept. No. 53*. (Available from NOAA Weather Bureau, Miami office.)
- 1969 Experiment in forecasting hurricane development with real data, *ESSA Tech. Memorandum ERLTM-NHRL 85*, Miami, Fla.
- Moncrieff, M. W. and Green, J. S. A. 1972 The propagation of steady convective overturning in shear, *Quart. J. R. Met. Soc.*, **98**, 336-352.
- Moncrieff, M. W. and Miller, M. J. 1976 The dynamics of simulation of tropical cumulonimbus and squall lines, *Ibid.*, **102**, 373-394.
- Núñez, E. and Gray, W. M. 1977 A comparison between West Indies hurricanes and Pacific typhoons, Paper prepared for the *11th Technical Conference on Hurricanes and Tropical Meteorology*, Dec. 13-16, Miami, Beach, FL, 528-534.
- Ogura, Y. 1964 Frictionally controlled, thermally driven circulation in a circular vortex with application to tropical cyclones, *J. Atmos. Sci.*, **21**, 610-621.
- Oliver, V. J. and Anderson, R. K. 1969 Circulation in the tropics as revealed by satellite data, *Bull. Amer. Met. Soc.*, **50**, 702-706.
- Ooyama, K. 1964 A dynamical model for the study of tropical cyclone development, *Geoffis. Intern.*, **4**, 187-198.
- 1969 Numerical simulation of the life cycle of tropical cyclones, *J. Atmos. Sci.*, **26**, 3-40.
- Palmén, E. H. 1948 On the formation and structure of tropical cyclones, *Geophysica*, Helsinki, **3**, 26-38.
- 1957 A review of knowledge on the formation and development of tropical cyclones, *Proc. Tropical Cyclone Symp.*, Brisbane, Dec. 1965, Wilke and Co., Ltd., Melbourne 213-231.
- Perlroth, I. 1967 Hurricane behavior as related to oceanographic environmental conditions, *Tellus*, **19**, 258-268.
- 1969 Effects of oceanographic media on equatorial Atlantic hurricanes, *Ibid.*, **21**, 230-244.
- Riehl, H. 1954 *Tropical meteorology*, McGraw-Hill, New York.
- 1961 On the mechanisms of angular momentum transports in hurricanes, *J. Met.*, **18**, 113-115.
- 1967 Varying structure of waves in the easterlies, *Dynamics of Large Scale Atmospheric Processes. Proceeding of the International Symposium*, Moscow, 1965, 411-416.
- 1975 Further studies on the origin of hurricanes, *Atmos. Sci. Paper No. 235*, Colorado State Univ., Ft. Collins, Colorado.
- Riehl, H. and Malkus, J. S. 1958 On the heat balances in the equatorial trough zone, *Geophysica*, Helsinki, 503-537.
- 1961 Some aspects of hurricane Daisy, 1958, *Tellus*, **13**, 181-213.
- Rosenthal, S. L. 1970 A circularly symmetric primitive equation of tropical cyclone development containing an explicit water vapour cycle, *Mon. Weath. Rev.*, **98**, 643-663.
- 1971 The response of a tropical cyclone model to variations in boundary layer parameters, initial conditions, lateral boundary conditions and domain size, *Ibid.*, **10**, 767-777.
- 1978 Numerical simulation of tropical cyclone development with latent heat release by the resolvable scales. I: model description and preliminary results, *J. Atmos. Sci.*, **35**, 258-271.

- Ruprecht, E. and Gray, W. M. 1976a Analysis of satellite-observed tropical cloud clusters, I: Wind and dynamic fields, *Tellus*, **28**, 391-413.
- 1976b Analysis of satellite-observed tropical cloud clusters, II: Thermal, moisture and precipitation, *Ibid.*, **28**, 414-426.
- Sadler, J. C. 1967a On the origin of tropical vortices, *Working Panel on Trop. Dynamical Meteorology*, Naval Postgraduate School, Monterey, CA 39-75. (Available from US Navy ERPF, Monterey, CA.)
- 1967b The tropical tropospheric trough as a secondary source of typhoons and a primary source of tradewind disturbances, *Final Report*, Cont. AF19 (628)3860, AF Cambridge Research Labs., Bedford, MA, Rept. 67-12. (Available from Inst. of Geophysics, Univ. of Hawaii.)
- 1974 A role of the tropical upper tropospheric trough in early seasonal typhoon development, *Tech. Paper No. 9-74*, US Navy Environmental Prediction Research Facility Report. (Available from Inst. of Geophysics, Univ. of Hawaii.)
- 1976a Tropical cyclone initiation by the tropical upper tropospheric trough, *Tech. Paper No. 2-76*, *Ibid.*
- 1976b A role of the tropical upper tropospheric trough in early season typhoon development, *Mon. Weath. Rev.*, **104**, 1266-1278.
- Shapiro, L. J. 1977a Tropical storm formation from easterly waves: A criterion for development, *J. Atmos. Sci.*, **34**, 7, 1007-1021.
- 1977b A criterion for the development of tropical storms from easterly waves, Paper prepared for the *11th Technical Conference on Hurricanes and Tropical Meteorology*, Dec. 13-16, Miami Beach, FL.
- Shea, D. J. and Gray, W. M. 1973 The hurricane's inner core region: I. Symmetric and asymmetric structure, II: Thermal stability and dynamic characteristics, *J. Atmos. Sci.*, **30**, 1544-1576.
- Sheets, R. C. 1967a On the structure of hurricane Janice (1958). NHRL Rept. No. 76. (Available from NOAA Weather Bureau, Miami office.)
- 1967b On the structure of hurricane Ella (1962). NHRL Rept. No. 66. (Available from NOAA Weather Bureau, Miami office.)
- 1968 On the structure of hurricane Dora (1964). NHRL Rept. No. 83. (Available from NOAA Weather Bureau, Miami office.)
- Sundqvist, H. 1970 Numerical simulation of the development of tropical cyclones with a ten-layer model, Part. I, *Tellus*, **22**, 359-390.
- Whitaker, S. D. 1967 Quantitative determination of heat transfer from sea to air during passage of hurricane Betsy. M.S. thesis, Texas A & M Univ., College Station, TX.
- Williams, K. T. and Gray, W. M. 1973 A statistical analysis of satellite-observed trade wind cloud clusters in the western North Pacific, *Tellus*, **21**, 323-336.
- Wright, S. 1976 The comparable development of tropical storm Holly with a gulf tropical disturbance, *Mon. Weath. Rev.*, **104**, 1451-1454.
- Yamasaki, M. 1968 Numerical simulation of tropical cyclone development with the use of primitive equations, *J. Met. Soc. Japan*, **46**, 178-201.
- Yanai, M. 1961 A detailed analysis of typhoon formation, *Ibid.*, **39**, 187-214.
- 1968 Evolution of a tropical disturbance in the Caribbean Sea region, *Ibid.*, Series II, **46**, 86-108.
- Zehr, R. 1976 Tropical disturbance intensification, *Dept. of Atmos. Sci. Paper No. 259*, Colorado State Univ., Ft. Collins, Colorado. (Available from Dept. of Atmos. Sci., CSU.)